BIOLOGICAL REVIEWS
Cambridge Philosophical Society
Biol. Rev. (2021), pp. 000–000.
doi: 10.1111/brv.12758

Fluorescent nanoparticles as tools in ecology and physiology

Sanni M. A. Färkkilä[1*], E. Toby Kiers[2], Raivo Jaaniso[3], Uno Mäeorg[4], Roger M. Leblanc[5], Kathleen K. Treseder[6], Zhenhui Kang[7] and Leho Tedersoo[1]

[1]*Institute of Ecology and Earth Sciences, University of Tartu, Ravila 14a, 50411, Tartu, Estonia*
[2]*Department of Ecological Science, Vrije Universiteit Amsterdam, De Boelelaan 1085, NL-1081 HV, Amsterdam, Noord-Holland, The Netherlands*
[3]*Institute of Physics, University of Tartu, W. Ostwaldi Str 1, 50411, Tartu, Tartumaa, Estonia*
[4]*Institute of Chemistry, University of Tartu, Ravila 14a, 50411, Tartu, Estonia*
[5]*Department of Chemistry, Cox Science Center, University of Miami, 1301 Memorial Drive, Coral Gables, FL, 33124, U.S.A.*
[6]*Department of Ecology and Evolutionary Biology, School of Biological Sciences, University of California, Irvine, 3106 Biological Sciences III, Mail Code: 2525, 92697, Irvine, CA, U.S.A.*
[7]*Institute of Functional Nano and Soft Materials (FUNSOM), Jiangsu Key Laboratory for Carbon-based Functional Materials and Devices, Soochow University, Suzhou, 215123, China*

ABSTRACT

Fluorescent nanoparticles (FNPs) have been widely used in chemistry and medicine for decades, but their employment in biology is relatively recent. Past reviews on FNPs have focused on chemical, physical or medical uses, making the extrapolation to biological applications difficult. In biology, FNPs have largely been used for biosensing and molecular tracking. However, concerns over toxicity in early types of FNPs, such as cadmium-containing quantum dots (QDs), may have prevented wide adoption. Recent developments, especially in non-Cd-containing FNPs, have alleviated toxicity problems, facilitating the use of FNPs for addressing ecological, physiological and molecule-level processes in biological research. Standardised protocols from synthesis to application and interdisciplinary approaches are critical for establishing FNPs in the biologists' tool kit. Here, we present an introduction to FNPs, summarise their use in biological applications, and discuss technical issues such as data reliability and biocompatibility. We assess whether biological research can benefit from FNPs and suggest ways in which FNPs can be applied to answer questions in biology. We conclude that FNPs have a great potential for studying various biological processes, especially tracking, sensing and imaging in physiology and ecology.

Key words: quantum dots, fluorescent carbon nanoparticles, nanotechnology, nanoparticles in biology, fluorescence techniques, alternative quantum dots, bioimaging, biosensing, molecular tracking, fluorescent labelling

CONTENTS

* Address for correspondence (Tel: +358400853395; E-mail: sanni.maria.aurora.farkkila@ut.ee)

I. INTRODUCTION

Fluorescent nanoparticles (FNPs) are nanoscale organic, inorganic crystalline or amorphous clusters that emit specific wavelengths upon exposure to light. FNPs have been extensively developed and widely utilised for technological and medical applications for over two decades (Reshma & Mohanan, 2019) and can also be harnessed for imaging, tracking and sensing applications in biology. The power of FNP technology is related to their unique fluorescence features: production of steady, bright, and clearly defined fluorescent peaks. FNPs are generally more stable, absorb and emit light more efficiently and have longer fluorescence lifetimes compared to many other fluorescent materials such as dyes. FNPs with different emission wavelengths can also be used simultaneously – a feature that dyes usually lack (Resch-Genger *et al.*, 2008). FNPs are also multimodal, i.e. the dots can perform several functions simultaneously. For example, the same dot can deliver a drug compound to cancer tissue and serve as a fluorescent marker to confirm successful delivery (Bera *et al.*, 2010). Compared to isotopic methods, FNPs offer a non-invasive option for cell-level particle tracking.

While the properties of FNPs make them useful for tracking, sensing and visualising organisms and molecules (Fig. 1), FNPs have not been widely adopted in fundamental biological research. Landmark papers describing semiconductor nanoparticles emerged in the early 1980s (Brus, 1983; Rossetti, Nakahara & Brus, 1983; Reed *et al.*, 1986) and successful utilisation of cadmium chalcogenide quantum dots (Cd-containing QDs; Cd-QDs) in cell imaging was achieved in the late 1990s (Bruchez *et al.*, 1998; Chan & Nie, 1998). Since then, research into QDs has intensified and the potential for developing FNPs in biological research emerged. The possibility to conjugate (i.e. chemically attach) molecules onto FNPs (Chan & Nie, 1998; Mattoussi *et al.*, 2000) further increased potential applications, such as tracking of compounds. The future of QDs seemed as bright as the dots themselves (Rosenthal *et al.*, 2011; Massey *et al.*, 2015) and a few groups successfully employed QDs in imaging, tracking and sensing applications across an array of organisms (Pang & Gong, 2019; Whiteside *et al.*, 2019). However, in the late 2000s, reports of QD degradation and subsequent leaking of Cd from the particle core with induced toxic effects became an increasing concern (Pelley, Daar & Saner, 2009; Massey *et al.*, 2015) and the value of FNP technology was questioned.

Since the development of the first QDs, the nanoscale world has made great strides in introducing new technologies. Cd-QDs have been transformed in terms of their shells, coatings, dopings (additions of atomic impurities during synthesis) and conjugations, all of which have greatly improved their optical and chemical properties, biocompatibility and usability. Furthermore, new, non-cadmium FNPs have been developed with metal, metalloid and carbon cores. These are now slowly finding their way into the biological realm. Owing to these recent developments, wider adoption of this technology in fields such as ecology and physiology is on the horizon. A new generation of FNPs can be applied to investigating food-web structure, prey preferences in predators, seed and spore dispersal dynamics in plants and fungi, nutrient cycling dynamics in microbial networks, and migration and behavioural patterns of micro-organisms in soil and water columns.

This review aims to summarise current research on FNPs. Our objective is to encourage biologists, unfamiliar with

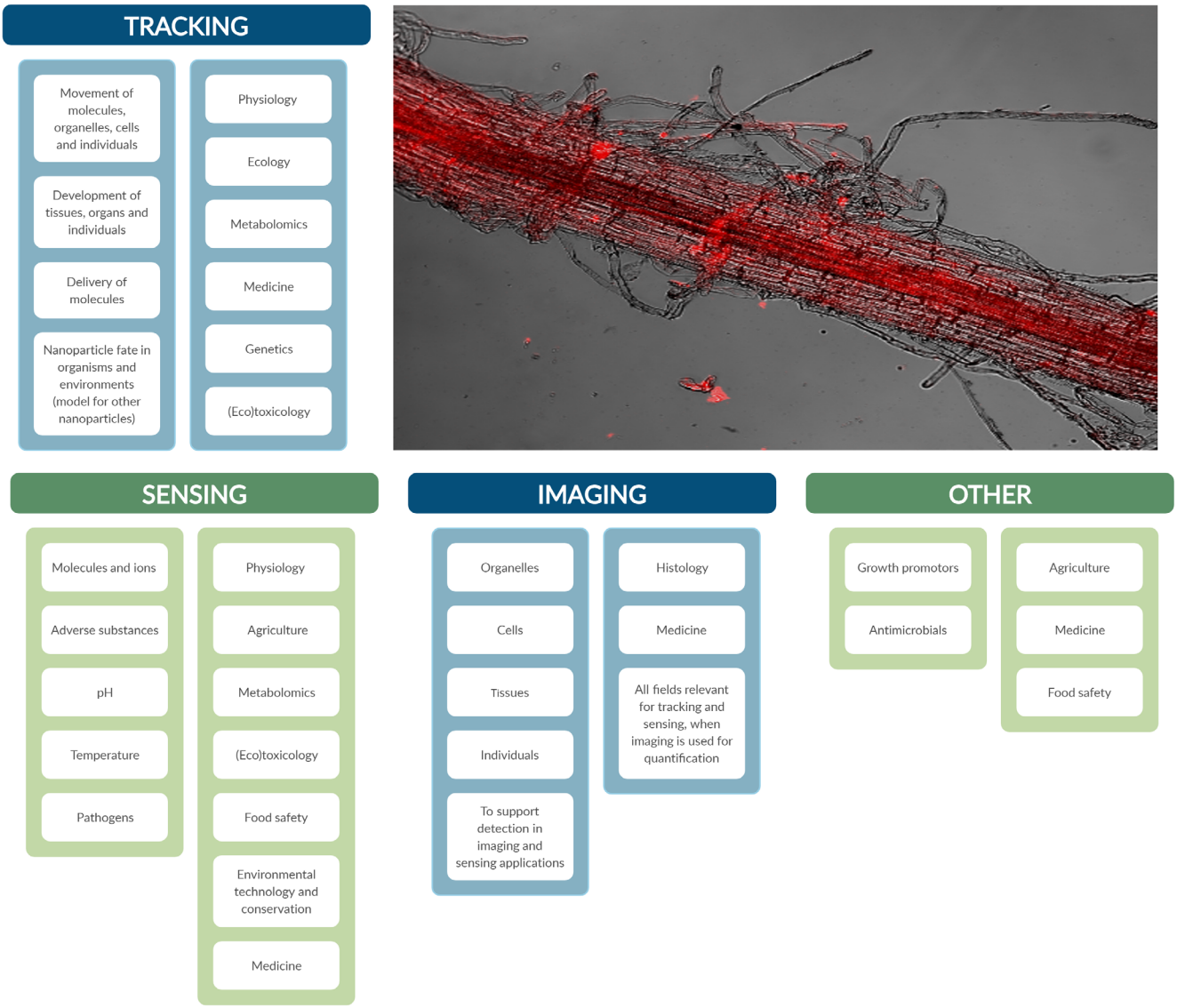

Fig. 1. Fluorescent nanoparticle (FNP) applications for various biological fields. The image (courtesy of Matthew Whiteside) features glycine-conjugated quantum dots (QDs) within a grass root colonized by arbuscular mycorrhizal fungi.

concepts such as optical physics and nanomaterial science, to consider various types of FNPs in their research. We mainly focus on the application of FNPs and their advantages and disadvantages in various fields of biology rather than their chemical and physical properties, which have been comprehensively reviewed elsewhere (Drbohlavova *et al.*, 2009; Zuo *et al.*, 2016; Schiffman & Balakrishna, 2018). We briefly address ecotoxicological issues relevant to specific applications, as these aspects have been broadly reviewed in general (Pelley *et al.*, 2009; Rocha *et al.*, 2017; Sharma *et al.*, 2017). We mainly address FNPs of two different categories: fluorescent carbon nanoparticles (FCNPs) and semiconductor quantum dots (SQDs). We provide a synthesis of existing biological research items related to FNPs *via* a selection of landmark papers as well as more recent, novel applications that are most relevant to ecology and physiology. We also discuss quantification methods and compare biologically relevant FNP properties to aid particle selection. Finally, we propose theoretical and practical approaches to plan research with FNPs and address knowledge gaps.

II. TYPES OF FLUORESCENT NANOPARTICLES (FNPs)

(1) Semiconductor quantum dots (SQDs)

Semiconductor quantum dots are nanocrystals that fluoresce in a specific wavelength upon excitation with another wavelength of light. The term semiconductor refers to a material

that has an intermediate capacity to conduct electricity. The word 'quantum' refers to the so-called quantum confinement effect on the properties of QDs – small dot size limits movement of electrons, forcing them to exist at discrete levels of energy. As a result, properties of QDs differ enormously from those of the same bulk material (Drbohlavova *et al.*, 2009; Rosenthal *et al.*, 2011). The optimal light wavelengths are referred to as excitation and emission peaks, which usually depend directly on particle size (i.e. quantum size effect): the larger the dot, the longer the wavelengths of excitation and emission (Drbohlavova *et al.*, 2009; Rosenthal *et al.*, 2011). In some particle types, the emission colour is changed by altering the relative abundances of different elements in the core or on the surface, which removes the possible effect of particle size in complex experiments (Whiteside *et al.*, 2019). SQDs are traditionally classified into groups based on the location of the core elements in the periodic table. These include group IV, group III–V, group II–IV and group IV–VI QDs and complex QDs, which all include several particle types (IV–VI QDs include several subgroups). However, these groupings are rarely utilised in biological research papers, and the utilisation of SQDs is intensely skewed towards Cd-QDs. Therefore, we address Cd-QDs separately, while other SQDs are addressed in parallel. FNP classification and terminology are discussed further in Section VI.

(*a*) Cadmium-containing QDs

The best-known FNPs, which we refer to also as cadmium quantum dots (Cd-QDs) for clarity, represent Cd-containing semiconductor nanocrystals that usually include the chalcogenides – sulphur (S), selenium (Se) or tellurium (Te) – as companion anions. The diameter of these QDs is typically 2–10 nm, sometimes up to 20 nm (Drbohlavova *et al.*, 2009; Rosenthal *et al.*, 2011), i.e. comparable in size to biological macromolecules such as proteins.

Cd-QDs have been used primarily for imaging purposes and as nanocarriers. There is also active research in QDs for molecular diagnostics and therapeutics, with a focus on imaging in the near infra-red region (the so-called biological window) and use in single molecular tracking (Dahan *et al.*, 2003; Li *et al.*, 2010; Liu *et al.*, 2012; Wagner *et al.*, 2019). Medical applications include a QD-microbead molecular tagging system that enables colour coding and identification of up to tens of thousands of biological molecules (Han *et al.*, 2001), QD labelling of various receptors to study their location and activity (Dahan *et al.*, 2003; Chung *et al.*, 2010), biomarkers and drug testing applications for various diseases such as SARS-CoV-2 (Li *et al.*, 2010; Gorshkov *et al.*, 2020) and real-time tracking of viral infection inside living cells (Liu *et al.*, 2012).

Quantum dots coated with a shell of less-toxic material such as, e.g. zinc sulphide (ZnS), are nowadays the standard type utilised in biological research, as shells render the core-cadmium less chemically and biologically available and improve other features such as photostability and biocompatibility (Winnik & Maysinger, 2013). Additionally, dopings, coatings and conjugations may improve the biocompatibility and optical properties of QDs. Elements such as nitrogen (N), phosphorus (P) or boron (B) can be incorporated into the dot during the preparation process *via* doping to fine-tune the electron structure, which can further improve the optical properties of QDs. The dopants can also be used in combination (co-doping) (Biju, Itoh & Ishikawa, 2010; Rosenthal *et al.*, 2011). Coating particles by amphiphilic polymer encapsulation (AMP, polymer coating), which forms a layer of reactive polar polymers on top of non-polar dots, enhances their water solubility and hence compatibility with biological systems (Hezinger, Teßmar & Göpferich, 2008; Rosenthal *et al.*, 2011). Dots can also be coated in a layer of silica (SiO_2), which improves stability and reduces toxicity (Selvan, Tan & Ying, 2005), or double-layered with AMP and silica (Hu & Gao, 2010). Commercially available QDs usually have a coating with reactive groups, such as carboxylic (–COOH) or amine groups ($-NH_2$), onto which users can easily conjugate their molecule of interest through the 1-ethyl-3-(−3-dimethylaminopropyl) carbodiimide hydrochloride/N-hydroxysuccinimide (EDC/NHS) amidation reaction (Chan & Nie, 1998). Common coatings include polyethylene glycol (PEG), polyethyleneimine (PEI), polyacrylic acid (PAA), tri-n-octylphosphine oxide (TOPO) and thiols (-SH) (Green, 2010; Rosenthal *et al.*, 2011). Once conjugated to nutrient compounds (Whiteside *et al.*, 2019), biological molecules such as proteins (Brandt *et al.*, 2015), hormones (Erland *et al.*, 2019), DNA strands (Ma *et al.*, 2008), antibodies (Eggenberger *et al.*, 2007) and sensory compounds (So *et al.*, 2006) can be targeted and tracked to specific tissues or cellular locations. Various structural modifications of QDs are illustrated in Fig. 2.

(*b*) Other semiconductor QDs

Besides Cd-QDs, myriad QD nanoparticles with alternative core elemental composition have been developed (Reed *et al.*, 1986; Canham, 1990; Mićić *et al.*, 1996; Sooklal

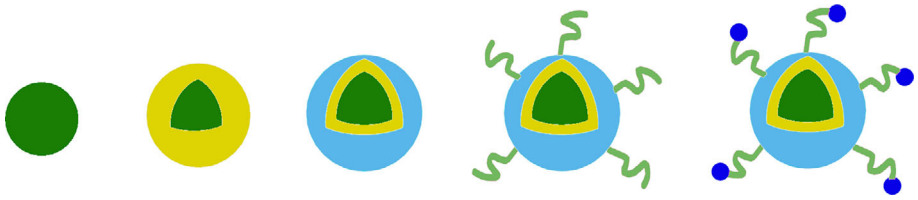

Fig. 2. Simplified structure of quantum dots (QDs) with different structural modifications. From left to right: plain QD, QD with shell (core/shell QD), coated core/shell QD, coated core/shell QD with functional groups (capped), coated and capped core/shell QD with molecular conjugates.

et al., 1996; Malik, O'Brien & Revaprasadu, 1999). The core elements may include various metals or metalloids, such as silicon (Si), copper (Cu), indium (In), zinc (Zn), germanium (Ge), phosphorus (P), arsenic (As), lead (Pb), tin (Sn), etc. Many of these particles also exhibit quantum confinement. In fact, the term quantum dot was originally coined for particles that did not have Cd in the core (Reed *et al.*, 1986). These alternative core elemental composition dots range from 1.4 to 25 nm in size and from 0 to 80% in quantum yield. They have been utilised in the bioimaging of various cells and tissues as well as biomarkers and sensors for antibodies (e.g. Bharali *et al.*, 2005; Pradhan *et al.*, 2007; Yong *et al.*, 2009; Zhou *et al.*, 2014; Liu *et al.*, 2016*a*,*b*; Chang *et al.*, 2017; García-Cortés *et al.*, 2017, Lei *et al.*, 2018). Silicon-cored QDs (SiQDs, also referred to as Si-dots) are often treated separately from other SQDs, because they do not contain heavy metals and are therefore theoretically more suited for biological applications (Chinnathambi *et al.*, 2014). While these are mostly used in technical applications, such as LEDs, batteries and solar cells (McVey & Tilley, 2014), they have also been utilised in targeted imaging of tumours, lymph nodes, cells, organelles and as carriers for drugs, microRNA (miRNA) and small interfering RNA (siRNA) (Erogbogbo *et al.*, 2008, 2011; Klein *et al.*, 2009; Park *et al.*, 2009; Nishimura *et al.*, 2013).

(2) Fluorescent carbon nanoparticles (FCNPs)

Fluorescent carbon nanoparticles (FCNPs) are comparable to QDs in size, but the semiconductor core is replaced by carbon, and other elements included are mainly oxygen (O), nitrogen (N) and hydrogen (H). The discovery of these is ascribed to Xu *et al.* (2004), who reported two new classes of carbon-based fluorescent nanomaterials isolated as a by-product of carbon nanotube purification. FCNPs are referred to using various terms, depending on the way they are synthesised and structured. Obscure terms, such as 'carbon dot (CD)', are commonly used to refer to particles of extremely varied properties. New terms and acronyms are often proposed as research groups claim they have developed new types of particles (Essner *et al.*, 2018; Tao *et al.*, 2019). For these reasons, researchers need to be careful when navigating the scientific literature. Several attempts have been made to unify this terminology (Cayuela *et al.*, 2016; Tao *et al.*, 2019). Here we treat all arbitrarily named FCNPs as carbon quantum dots (CQDs), following recent literature (Tao *et al.*, 2019). Terminological issues are further addressed in Section VI.

CQDs are typically <10 nm in size and vary in structure (amorphous or crystalline) and shape (diamond or globular), depending on precursors and synthesis methodology (Baker & Baker, 2010; Lim, Shen & Gao, 2015; Park *et al.*, 2016; Namdari, Negahdari & Eatemadi, 2017). Due to a variety of synthesis methods, the origin of fluorescence in FCNPs has been debated. Various authors have attributed this to factors other than quantum confinement effects, such as surface electronic states, edge effects, free surface states, zig-zag structures or conjugated molecular structures (Qi *et al.*, 2016). FCNPs can be manufactured with several different methodologies, which are classified as top-down and bottom-up methods. Top-down methods generally involve breaking the FNPs apart from large particles through oxidation, laser ablation, extraction or electrochemical release from various source materials such as soot, fruits or wastes (Lim *et al.*, 2015; Zhang *et al.*, 2018*a*). Conversely, bottom-up methods involve synthesis from molecular precursors, such as carbohydrates, amino acids or alcohols *via* molecular aggregation or through hydrothermal, ultrasound, pyrolytic, electrochemical or microwave procedures (Goryacheva, Sapelkin & Sukhorukov, 2017*a*). Like SQDs, FCNPs are often doped to improve their properties. Dopants change the properties of the dots by withdrawing, donating or trapping electrons. FCNPs should also be passivated – covered with a protective coating – to improve their fluorescence and stability, as well as to reduce unspecific binding and aggregation (Asadian, Ghalkhani & Shahrokhian, 2019). Minimally cytotoxic coating options include PEG or poly-(propionyl ethylenimine-co-ethylenimine) (PPEI-EI), although other options such as poly(acrylic acid) (PAA) or branched poly(ethylenimine) (BPEI) can also be used at low concentrations (Ding, Zhu & Tian, 2014).

Due to their small size and natural composition, FCNPs connected to suitable surface ligands have great potential as diagnostic tools and drug carriers, as they can effectively reach specific tissues. For example, the blood–brain barrier (BBB) complicates treatment of central nervous system diseases by inhibiting the passage of nearly all molecular drugs and nanoparticles due to their high molecular mass, but CQDs conjugated to transferrin can cross this barrier in zebrafish (*Danio rerio*; Li *et al.*, 2016*a*). Furthermore, unconjugated CQDs synthesised from D-glucose and L-aspartic acid could cross the BBS and specifically target cancerous tissue in mouse (*Mus musculus*) brain (Zheng *et al.*, 2015*a*). Similarly, diagnosis of bone-related diseases, such as osteoporosis, typically depends on methods involving harmful radiation, because other methods are hampered by the thickness of the tissues surrounding bones and the inertness of the bone itself, but carbon nanopowder-derived CQDs can specifically target and attach to bone and thus enable imaging (Peng *et al.*, 2017). Unlike conventional drugs or diagnostic tools, FCNPs can be multimodal. For example, a CQD-based nanocarrier complex both delivered and released a drug specifically in a cancerous tissue, and this was confirmed by fluorescence observed upon drug release (Feng *et al.*, 2016). Furthermore, carbon-based FNPs are increasingly utilised in antimicrobial applications, such as wound dressings, because of their bactericidal properties resulting from ROS (reactive oxygen species) generation (Ristic *et al.*, 2014; Sun *et al.*, 2014; Lin, Bao & Wu, 2019; Yadav *et al.*, 2019; Gao *et al.*, 2020). Based on these medical examples, carbon-based FNPs have an immense potential for biological applications, particularly in labelling and tracking of different compounds in organisms and communities in the fields of animal and plant physiology and ecology.

Graphene quantum dots (GQDs) differ from CQDs in their arrangement of carbon in hexagonal lattices with a size up to 100 nm. While CQDs are generally 3D assemblies of molecular chromophores, GQDs have a 2D crystalline structure and their properties depend on the orientation of the lattice units (edge effect). Because of this structure, GQDs frequently exhibit quantum confinement, whereas many other FCNPs do not (Pan *et al.*, 2010; Tian *et al.*, 2018). However, most of their biologically relevant properties resemble those of other FCNPs, making their separation somewhat arbitrary, although well established in the relevant literature. While GQDs have been utilised in molecular carriers, photocatalysts and solar cell components (Tian *et al.*, 2018), they have been used only in ion- and chemical-sensing applications in biological research so far. However, this is likely partly explained by the fact that GQDs are still a relatively recent technology (Pan *et al.*, 2010).

Carbonised polymer dots (CPDs) are prepared from semiconductive polymers, such as polyfluorenes, poly(phenylene ethylene) and poly(phenylene vinylene), that are connected by cross-linking of π-electron systems or by aggregation (Wu & Chiu, 2013). Cross-linked particles are termed conjugated polymer dots or conjugated polymer nanoparticles, while the aggregation-type particles are called unconjugated polymer dots. In some sources, polymer dots in general are regarded as a sub-type of FCNPs (Li *et al.*, 2019*b*). In others, only unconjugated dots are considered FCNPs (Zhu *et al.*, 2015), or all polymer dots are treated as a distinct type (Wu & Chiu, 2013). The term carbonised polymer dot was recently introduced to solve this confusion (Tao *et al.*, 2019). As the polymers involved in polymer dots are heavily carbon-based, we consider these a subcategory of FCNPs, following Xia *et al.* (2019). CPDs range from 1 to 50 nm in size and are inherently insoluble in water, similarly to their polymeric precursors. Coating the particle with other polymers or silica creates an amphiphilic surface, but leaves the core hydrophobic, which increases stability and density in water-based solvents (Wu & Chiu, 2013). This structure also renders CPDs an attractive alternative option for developing molecular carriers of drugs, because their mouldable structure and inside hydrophobicity allow 'storing' of therapeutics (Wu & Chiu, 2013; Massey *et al.*, 2015; Zhu *et al.*, 2015). Conjugated CPDs were developed in the early 2000s (Landfester *et al.*, 2002) and used in bioimaging several years later (Wu *et al.*, 2008). Since then, conjugated CPDs have been used as drug carriers in photodynamic therapy and in sensing cancer-related enzymes (Wang & He, 2018; Cheng *et al.*, 2019; Cui *et al.*, 2019; Kim *et al.*, 2020). They have also been utilised as disease biomarkers and medical biosensors of dopamine and hypochlorite (Alizadeh & Salimi, 2019; Wang *et al.*, 2019).

Nanodiamonds (NDs) are small diamonds, 2–10 nm in size. However, they are frequently referred to by various names, depending on their shape, size and surface modifications (Mochalin *et al.*, 2012). Although nanodiamonds have been explored for technical and, to some extent, for medical applications (Chow *et al.*, 2011; Chang *et al.*, 2013; Gismondi *et al.*, 2015; Bondon *et al.*, 2020; Liu, Chang & Chang, 2020), they have not been utilised in physiological or ecological research so far. An interesting additional possibility is the use of NDs for magnetic resonance imaging (MRI), which can provide images analogous to X-rays without the need for harmful radiation (Liu *et al.*, 2020).

(3) Rare-earth doped nanoparticles

Rare-earth-doped FNPs are a complex group of particles that constitute elements of the f-block of the periodic table, as fluorescent entities doped into dielectric nanocrystals. Of these, only the so-called upconversion nanoparticles (UCNPs) have been used in bioapplications thus far. UCNPs fluoresce due to the so-called photon upconversion, a phenomenon in which light excitation at a longer wavelength leads to light emission at a shorter wavelength – opposite to the above-discussed FNPs. UCNPs have been utilised in technical and medical applications, such as imaging and treatment of tumours, inactivation of viruses, siRNA delivery and tracking of cell transplants (Idris *et al.*, 2009; Jiang *et al.*, 2009; Wang *et al.*, 2011; Lim *et al.*, 2012; Yan *et al.*, 2019). The most frequently used type in life science applications seems to be made of a $NaYF_4$ core doped with ytterbium (Yb) and erbium (Er).

III. FLUORESCENT NANOPARTICLES IN BIOLOGICAL RESEARCH

In this section, we summarise research related to various FNPs, including particle type, application, target compounds and organisms involved (Table 1). Carboxyl-capped, CdSe/ZnS QDs are the most commonly utilised FNP type thus far.

(1) Cadmium-containing quantum dots (Cd-QDs)

(a) Ecology

In ecological studies, QDs are most commonly utilised in food chains, mostly from an ecotoxicological perspective. For example, carboxyl-capped CdSe/ZnS QDs were transferred from an alga *Pseudokirchneriella subcapitata* to a water flea *Ceriodaphnia dubia* (Bouldin *et al.*, 2008), and from a crustacean *Artemia franciscana* to a zebrafish (*Danio rerio*) during feeding (Lewinski *et al.*, 2011), elegantly confirming prey–predator relationships between these organisms. Both studies found the toxicity of QDs to be lower than expected, with no biomagnification. Likewise, there was no significant biomagnification of carboxyl-capped CdSe/ZnS QDs from *Escherichia coli* bacteria and *Tetrahymena pyriformis* ciliates to the rotifer *Brachionus calyciflorus* (Holbrook *et al.*, 2008). By contrast, a study on trophic transfer of CdSe QDs between bacteria (*Pseudomonas aeruginosa*) and ciliates (*Tetrahymena thermophile*) revealed significant biomagnification, as Cd concentrations of ciliates exceeded their QD-incubated bacterial prey fivefold (Werlin *et al.*, 2011). CdTe QDs were 1.4-fold

Table 1. Summary of the research on fluorescent nanoparticles in the life sciences included in this review (excluding strictly medical applications)

Type	Modification	Application	Target(s) if applicable	Organism(s)	Reference
Carbon quantum dot (CQD)		Bacterial enhancement		*Azotobacter chroococcum*	Wang *et al.* (2018*a*)
		Imaging (animal)		*Caenorhabditis elegans*	Chen *et al.* (2014*b*); Pramanik *et al.* (2016)
		Imaging (bacteria)		*Pseudomonas aeruginosa*	Ritenberg *et al.* (2016)
		Imaging (bacteria/ fungal cellular)		*Bacillus subtilis*, *Aspergillus aculeatus* *Mycobacterium tuberculosis*, *Pseudomonas aeruginosa*, *Magnaporthe oryzae*, *Fusarium avenaceum*	Kasibabu *et al.* (2015*a*, *b*); Mehta *et al.* (2015)
		Imaging (fungal cellular)		*Penicillium* sp.	Bhamore *et al.* (2018)
	Cellulose conjugated	Imaging (plant cellular)	Cell walls	*Allium cepa*, *Vigna radiata*, *Arabidopsis thaliana*	Li *et al.* (2017)
		Plant growth enhancement		*Arabidopsis thaliana*, *Trifolium repens* *Arachis hypogaea* *Brassica rapa* var. *parachinensis* *Chlorella vulgaris* *Citrus maxima* *Oryza sativa* *Vigna radiata* *Triticun aestivum*	Li *et al.* (2019*a*); Su *et al.* (2018); Zheng *et al.* (2017); Zhang *et al.* (2018*a*); Li *et al.* (2019*b*); Li *et al.* (2018*c*); Tripathi & Sarkar (2015); Li *et al.* (2016*b*); Wang *et al.* (2018*b*)
	Glucose functionalised Au NP conjugated			*Triticum aestivum*	Swift *et al.* (2021)
		Sensing (chemical)	Carbendazim (fungicide)		Yang *et al.* (2018*a*)
			DNP and 4,8-DiMeIQx (industrial chemicals)		Cayuela *et al.* (2013)
			Enrofloxacin (antibacterial agent)		Guo *et al.* (2019)
	Antibody conjugated		Glyphosate (herbicide)		Wang *et al.* (2016)
			Hydrazine (industrial chemical)		Sha *et al.* (2018)
	Silver NP conjugated		Phoxim (insecticide)		Zheng *et al.* (2018)
			p-Nitrophenol (p-NP) (industrial chemical)		Zhang *et al.* (2019)
			Pyridine (industrial chemical)		Campos *et al.* (2015)
	Ovalbumin (OVA) conjugated, in complex with antibody-conjugated silver NP		Zearalenone (mycotoxin)		Li *et al.* (2018*b*)
		Sensing (ionic)	Cr(VI)		Vaz *et al.* (2017)
			Cu^{2+}		Li *et al.* (2020*a*)
			Fe^{2+}, Fe^{3+}, Co^{2+}, Ni^{2+}, Cu^{2+}, Zn^{2+}, Cd^{2+}, Hg^{2+}, Pb^{2+}, Ag^{+}, Cr^{3+}, Ce^{3+}, and Eu^{3+}		Pan *et al.* (2015)
			Fe^{3+}		Shi *et al.* (2016)
			Hg^{2+}		Lu *et al.* (2012)
			I^{-}		Du *et al.* (2013)
			Pb^{2+}		Xu *et al.* (2018)
					Plácido *et al.* (2019)

Table 1. *(Cont.)*

Type	Modification	Application	Target(s) if applicable	Organism(s)	Reference
			Pb^{2+},$Cu^{2+}$$Cd^{2+}$ and Ni^{2+}		Gao *et al.* (2018)
			Pt^{2+}, Au^{3+}, and Pd^{2+}		Zhang *et al.* (2019*a*)
		Sensing (pH)			Lin *et al.* (2017)
	Carboxyl capped, indole propionic acid conjugated	Sensing (plant molecular)	Indole propionic acid receptor	*Vigna radiata*	
	Polyacrylic acid or polyethylenimine coated	Translocation (plant)		*Cucurbita* sp.	Qian *et al.* (2018)
				Zea mays	Chen *et al.* (2016*a*)
				Dianthus cariophyllus	Han *et al.* (2017)
CdS	L-cysteine or thioglycerol capped	Sensing (ionic)	zinc (II), copper (II)		Chen & Rosenzweig (2002)
	Thiolated oligonucleotide conjugated	Sensing (molecular)	Nucleic acid		Willner *et al.* (2001)
		Sensing (molecular), Photocatalysis	Formaldehyde		Vastarella & Nicastri (2005)
					Curri *et al.* (2002)
CdS/ZnS	Trichloropyridinol (TCP) antibody conjugated	Sensing (chemical)	TCP, metabolite of chlorpyrifos (CPF) (pesticide)		Zou *et al.* (2010)
CdSe	Oleic acid coated or mercaptopropionic acid (MPA) coated	Translocation (plant)		*Oryza sativa*	Nair *et al.* (2011)
		Trophic transfer		*Shewanella onedensis*, *Caenorhabditis elegans*	Tian *et al.* (2017)
				Pseudomonas aeruginosa, *Tetrahymena thermophila*	Werlin *et al.* (2011)
CdSe/CdS	Silica encapsulated, trimethoxysilylpropyl urea and acetate coated or streptavidin biotin conjugated	Cell imaging (animal)		*Mus musculus*	Bruchez *et al.* (1998)
CdSe/CdS/Cd0.5Zn0.5S/ZnS	Hydrosulfide-3-acetyl-deoxynivalenol and bovine serum albumin (BSA)-conjugated conjugated	Sensing (chemical)	Deoxynivalenol (mycotoxin)	*Fusarium* sp., *Zea mays*	Zhang *et al.* (2018*b*)
CdSe/CdZnS	Polyethylenimine (PEI) or poly(ethylene glycol) or anionic poly(acrylic acid) (PAA-EG)	Translocation (plant)		*Populus deltoides* × *nigra*	Wang *et al.* (2014)
	Carboxyl capped	Trophic transfer		*Arabidopsis thaliana*, *Trichoplusia ni*	Koo *et al.* (2015)
CdSe/ZnS	Topo capped, polymer coated, DNA conjugated	Genetics (animal)	Ribosomal protein 49 (*Rp49*), Actin 5C (*Act5C*), dorsal-related immunity factor (*Dif*) and diptericin (*Dpt*)	*Drosophila*	Choi *et al.* (2009*b*)
	Mercaptoacetic acid (MAA) coated, DNA labelled	Genetics (plant)	Chromosomes	*Zea mays*	Ma *et al.* (2008)
	Polymer coated, carboxyl capped, luciferase conjugated	Imaging (animal)		*Mus musculus*	So *et al.* (2006)
	Carboxyl capped, antibody conjugated	Sensing (chemical)	Benzothiostrobin (Fungicide)	*Fragaria* sp.	Wu *et al.* (2019)

(Continues)

Table 1. *(Cont.)*

Type	Modification	Application	Target(s) if applicable	Organism(s)	Reference
	Dihydrolipoic acid (DHLA) capped, antibody fragment conjugated		2,4,6-trinitrotoluene (TNT)		Goldman *et al.* (2005)
	Dihydrolipoic acid (DHLA) capped, specific antibody conjugated		Cholera toxin, ricin, shiga-like toxin 1, and staphylococcal enterotoxin B		Goldman *et al.* (2004)
	Trioctylphosphine or trioctylphosphine oxide TOP/TOPO coated		Diquat (herbicide)	*Avena sativa*	Carrillo-Carrión *et al.* (2011)
	Carboxyl capped, antibody conjugated		Neonicotinoids (imidacloprid, imidaclothiz, and clothianidin) (insecticides)		Wang *et al.* (2017)
	Streptavidin conjugated	Tracking (animal cellular)		*Danio rerio*	Rieger *et al.* (2005)
	Carboxyl capped, poly-L-lysine conjugated	Tracking (animal individual)		*Daphnia magna*, *Daphnia pulex*, ostracods, *Chaoborus* sp., *Cloeon* sp.	Ekvall *et al.* (2013); Hylander *et al.* (2014); Heuschele *et al.* (2017); Langer *et al.* (2019); Ekvall *et al.* (2020)
	Dihydrolipoic acid (DHLA)-capped	Tracking (molecular)	Cyclin E (protein)	*Xenopus laevis*	Brandt *et al.* (2015)
	Carboxyl capped, melatonin/seratonin conjugated	Tracking (plant molecular)	Melatonin and seratonin	*Hypericum perforatum*	Erland *et al.* (2019)
	Silica encapsulated, antibody conjugated	Tracking (plant organelle)	Microtubules	*Nicotiana tabacum*	Eggenberger *et al.* (2007)
	Caboxyl capped	Translocation (plant)		*Arabidopsis thaliana*	Navarro *et al.* (2012)
	Carboxyl capped	Trophic transfer		*Caenorhabditis elegans*, *Escherichia coli*	Kim *et al.* (2016)
	Poly(acrylic acid)-octylamine copolymer (PAA) coated			*Danio rerio*, *Artemia franciscana* sp.	Lewinski *et al.* (2011)
	Carboxyl capped			*Pseudokirchneriella subcapitata*, *Ceriodaphnia dubia*	Bouldin *et al.* (2008)
	Carboxyl capped			*Leptocheirus plumulosus*, *Isochrysis galbana*	Jackson *et al.* (2012)
	Antigen conjugated	Sensing (chemical)	Deoxynivalenol (DON), ZEN, AfB1, T2-toxin (T2) and fumonisin B1 (FB1) (mycotoxins)		Beloglazova *et al.* (2014)
	Antibiotic antibody conjugated		Chloramphenicol (CAP), streptomycin (STM) and the fluoroquinolone compound, ofloxacin (OFL) (antibiotics)		Taranova *et al.* (2015)
	MPA capped, antibody labelled		Zearalenone (mycotoxin)		Beloglazova *et al.* (2012)
	Renilla luciferase (BRET) and nona-arginine R9 peptide conjugated,	Tracking (animal cellular)	Gametes	*Sus scrofa domesticus*	Feugang *et al.* (2015)

Table 1. *(Cont.)*

Type	Modification	Application	Target(s) if applicable	Organism(s)	Reference
	plasminogen antibody functionalized				
	Carboxyl capped, glutathione conjugated	Tracking (fungal individual)		*Saccharomyces cerevisiae*	Gustafsson *et al.* (2014)
	Carboxyl capped, mercaptoacetic acid coated, amino acid bound	Tracking (plant molecular)	Gamma-aminobutyric acid (GABA) binding sites	*Nicotiana tabacum*	Yu *et al.* (2006)
	Carboxyl capped, protein conjugated	Tracking (plant molecular)	Stigma/stylar cysteine-rich adhesin (SCA)	*Lilium longiflorum*	Ravindran *et al.* (2005)
	Carboxyl capped, hydroxyapatite conjugated	Tracking (plant/fungal molecular)	Hydroxyapatite	*Daucus carota*, *Medicago truncatula*, *Rhizophagus irregularis*	Whiteside *et al.* (2019)
	Carboxyl capped, polymer layered	Trophic transfer		*Astasia longa*, *Danio rerio*, *Moina macrocopa*	Lee & An (2015)
	Carboxylated and biotinylated			*Escherichia coli*, *Tetrahymena pyriformis*, *Brachionus calyciflorus*	Holbrook *et al.* (2008)
	Glycine-, mercaptosuccinic acid-, cysteine- and cysteamine-conjugated			*Lolium perenne*, *Allium cepa*, *Ctenopseustis herana*	Al-Salim *et al.* (2011)
	Carboxyl capped, polymer layered			*Saccharomyces cerevisiae*, *Folsomia candida*, *Armadillidium vulgare*	Chae *et al.* (2016)
	N-acetyl-L-cysteine capped	Sensing (chemical)	Gallic acid		Tan *et al.* (2020)
	Ni^{2+} – modulated homocysteine-capped		Histidine		Wu & Yan (2010)
	Polymer coated, carboxyl capped, amino acid conjugated	Tracking (plant/fungal molecular)	Amino acids	*Poa annua*, *Penicillium solitum*, *Sorghum bicolor*, *Glomus intraradices*, *Glomus etunicatum*, *Glomus mosseae*, *Glomus aggregatum*, unidentified mycorrhizal fungi	Hynson *et al.* (2015); Whiteside *et al.* (2009, 2012*a*,*b*)
CdSeS/ZnS	Carboxyl capped, apatite conjugated	Tracking (plant/fungal molecular)		*Daucus carota*, *Rhizophagus irregularis*, *Mediago truncatula*	van't Padje *et al.* (2020*a*, *b*, 2021)
CdTe	Cysteamine (CA)-capped	Sensing (ionic)	Hg^{2+}		Ding *et al.* (2015)
	TGA capped, antibody conjugated	Sensing (pathogen)		*Citrus tristeza*, *Citrus* sp.	Shojaei *et al.* (2016)
	Antibody conjugated			*Polymyxa betae*, *Beta vulgaris*, *Hordeum vulgare*	Safarpour *et al.* (2012)
	DNA aptamer conjugated	Sensing (plant molecular)	Systemin (plant peptide hormone)	*Lycopersicon esculentum*	Liu *et al.* (2015)
	Dodecapeptide conjugated	Tracking (plant cellular)	Stem cells	*Arabidopsis thaliana*	Yu *et al.* (2014)
		Trophic transfer		*Escherichia coli*, *Paramecium caudatum*	Gupta *et al.* (2017)
	Glutathione capped	Sensing (ionic)	Fe^{2+} and Fe^{3+}		Wu *et al.* (2009)
CdTe/CdS		Tracking (animal)		*Tribolium castaneum*, *Bactrocera tryoni*, *Plutella xylostella*	Gurdasani *et al.* (2021)
CuInSexS2 – x/ZnS	Zinc oleate ligand coated	Tracking (plant tissue)	Pollen	*Lapeirousia anceps*, *Moegistorhynchus*	

(Continues)

Table 1. *(Cont.)*

Type	Modification	Application	Target(s) if applicable	Organism(s)	Reference
				longirostris Wachendorfia paniculata, *Sparaxis villosa*, *Arctotheca calendula*, *Oxalis purpurea*, *Apis mellifera capensis*	Minnaar *et al.* (2019); Minnaar & Anderson (2019)
Graphene quantum dots (GQDs)	Nanosheet connected	Sensing (chemical)	Methanol, ethanol and propanol		Parvizi *et al.* (2019)
	Nitrocellulose embedded		Quercetin, 4-nitrophenol and paraoxon		Álvarez-Diduk *et al.* (2017)
	Complex with g-C_3N_4, and a biotin-labelled aptamer		Zeatin (Cytokinin)		Wang *et al.* (2018)
			Tetracycline (antibiotic)		Zhang *et al.* (2020)
		Sensing (ionic)	Al^{3+}		Fan *et al.* (2014)
			Cd^{2+}		Li *et al.* (2012)
			Co^{2+}		Chen *et al.* (2016)
			Cr(VI)		Sheng *et al.* (2020)
			Fe^{3+}, $Cu^{2+}$and Ag^{+}		Shen *et al.* (2017)
			Hg^{2+}		Shi *et al.* (2015)
			Ni^{2+}		Huang *et al.* (2013*a*)
			Pb^{2+}		Bian *et al.* (2016)
		Sensing (pH)			Zhang *et al.* (2019*a*)
InP/ZnS	N-terminus immobilized, Hsp 90α functionalized	Tracking (plant molecular)	Heat shock protein 90 (Hsp 90) inhibitors	*Curcuma longa*	Hu *et al.* (2018)
		Translocation (animal)		*Hydra vulgaris*	Veronesi *et al.* (2019)
Nanodiamonds (NDs)	Dextran- or bovine serum albumin (BSA) coated	Imaging (animal)		*Caenorhabditis elegans*	Mohan *et al.* (2010)
Carbonised polymer dots (CPDs)		Sensing (ionic)	Cr(VI)		Zare-Moghadam *et al.* (2020)
	Carboxyl capped		Pb^{2+}		He *et al.* (2020)
		Sensing (molecular)	Cytochrome C		Shamsipur *et al.* (2019)
	Carboxyl capped, in conjuction with a DNA walker		MicroRNA (miRNA)		Luo *et al.* (2019)
			Glutathione, ascorbic acid, N-acetyl-L-cysteine, superoxide dismutase and catalase		Zhao *et al.* (2020)
	Congo Red and mitochondria-targeting group triphenylphosphonium (TPP) conjugated	Sensing (pH)	Mitochondria		Sun, Ling & Gao (2017)
Quantum dots (QDs) of unidentified composition	Streptavidin conjugated to biotin	Genetics (plant)	Chromosomes	*Allium fistulosum*	Müller *et al.* (2006)
	Streptavidin conjugated to oligonucleotide DNA		miRNA	*Oryza sativa indica*	Liang *et al.* (2005)
	Streptavidin conjugated, conjugater to antigen/ amplicon or biotin-BSA	Sensing (bacteria)		*Staphylococcus aureus*	Chen *et al.* (2014*a*)
Silicon-cored quantum dots (SiQDs)		Imaging (animal)		*Danio rerio*	D'Amora *et al.* (2019)
		Plant growth enhancement		*Cucumis sativus*	Li *et al.* (2019*c*)

Table 1. *(Cont.)*

Type	Modification	Application	Target(s) if applicable	Organism(s)	Reference
	In solution with acetylcholinesterase (AChE) and choline oxidase (ChOx)	Sensing (chemical)	Carbaryl, parathion, diazinon, and phorate (pesticides)		Yi *et al.* (2013)
		Sensing (ionic)	Cu^{2+}		Zhao *et al.* (2014)
			Fe^{3+}		Linehan *et al.* (2019)
	Mercaptosilane-coated, transferrin (Tf)-protein conjugated	Tracking (molecular)	Tf receptor		Nishimura *et al.* (2013)
SnS_2		Sensing (ionic)	Fe^{3+}		Srivastava *et al.* (2020)
Upconversion nanoparticles (UCNPs), NaLuF4: Yb^{3+},Er^{3+}/ Tm^{3+}	Oleic-acid functionalized, PEG coated, dye conjugated	Imaging (animal)		Medusozoa	Chen *et al.* (2015*b*)
UCNP, Y_2O_3: Er^{+3} Yb^{+3}				*Solenopsis xyloni*	Alkahtani *et al.* (2017)
UCNP, NaYF4: Yb, Er	Oleic acid-capped, aptamer and magnetic nanoparticle conjugated	Sensing (chemical)	Chloramphenicol (antibiotic)		Wu *et al.* (2015)
UCNP, NaGdF4: Yb^{3+},	Er^{3+}@NaYF4	Oleic acid and PEG coated, dye conjugated	Sensing (chemical)	Nitrates	
Hu *et al.* (2019)					
UCNP, NaYF4:Yb, Tm@NaYF4	DNAzyme conjugated	Sensing (ionic)	Zn^{2+}	*Danio rerio*	Yang *et al.* (2018*b*)
UCNP, NaYF4: Yb^{3+},Er^{3+}	Silica coated, carboxyl capped	Translocation		*Raphanus sativus*, *Lemna minor*	Modlitbová *et al.* (2019)
UCNP, NaYF4: Yb,Er	L- hydroxyethane-1,1-diphosphonic acid (HEDP) functionalized	Translocation		*Arabidopsis thaliana*, *Phalaenopsis* sp.	Hischemöller *et al.* (2009)
UCNP, NaYF4: Yb,Er	L- hydroxyethane-1,1-diphosphonic acid (HEDP) functionalized	Translocation		*Cucurbita maxima*	Nordmann *et al.* (2015)
UCNP, NaYF4	Citric-acid coated	Translocation		*Vigna radiata*	Peng *et al.* (2012)
ZnCdSe/ZnS	Carboxyl capped, PEGylated, antibody conjugated	Sensing (chemical)	Acetamiprid (insecticide)		Liu *et al.* (2019)
ZnS	Glutathione capped	Imaging (fungal cellular)		*Rhizopus oryzae*	Desai *et al.* (2019)
	Mercaptophenylboronic acid capped	Sensing (chemical)	Transferrin		Chang *et al.* (2017)
	(3-aminopropyl) triethoxysilane and an As(III) ionic imprinted polymer coated	Sensing (ionic)	As(III) and As(V)		Jinadasa *et al.* (2020)
	Glutathione capped		Cu^{2+} and Hg^{2+}		Desai *et al.* (2019)
	Cetyltrimethylammonium bromide-capped, aptamer labelled		Hg^{2+}		Xie *et al.* (2012)
	Glutathione capped		Pb^{2+}		Chen *et al.* (2016*b*)

biomagnified in a food chain between *E. coli* and the ciliate *Paramecium caudatum* (Gupta *et al.*, 2017). However, both experiments were restricted to a single day and thus did not assess long-term biomagnification or bioaccumulation potential. Transfer of CdSe/ZnS and CdSe QDs from bacteria to the flatworm *Caenorhabditis elegans* upon feeding revealed no toxicity (Kim, Kwak & An, 2016; Tian *et al.*, 2017), but the dots were metabolised into SeO and Na_2SeO_3 in the flatworm gut (Tian *et al.*, 2017). Similarly, a study comparing the uptake of CdSe/ZnS QDs from the water column and through consumption of QD-incubated algae (*Isochrysis galbana*) by the amphipod *Leptocheirus plumulosus* showed that the QDs taken up from the water column were intact, while QDs obtained through algal feeding were biotransformed into toxic compounds (Jackson *et al.*, 2012). Trophic transfer of CdSe/ZnS QDs has also been demonstrated in a protozoa–zooplankton–fish food web, with no adverse effects or biomagnification (Lee & An, 2015).

In terrestrial food chains, self-synthesised CdSe/CdZnS QDs with three different coatings [anionic PAA-ethylene glycol (EG), cationic PEI, and near-neutral poly(maleic anhydride-alt-1-octadecene) (PMAO) – PEG] moved to the roots and leaves of hydroponically grown thale cress (*Arabidopsis thaliana*) and subsequently to the herbivorous insect *Trichoplusia ni* (Koo *et al.*, 2015). Among FNP types, QDs with an anionic coating exhibited the greatest stability and transfer to roots and leaves, whereas QDs with cationic and neutral coatings were more prone to aggregation, and cationic QDs leached Cd. Insects feeding on QD-treated plants fluoresced and exhibited reduced fitness. CdSe/ZnS QD transfer has also been demonstrated in a yeast–insect–insect food web with no adverse effects or bioaccumulation (Chae, Kim & An, 2016). Finally, to reach a broader understanding of QD fate in terrestrial ecosystems, CdSe/ZnS QDs with four different conjugates (glycine, mercaptosuccinic acid, cysteine and cysteamine) were tracked from the water column into ryegrass (*Lolium perenne*), onion (*Allium cepa*), chrysanthemum (*Chrysanthemum* sp.) and thale cress plants, and from larvae to adults in brownheaded leafrollers (*Ctenopseustis herana*). Limited uptake of QDs from the water column was observed in cut stems, whereas rooted plants did not take up QDs. Leafroller larvae fed with QD materials accumulated QDs in their haemolymph, whereas some fluorescence and elevated Cd concentrations occurred in adult moths (Al-Salim *et al.*, 2011).

Although food-web studies have focused on toxicity assessment, they indicate trophic transfer of QD particles, which shows great potential for tracking applications in multi-organism systems. Biomagnification and adverse effects were problematic in unshelled QDs but not in shelled QDs. Thus, food sources labelled with shelled QDs could be utilised to discover nutritional preferences and prey–predator dynamics.

(*b*) Plants

Cadmium-containing QDs have been widely used in plant molecular research to document various physiological processes since the emergence of the first tracking applications in the mid-2000s. Tracking of the plant adhesion protein stigma/stylar cysteine-rich adhesin (SCA) in lily (*Lilium longiflorum*) pistils by SCA conjugated carboxyl-capped CdSe/ZnS QDs indicated that this protein is likely taken into plant pollen tubes through endocytosis at the tip of the tube (Ravindran *et al.*, 2005). Carboxyl-capped CdSe/ZnS QDs bound to the amino group in γ-aminobutyric acid (GABA) in tobacco (*Nicotiana tabacum*) pollen revealed a fluorescent circle around the protoplast only with conjugated QDs, implying that GABA receptors are located in the plant cellular membrane (Yu *et al.*, 2006). Since these pioneering experiments, QDs have been successfully utilised to determine binding sites for many other plant chemicals, such as jasmonic acid, calmodulin and salicylic acid (reviewed by Pang & Gong, 2019). QDs also found their way to cellular-level tracking. For example, CdSe/ZnS/SiO_2 QDs were successfully used to visualise cell division in tobacco plants by covalently linking these to antitubulin antibodies (Eggenberger *et al.*, 2007). Similarly, thioglycolic acid (TGA)-capped CdTe QDs conjugated to the stem cell-associated peptide CLAVATA3 were demonstrated to be useful for tracking the fate of thale cress root meristem cells during plant development (Yu *et al.*, 2014). More recently, a study utilised carboxyl-capped CdSe/ZnS QDs conjugated to melatonin and serotonin to study plant uptake and localisation of these compounds in St John's wort (*Hypericum perforatum*) under thermal stress (Erland *et al.*, 2019). The hormone–QD conjugates were taken up by cultured roots with differing localisation patterns, which were disrupted upon exposure to heat stress.

Plant uptake of QDs varies greatly among studies. Water-soluble mercaptopropionic acid (MPA)-capped CdSe QDs were taken up by roots of rice (*Oryza sativa*) (Nair *et al.*, 2011). Uptake and translocation of CdSe/CdZnS QDs with a cationic (PAA-EG) coating was 10-fold faster than with an anionic (PEI) coating in hybrid poplar (*Populus deltoides* × *nigra*) cuttings, but translocation to shoots was negligible in both cases (Wang *et al.*, 2014). Similarly, root uptake of QDs with cationic coatings was higher than for QDs with anionic coatings in thale cress but a substantial translocation to leaves occurred in this experiment (Koo *et al.*, 2015). Conversely, QDs remain adsorbed onto root surfaces in some studies, for example carboxyl-capped CdSe/ZnS QDs in thale cress (Navarro, Bisson & Aga, 2012) and MPA-capped CdTe, CdTe/ZnS, and CdTe/CdS/ZnS QDs in common onion (Modlitbová *et al.*, 2018*b*).

Commercial streptavidin-conjugated QDs have been utilised in plant genetics. For example, Liang *et al.* (2005) developed a tool for profiling expression of 11 rice miRNAs involving a microarray of oligonucleotide probes, biotin-conjugated miRNAs and streptavidin-conjugated QDs. The microarray with bound miRNAs was incubated with QDs, which revealed the relative proportions of the 11 miRNAs in samples based on differences in fluorescent intensities of the probes. Biotin-labelled QD-streptavidin conjugates also allowed specific *in situ* observation of hybridisation in

Welsh onion (*Allium fistulosum*) *via* the attachment of labelled QDs to plant chromosomes, but the method was less sensitive than labelling with a fluorescent dye (Müller *et al.*, 2006). However, oligonucleotide-conjugated, mercaptoacetic acid (MAA)-capped CdSe/ZnS QDs outperformed traditional fluorescent dyes in maize (*Zea mays*) (Ma *et al.*, 2008).

In summary, plant physiological research has greatly benefitted from QDs for tracking biomolecules, determining binding sites as well as monitoring development and cellular processes such as hybridisation and cell division. Experiments have revealed inconsistent uptake of QDs, suggesting the need for specific studies. Nonetheless, the described research efforts provide a firm foundation for exploring various plant molecular and physiological processes with QDs.

(*c*) Animals

A few studies have utilised QDs in zoological research. Streptavidin-conjugated CdSe/ZnS QDs injected into a zebrafish blastomere at the two-cell stage were transferred from mother to daughter cells through cell division *via* cytoplasmic bridges and exhibited bright fluorescence even in late developmental stages such as organogenesis (Rieger *et al.*, 2005). A CdSe/ZnS QD complex involving a fluorescent dye, a cell-penetrating peptide and an antibody related to fertilisation regulation was utilised for tracking the movement of domestic pig (*Sus scrofa domesticus*) spermatozoa in female reproductive tracts (Feugang *et al.*, 2015). The QD complexes specifically attached to male gametes, indicating that plasminogen is present in sperm cells. Since the complex did not hinder the movement of spermatozoa, it could be used for *in vivo* tracking of fertilisation success. This application also demonstrates the usefulness of QD technologies for deep tissue imaging of large animals, which is challenging with more traditional methods that are less specific and bright (Feugang *et al.*, 2015). CdSe/ZnS QDs capped with dihydrolipoic acid (DHLA) were used to track a protein that regulates the cell cycle in African clawed frog (*Xenopus laevis*) embryos in vivo (Brandt *et al.*, 2015). Additionally, gene expression in fruit fly (*Drosophila* sp.) cells was determined by MAA-capped, polymer-coated CdSe/ZnS QDs of three different emission colours, which were connected to DNA oligonucleotides specific for various mRNA molecules present in the cells. The mRNAs selected as targets were present in large (housekeeping gene mRNAs *Rp49* and *Act5C*) or small concentrations (mRNAs of the immunity-related *Dif* gene) or their expression could be quantitatively induced (*Dpt* mRNA transcribed upon bacterial infection). The results revealed that the QD probes were specific, sensitive and could provide quantitative information about the amounts of mRNAs inside cells (Choi *et al.*, 2009*b*).

In environmental settings, positively charged, carboxyl-capped, poly-L-lysine-conjugated CdSe/ZnS QDs were successfully implemented to track the movement of water flea (*Daphnia magna*) individuals using video cameras equipped with ultraviolet (UV) filters (Ekvall *et al.*, 2013). Labelling the water fleas with QDs allowed behavioural observations of water flea individuals including the distance and speed of their movement in response to UV light. Based on differently coloured QDs, the cameras were able to distinguish eight labelled individuals (Ekvall *et al.*, 2013). The same experimental procedure was subsequently used to study how genetically and ontogenically different water flea individuals respond to multiple UV-light exposures (Hylander *et al.*, 2014, Heuschele *et al.*, 2017), predation in three-species networks (Langer *et al.*, 2019) and to these stressors combined (Ekvall *et al.*, 2020). These studies indicate that the reaction of water fleas to UV light depends on their age, size and capacity to develop tolerance to it (Hylander *et al.*, 2014, Heuschele *et al.*, 2017). Furthermore, water fleas adjust their swimming speed, depth and distance to other individuals in response to predation (Langer *et al.*, 2019) and respond adequately to the greatest risks (Ekvall *et al.*, 2020).

QD-tagging of flying insects was also examined recently, in a study in which CdTe/CdS QDs were used to tag the red flour beetle (*Tribolium castaneum*) (Gurdasani *et al.*, 2021). As the QDs had no surface ligands to help them bind chemically to the insects, they were poorly retained on individuals that were in contact with abrasive surfaces, but the authors did manage to QD-tag and release nearly 7000 insects in 3 days, and to establish that the QDs were non-toxic and did not hinder flight (Gurdasani *et al.*, 2021). This indicates that QDs with proper surface modifications could provide a novel solution for efficient tagging of substantial numbers of flying insects, including important pest species.

Taken together, QDs have been applied to zoological research spanning from molecules to individuals. Although strictly biological applications are still relatively uncommon, the research shows that QDs can be utilised to further our understanding of animal physiology, behaviour and ecology.

(*d*) Fungi

In a pioneer study, the uptake and translocation of glycine and arginine labelled with carboxyl-capped CdSe/ZnS QDs was followed from arbuscular mycorrhizal fungi to roots and leaves of annual meadowgrass (*Poa annua*) (Whiteside, Treseder & Atsatt, 2009). In a follow-up experiment using the same type of QDs conjugated to 20 different amino acids, eight of the amino acids were taken up more by mycorrhizal plants than by uncolonised plants (Whiteside, Garcia & Treseder, 2012*b*). Furthermore, a similar study revealed that fungi in N-fertilised soil prefer glycine to chitosan, while fungi in unfertilised soil show no preference (Whiteside *et al.*, 2012*a*; Hynson, Allison & Treseder, 2015). To study nutrient allocation dynamics within a mycorrhizal network, carboxyl-capped CdSeS/ZnS QDs fluorescing in two colours were conjugated to hydroxyapatite – a form of rock phosphate. Using both confocal microscopy and fluorescence analysis *via* a microplate reader, it was demonstrated that fungal networks capitalise on trade with host plants by first moving the QD-tagged hydroxyapatite to areas of high plant demand (Whiteside *et al.*, 2019). QD-tagged hydroxyapatite was then used to show how the nutritional status of

host roots affects P allocation patterns of the fungus (van't Padje *et al.*, 2020*a*). Using an experimental arrangement of two *in-vitro* roots connected by a single fungal network, the researchers tracked QD-tagged hydroxyapatite of three colours to show how host demand influenced both allocation patterns to roots over time and storage patterns in the fungus itself. In a second experiment with single root systems, the researchers injected this compound into different locations across the fungal network and found that the fungus was able to control the location, time and amount of P transfer to the host (van't Padje, Werner & Kiers, 2020*b*). Finally, QD-tagged apatite revealed that mycorrhizal symbiosis did not enhance plant P accumulation of heat stressed or waterlogged barrel clover (*Mediago truncatula*), but the plants took up 80% less P post-treatment than before treatment, indicating potential P saturation prior to exposure to the abiotic stresses (van't Padje *et al.*, 2021).

Research on baker's yeast (*Saccharomyces cerevisiae*) revealed that amino-terminated CdSeS/ZnS QDs conjugated to glutathione could be used for labelling two different yeast strains in mixed cultures (Gustafsson *et al.*, 2014). The QDs introduced to cultures with known proportions of the two strains were readily taken up by yeast cells and transferred from mother cells to daughter cells, enabling the separation of stains even after a complete fermentation cycle of approximately 120 h. Furthermore, there was significantly less variation between replicates in the ratios of stains observed *via* the QD method compared with microsatellite DNA analysis, indicating good quantitative performance (Gustafsson *et al.*, 2014).

(*e*) Biosensing

QD-based biosensing applications emerged in the early 2000s. The first products were a semi-quantitative DNA sensor with oligonucleotide-conjugated CdS QDs (Willner, Patolsky & Wasserman, 2001) and a sensor for Zn^{2+} and Cu^{2+} ions based on CdS QDs conjugated with thioglycerol and L-cysteine [limit of detection (LOD), 0.8 and 0.1 μM, respectively; Chen & Rosenzweig, 2002]. Two formaldehyde sensors based on CdS QDs were elaborated soon thereafter (Curri *et al.*, 2002; Vastarella & Nicastri, 2005). Multiple chemical sensors were developed for mostly medical applications (Zhang *et al.*, 2017), such as a CdTe QD sensor capped with Ni modified homocysteine for detecting histidine in urine samples (LOD 0.3 μM; Wu & Yan, 2010). A more complex example is Föster resonance energy transfer (FRET) sensors, which have been used for the detection of the explosive 2,4,6-trinitrotoluene (TNT) in soil (Goldman *et al.*, 2005) and for determining the proteolytic activity of four proteases (Medintz *et al.*, 2006). These sensors are based on the energy transfer between DHLA-capped CdSe/ZnS QDs and fluorescent dye complexes that interact with the sensing target. The TNT sensor reached a limit of detection of 20 μg/l (Goldman *et al.*, 2005) while the protease activity sensor achieved similar measures of rate and speed of the enzymatic reactions as the traditionally used Michaelis–Menten kinetics analysis (Medintz *et al.*, 2006). In addition, researchers have developed sensors for various metal ions, e.g. a glutathione-capped CdTe QD sensor for Fe^{2+} (LOD 5.00×10^{-3} μM; Wu, Li & Yan, 2009) and a cysteamine-capped CdTe QDs sensor for Hg^{+} (LOD 4.00×10^{-3} μM; Ding *et al.*, 2015). Similarly, CdSe/ZnS QD sensors conjugated to dopamine and to a dopamine-peptide were prepared for observing redox states in different positions of cells and for sensing cytoplasmic pH (7–11.5), respectively (Clarke *et al.*, 2006; Medintz *et al.*, 2010).

In recent years, much research has focused on QD applications in food safety and agriculture, particularly the detection of pathogens and toxins (Chern *et al.*, 2019). In a pioneering study, Goldman *et al.* (2004) developed specific antigen-conjugated CdSe/ZnS QDs for simultaneous detection of four toxins – cholera toxin, ricin, shiga-like toxin 1 and staphylococcal enterotoxin B – with LODs of 10, 30, 300 and 3 μg/l, respectively. Subsequently, a QD probe was used to detect the mycotoxins deoxynivalenol, zearalenone, aflatoxin B1, T2-toxin and fumonisin B1 simultaneously (LOD 3.2×10^{-3} μg/mg, 6×10^{-4} μg/mg, 2×10^{-4} μg/mg, 0.001 μg/mg and 0.0004 μg/mg, respectively; Beloglazova *et al.*, 2014). A more complicated sensor based on hydrosulfide-3-acetyl-deoxynivalenol and bovine serum albumin (BSA)-conjugated CdSe/CdS/Cd0.5Zn0.5S/ZnS QDs has since brought the detection limit for deoxynivalenol down to $\mathbf{1.22} \times 10^{-5}$ μg/mg (Zhang *et al.*, 2018*b*). A similarly complex sensor of the plasmodiophoromycete *Polymyxa betae*, a known carrier of beet necrotic yellow vein virus, was developed from CdTe QDs conjugated to specific antibodies together with a rhodamine antigen solution and a buffer solution, which displayed a change in absorbance in the presence of the virus (LOD 500 μg/l; Safarpour *et al.*, 2012). Likewise, a sensor based on the reaction between antibody-conjugated CdTe QDs and carbon nanoparticle-conjugated antigens could be used to detect citrus tristeza virus (LOD 220 μg/l; Shojaei *et al.*, 2016). In addition, several sensors have been developed for food science applications. For example, a sensor for detecting *Staphylococcus aureus* with a test strip involving streptavidin-capped, biotin-conjugated QDs (LOD 3 colony forming units (CFU)/ml or 30 CFU/g in milk powder and meat, respectively; Chen *et al.*, 2014*a*), and another for simultaneous detection of the antibiotics ofloxacin, chloramphenicol and streptomycin in milk with antibody conjugated CdSe/ZnS QDs (LOD 0.3, 0.12, and 0.2 μg/l; Taranova *et al.*, 2015) have been reported. Sensing of the antioxidant gallic acid in tea was achieved with N-acetyl-L-cysteine-capped CdTe QDs (LOD 0.56 μg/l; Tan, Li & Yang, 2020). Finally, QD sensors have been developed for pesticides and their derivatives, including trichloropyridinol (LOD 1.0 μg/l; Zou *et al.*, 2010), paraoxon and parathion (LOD $\mathbf{1.05} \times 10^{-5}$ μM and 4.47×10^{-6} μM, respectively; Zheng *et al.*, 2011), diquat (LOD 1×10^{-5} μg/mg; Carrillo-Carrión, Simonet & Valcárcel, 2011), imidacloprid, imidaclothiz and clothianidin (LOD 0.5, 0.5 and 1 μg/l, respectively; Wang *et al.*, 2017), acetamiprid (LOD 1 μg/l; Y. Liu *et al.*, 2019) and benzothiostrobin (LOD 25 μg/l; Wu

et al., 2019). Cd-QDs have also been used for sensing plant hormones. For example, a sensor for tomato systemin was developed based on aptamer-conjugated CdTe QDs doped with Zn^{2+} and graphene oxide (LOD 0.1 μM). Without systemin, the QDs were bound to graphene oxide, exhibiting no fluorescence, while systemin-bound QDs did not bind to graphene oxide and thus retained their fluorescence (Liu *et al.*, 2015).

Although various molecular sensors based on QDs have been reported, most are related to commercial or medical applications. Nonetheless, these studies still provide a starting point for physiological and ecological applications by enabling the preparation and utilisation of sensors for biologically important marker molecules and metabolites.

(2) Other semiconductor QDs

Semiconductor QDs not containing Cd have received limited attention in biology, likely because of their relatively low commercial availability. However, some biological applications have been reported in recent years, especially with indium-containing particles. For example, InP/ZnS-based probes have been used for identifying heat shock protein (hsp) inhibitors in turmeric (*Curcuma longa*), by a complex of hsp-conjugated QDs embedded into another type of nanoparticle. The probe enabled detection and identification of 12 potential inhibitors of the hsp (Hu *et al.*, 2018). Minnaar & Anderson (2019) and Minnaar, de Jager & Anderson (2019) successfully utilised $CuInSe_xS_{2-x}$/ZnS (core/shell) QDs in studying the transfer of pollen in various plant species. The dots were coated with zinc oleate ligands, dissolved in hexane and pipetted onto plant anthers. This method revealed that pollen of the plant *Lapeirousia anceps* accumulates in different parts of its pollinator (*Moegistorhnychus longirostris*) depending on the length of the floral tube, indicating a potential reproductive barrier between the long-tubed and short-tubed morphotypes of the species. Finally, a study on the uptake of shelled and unshelled InP/ZnS QDs in the freshwater polyp (*Hydra vulgaris*) revealed rapid degradation of both types of FNPs inside the polyps (Veronesi *et al.*, 2019).

Semiconductor QDs, especially particles including Zn, are being increasingly applied for biosensing purposes. Zn-chalcogenide-based QDs have been utilised for mercury (LOD 1.5×10^{-3} μM; Xie *et al.*, 2012), lead (LOD 0.45 μg/l; J. Chen, Zhu & Zhang, 2016*b*), copper (LOD 3.13 μM; Desai *et al.*, 2019) and arsenic (LOD 2.96×10^{-5} μg/mg; Jinadasa *et al.*, 2020). Recently, SnS_2 QDs were used for detecting iron (LOD ∼0.84 μM; Srivastava, Singh & Srivastava, 2020). Additionally, Mn-doped, mercaptophenylboronic acid-capped ZnS QDs were utilised for detecting glycoprotein transferrin from serum *via* its enhancement of QD fluorescence (LOD 5.69×10^{-3} μM; Chang *et al.*, 2017). Glutathione-capped ZnS QDs were used to image cells of the mould *Rhizopus oryzae* (Desai *et al.*, 2019).

SiQDs have been used for tracking transferrin receptor activity in rat kidney cells by conjugating the SiQDs to transferrin. This method allowed tracking individual transferrin molecules for 10-fold longer compared with fluorescent dyes (Nishimura *et al.*, 2013). SiQDs have also been used for imaging water flea embryos, as SiQDs were localised in the gut, yolk sac and eye lenses (D'Amora *et al.*, 2019). Furthermore, SiQD sensors have been developed for copper (LOD 0.008 μM; Zhao *et al.*, 2014) and iron (LOD 1.3 μM; Linehan, Carolan & Doyle, 2019), as well as for the pesticides carbaryl, parathion, diazinon and phorate (LOD 7.25×10^{-3} μg/l, 3.25×10^{-2} μg/l, 6.76×10^{-2} μg/l and 0.19 μg/l, respectively; Yi *et al.*, 2013).

In summary, non-cadmium SQDs, while abundant and diverse, have remained underutilised and overshadowed by Cd-QDs in biological applications. Nonetheless, these can provide alternative opportunities for ecological and physiological research if explored more deeply.

(3) Fluorescent carbon nanoparticles (FCNPs)

Unlike Cd-QDs, most FCNPs lack coating or conjugation, with some exceptions. For example, cellulose-bound CQDs, prepared by mixing α-cellulose with CQD solution, were used to map plant cell wall structure. The CQDs incorporated into plant cell walls fluoresced differently within tissues of various plant species (Li *et al.*, 2017). Similarly, carboxyl-capped CQDs were used for labelling receptors of the growth hormone indole propionic acid (IPA) in mung bean (*Vigna radiata*) seedlings. Plant tissues were incubated with IPA-conjugated CQDs and examined under a fluorescence microscope, revealing that IPA receptors are located mainly in the membranes of the plant stele (Lin *et al.*, 2017). CQDs were taken up and translocated to petal border cells of cut carnation (*Dianthus* sp.) plants *via* transpiration flow. The authors also reported that CQD-incubated fluorescent flowers were more attractive to insects than non-fluorescent ones, although no methodology or experimental data on these findings were presented (Han *et al.*, 2017). Another study utilising CQDs with different coatings (none, PAA, and PEI) revealed that pumpkin (*Cucurbita pepo*) seedlings translocated all types of CQDs to roots and shoots, while the coatings affected translocation patterns: CQD-PEI occurred throughout root tissue, while the other two types were present only in root epidermis. All CQDs entered leaves, with CQD-PEI showing the strongest fluorescence (Qian *et al.*, 2018). A similar study revealed systematic translocation of uncoated CQDs throughout maize plants as well as their excretion from leaves (Chen *et al.*, 2016*a*). Recently, amine-coated CQDs without functionalisation and with glucose conjugation were shown to be taken up by wheat (*Triticum aestivum*) (Swift *et al.*, 2021). The glucose-bound CQDs improved crop yield and photosynthesis rate, while the unfunctionalised CQDs did not differ from controls.

FCNPs have also been used in imaging and visualising organisms, for example flatworm bodies (Chen *et al.*, 2014*b*; Pramanik *et al.*, 2016) as well as bacterial (*Bacillus subtilis*, *Pseudomonas aeruginosa*, *Mycobacterium tuberculosis*) and fungal (*Aspergillus aculeatus*, *Fusarium avenaceum*, *Magnaporthe oryzae*, *Penicillium* sp.) cells (Kasibabu *et al.*, 2015*a*,*b*; Mehta

et al., 2015; Ritenberg *et al.*, 2016; Bhamore *et al.*, 2018), although mostly as proof of concept to accompany a new synthesis methodology. CQD-assisted imaging was utilised to observe changes in the biofilm of *Pseudomonas aeruginosa* in response to growth inhibitors and altered temperature (Bhamore *et al.*, 2018).

Nanodiamonds introduced to flatworms *via* feeding or injection dispersed differently depending on the exposure route and enabled imaging (Mohan *et al.*, 2010). Plain NDs obtained through feeding remained in the gut and were excreted normally, while NDs conjugated to carboxymethyldextran (CMDx) and bovine serum albumin (BSA) were retained in intestinal cells for >24 h. Furthermore, NDs injected to the gonads of the worms were found to transfer to embryos and offspring (Mohan *et al.*, 2010).

Most sensing applications of FCNPs are related to determining the concentration of ions (Anas *et al.*, 2019). For example, a single type of CQD distinguished 13 metal ions at a concentration of 100 μM based on their differing emission profiles (Pan *et al.*, 2015). Various CQDs have been reported for sensing ions of mercury (LOD 2.3×10^{-3} μM; Lu *et al.*, 2012), lead (LOD $\mathbf{5.5 \times 10^{-5}}$ μM; Xu *et al.*, 2018), copper (LOD 5×10^{-5} μM; Li *et al.*, 2020*a*), iron (LOD 1.8×10^{-3} μM; Shi *et al.*, 2016), iodine (LOD 0.43 μM; Du *et al.*, 2013), nickel (LOD 0.1 μM; Plácido *et al.*, 2019), cadmium (LOD 0.012 μM; Plácido *et al.*, 2019), chromium (LOD 30 μg/l; Vaz *et al.*, 2017) as well as platinum, gold and palladium (LOD 0.886, 3.03 and 3.29 μM, respectively; Gao *et al.*, 2018). Similarly, GQD-based sensors have been developed for chromium (LOD 0.091 μM; Sheng *et al.*, 2020), lead (LOD 0.03 μM; Bian *et al.*, 2016), mercury (LOD 8.6×10^{-3} μM; Shi *et al.*, 2015), cadmium (LOD 0.013 μM; Li *et al.*, 2012), cobalt (LOD 0.2 μM; Chen *et al.*, 2016), aluminium (LOD 3.64 μM; Fan *et al.*, 2014), nickel (LOD 4.1 μM; Huang *et al.*, 2013*a*) as well as iron, copper and silver (LOD 8×10^{-3} μM, 0.25 and 0.05 μM, respectively; Shen *et al.*, 2017). In addition, CQDs have been used as bioindicators of cytoplasm pH due to a linear relationship between fluorescence intensity and pH (range 1.0–13.0; Zhang *et al.*, 2019*a*). These results indicate that FCNPs have a great potential for detecting chemical properties in cells and environmental samples as well as for locating heavy metals and microelements.

Researchers have also explored FCNPs as sensors for more complex chemicals (Asadian *et al.*, 2019). For example, CQDs were used to probe the anthropogenic pollutants 2,4-dinitrophenol (LOD 400 μg/l), 2-amino-3,4,8-trimethyl-3H- imidazo[4,5-f]quinoxaline (4,8-DiMeIQx) (LOD 1290 μg/l; Cayuela, Laura Soriano & Valcárcel, 2013) and the wastewater pollutant enrofloxacin (LOD 160 μg/l; Guo *et al.*, 2019). CQD-based probes have been developed for the hazardous chemicals p-nitrophenol (LOD 0.11 μM; Zhang *et al.*, 2019), hydrazine (LOD 39.7 μM; Sha *et al.*, 2018), pyridine (LOD 30 μM; Campos *et al.*, 2015), the mycotoxin zearelone (LOD 0.1 μg/l; Li *et al.*, 2018*b*), the herbicide glyphosate (LOD 8 μg/l; Wang *et al.*, 2016), the fungicide carbendazim (LOD 0.002 μM; Yang *et al.*, 2018*b*) and the insecticide phoxim (LOD 0.04 μM; Zheng *et al.*, 2018). Similarly, complex GQD sensors have been reported for the antioxidant quercetin as well as the pollutants 4-nitrophenol and paraoxon (LOD 23.5, 43.6 and 39.7 μM, respectively; Álvarez-Diduk, Orozco & Merkoçi, 2017), the plant cytokinin zeatin (LOD 3.1×10^{-5} μM; Wang *et al.*, 2018) and the antibiotic tetracycline (LOD 0.95 μg/l; Zhang *et al.*, 2020). A GQD-based sensor for monitoring vapours of methanol, ethanol and propanol has also been developed (LOD 4.3, 4.9 and 10.5 ppm, respectively; Parvizi *et al.*, 2019).

Carbonised polymer dots (CPDs) have been used in sensing the ions of copper (LOD 3.5×10^{-4} μM; Shamsipur *et al.*, 2019), iron (LOD 3×10^{-5} μM; Shamsipur *et al.*, 2019), lead (LOD $\mathbf{1.7 \times 10^{-7}}$ μM; He *et al.*, 2020) and chromium (LOD 0.03 μM; Zare-Moghadam *et al.*, 2020) as well as pH (range 2.57–8.96; Sun, Ling & Gao, 2017). Additionally, carboxyl-capped CPDs were used in a complex biosensor for detecting a target miRNA from an RNA mixture (LOD 1.7×10^{-10} μM; Luo *et al.*, 2019). Tributyl phosphate-doped CPDs were utilised for sensing cytochrome c (LOD 3.27×10^{-5} μM) – a molecular marker of the initial stages of cell death – and thus the onset of apoptosis (Shamsipur *et al.*, 2019). Detection of total antioxidant capacity with glutathione, ascorbic acid, N-acetyl-L-cysteine and superoxide dismutase as targets was achieved with CPDs (Zhao *et al.*, 2020).

Taken together, utilisation of FCNPs for applications spanning from imaging and translocation to sensing are rapidly increasing, and their potential for biology-related applications, including physiology and ecology is becoming more evident. Still, many possibilities, such as multi-organism transfer and molecule tracking, remain unexplored.

(4) Upconversion nanoparticles

Upconversion nanoparticles (UCNPs) have also been utilised in a few plant uptake experiments, imaging of animals and sensory applications. Translocation of UCNPs from roots to shoots and leaves in radish (*Raphanus sativus*), orchid (*Phalaenopsis* sp.), pumpkin, thale cress, and mung bean have been reported, demonstrating the potential of UCNPs for plant imaging (Hischemöller *et al.*, 2009; Peng *et al.*, 2012; Nordmann *et al.*, 2015; Modlitbová *et al.*, 2019). Imaging experiments with UCNPs have also been performed in small animals such as jellyfish and ants (Chen *et al.*, 2015*b*; Alkahtani *et al.*, 2017). UCNP-based tools have been developed for sensing the spatiotemporal localisation of Zn ions in zebrafish during embryo development (Hu *et al.*, 2019) and for detection of nitrate (LOD 100 μg/l) in Chinese cabbage (*Brassica rapa*; Yang *et al.*, 2018*c*). Similarly, an aptamer sensor for the antibiotic chloramphenicol (LOD 0.01 μg/l; Wu *et al.*, 2015) has been developed for food safety purposes.

IV. QUANTIFICATION OF FNPs

Quantification of FNPs from images and directly from samples can be achieved in several ways, most of which require

prior excitation of dot fluorescence. Generally, fluorescence excitation is achieved with a light source or radioactive energy (Liu *et al.*, 2010). Light sources that have been used include continuous wave (CW) or pulsed lasers (Whiteside *et al.*, 2009), Hg lamps (Whiteside *et al.*, 2009; Nishimura *et al.*, 2013), Xe lamps (Ma *et al.*, 2008; Cayuela *et al.*, 2013; Brandt *et al.*, 2015) and LEDs (Minnaar & Anderson, 2019; Minnaar *et al.*, 2019). Additionally, FNP fluorescence can be achieved indirectly *via* excitation of another chromophore and subsequent FRET between the chromophore and the FNP (Chou & Dennis, 2015; Afsari *et al.*, 2016; Goryacheva *et al.*, 2017*b*). Notably, in FRET applications, many sensors utilise FNPs as the energy donor (Brandt *et al.*, 2015; Yang *et al.*, 2018*a*; Zhang *et al.*, 2020). Furthermore, activation without an external light source is possible *via* bioluminescence resonance energy transfer (BRET), in which a light-emitting compound, such as luciferase, provides the activating light energy for FNPs (So *et al.*, 2006; Hsu *et al.*, 2013; Feugang *et al.*, 2015).

Nanoparticle quantification directly from samples can be achieved by multiple methods with varying accuracy, depending on FNP and application type. In sensory applications, in which the quantification of target compounds is based on the fluorescence spectra, this can be measured using a fluorescence spectrophotometer, microplate reader or near-infrared (NIR) spectroscope (Martynenko *et al.*, 2017). In practice, the amount of target compound in samples is usually determined by the comparison of sample fluorescence spectra to reference spectra obtained from solutions with known concentrations of the target (Sun *et al.*, 2017). However, other compounds and ions present in complex biological solutes may also affect the fluorescence spectra of the sample, whereas the quality of excitation light can influence the efficiency of light emission, rendering concentration estimates less reliable (Hoy *et al.*, 2013; Yao, Yang & Duan, 2014; Martynenko *et al.*, 2017). Time-gated methods, such as time-resolved photoluminescence spectroscopy (TRPL) and fluorescence lifetime imaging microscopy (FLIM), can provide a more reliable alternative. These techniques also involve measuring sample fluorescence spectra, but this is performed multiple times at various time points while also measuring fluorescence decay. Such decline in fluorescence intensity can be used to decipher FNP fluorescence from that of other compounds present in the sample (Mandal *et al.*, 2013; Yao *et al.*, 2014; Merkl *et al.*, 2016; Martynenko *et al.*, 2017). Of these techniques, FLIM is the most informative, because it measures the fluorescence lifetime for each pixel, as opposed to the whole frame as in TRPL (Yao *et al.*, 2014). Simple absorbance measurements are sometimes used to determine FNP concentrations in samples, although the accuracy of this method is generally limited to nanomolar concentrations (Martynenko *et al.*, 2017). For Cd-QDs and some other SQDs, the most common approach is to quantify the amount of FNPs indirectly *via* analysis of concentrations of Cd or other core metals in a sample, using inductively coupled plasma mass spectrometry (ICP-MS; Lewinski *et al.*, 2010; Jackson *et al.*, 2012; Yaghini *et al.*, 2016; Martynenko *et al.*, 2017; Majumdar *et al.*, 2019; Lian *et al.*, 2019). Quantification of FCNPs and attached target compounds can also be achieved with matrix-assisted laser desorption-ionisation time-of-flight mass spectroscopy (MALDI-TOF; Khan *et al.*, 2015).

In sample images, FNPs can be quantified based on determining the number of fluorescent pixels. Image-processing and analysis software can be used to outline an area exhibiting fluorescence, a region of interest (ROI), and then determine its size and FNP density by pixel counting (Bouldin *et al.*, 2008; Ma *et al.*, 2008). Similarly, the intensity of fluorescence, which indirectly indicates the amount of FNPs in the ROI, can be calculated by comparing it to a non-fluorescent, identically sized area of a picture. Comparisons are usually based on the average or maximum and minimum fluorescence intensities of each pixel in the ROI and control area (Ballou *et al.*, 2004; Chibli *et al.*, 2011; Nishimura *et al.*, 2013; Boschi & de Sanctis, 2017; Erland *et al.*, 2019). Especially when comparing larger areas, such as whole micro-organisms, FNP-incubated individuals and control individuals can be compared for the same parameters (Bouldin *et al.*, 2008). Fluorescence lifetimes between target and control areas can also be compared from FLIM images (Yao *et al.*, 2014). Simple counting of the number of fluorescence-exhibiting organisms, cells or other structures, either manually or *via* artificial intelligence (AI)-based automated counting, is also useful in certain applications (Yong *et al.*, 2009; Ristic *et al.*, 2014).

Several methods have been developed for determining FNP movements. Particle positions in the x and y axes in each frame are determined in time and this information is used to calculate trajectories and diffusivity of particles in the target tissues (Ekvall *et al.*, 2013; Nishimura *et al.*, 2013; Liu *et al.*, 2016*a*).

V. THE PROS AND CONS OF VARIOUS FLUORESCENT TOOLS

(1) FNPs compared with other fluorescence tools

While fluorescent dyes, proteins and heavy isotopes have historically been used in biological research, FNPs provide a viable alternative, especially for fluorescent dyes and proteins, due to their size-dependent emission and their straightforward separation of symmetric excitation and emission peaks (Resch-Genger *et al.*, 2008; Himmelstoß & Hirsch 2019; Reshma & Mohanan, 2019; Wagner *et al.*, 2019). In particular, QDs exhibit higher molar absorption coefficients and quantum yields (QYs) than dyes, indicating that QDs can absorb more light energy and emit light more efficiently. Additionally, the fluorescent lifetime of FNPs (5–100 ns) is usually longer than in dyes (1–5 ns), and FNPs are thermally and photochemically more stable. The signal-to-noise ratio is also relatively higher for FNPs, indicating greater accuracy (Bruchez *et al.*, 1998; Resch-Genger *et al.*, 2008; Winnik & Maysinger, 2013; Yaghini *et al.*, 2016; Reshma & Mohanan, 2019). Finally, the

stability and longevity of FNPs in biological systems are usually much longer than those of dyes; for example, CdSe/ZnS QDs retain their stability and labelling activity in living cells for over a week (Jaiswal *et al.*, 2003). An obvious additional advantage of FNPs is the ease of multi-colour labelling (van't Padje *et al.*, 2020*a*,*b*). While organic dyes can typically only be used one at a time, because each dye has a different composition, size and different chemical properties, it is possible to track multiple FNP-bound targets simultaneously; i.e. each target can be conjugated to a different-coloured dot and excited by the same source of light (Wagner *et al.*, 2019). The ease of use, cost-effectiveness, small size and well-established protocols represent the main benefits of fluorescent dyes.

The pros and cons of fluorescent proteins generally correspond to those of fluorescent dyes. Fluorescent proteins are smaller, cheaper and relatively less toxic than many FNPs. However, fluorescent proteins exhibit lower photostability, shorter fluorescence lifetime (∼5 ns) and an asymmetric emission profile. Furthermore, fluorescent proteins are relatively less suited for multicolour labelling, because the fluorescence cannot be tuned as one type of protein creates only one colour of emission (Himmelstoß & Hirsch, 2019). Fluorescent proteins are generally more suitable for NIR imaging than dyes, but the protocols for the application of these are comparatively less established (Himmelstoß & Hirsch, 2019).

FNPs can be used in place of isotopic methods for tracking the movement of different compounds in biological systems. Radioactive and stable isotope labelling experiments have been used in biological research for nearly a century to study the movement of molecules, such as nutrients or defensive compounds (Hevesy, 1939; Newsome *et al.*, 2007). However, since the measurements typically involve the addition of an isotopically labelled compound to one spot and the subsequent analysis of the amount of the labelled compound in another spot, they provide no information about the mechanism of movement. Furthermore, the analysis of isotopic content usually requires destructive sampling, rendering temporal observations in living organisms difficult. Additionally, isotopic studies often provide little information about the location of the compounds at the cellular level, although autoradiography may solve this for radioactive isotopes (Bücking & Heyser, 2001). Conversely, *in vivo* analysis of FNP-linked compound movement and localisation within organisms and tissues is relatively easy (Chae *et al.*, 2016; Li *et al.*, 2016*a*). For some elements such as phosphorus (P), hazardous radioactive isotopes with relatively short half-lives represent the only labelling option. Further, even if stable isotopes exist, as for carbon and nitrogen, many biological, chemical and physical processes discriminate against heavier isotopes. The natural abundances of stable isotopes can also vary even among tissues of a single individual (Cernusak *et al.*, 2009). Thus, the pattern and magnitude of movement and presence of isotopic labels may not accurately represent those of their common counterparts. Taken together, the use of FNPs instead of isotopes may alleviate some of the associated problems, although some extent of size-dependent discrimination against FNP labels is likely and requires urgent assessment for various biogeochemical and biophysical processes.

(2) Relative benefits and shortfalls of various FNPs

Choosing among FNPs is difficult, because all major FNP types have their advantages and disadvantages (Table 2) and reliable information is lacking for many FNP types. As toxicity concerns have overshadowed the utilisation of FNPs, especially Cd-QDs, these side effects are important to consider. Besides, there are also important considerations with regard to fluorescent properties, and factors such as cost-effectiveness, commercial and data availability, as well as type-specific limitations.

(*a*) Toxicity of FNPs

The toxicity of Cd-QDs is generally considered the main shortfall of these particles, but more research is needed for modified Cd-QDs (Tsoi *et al.*, 2013; Rocha *et al.*, 2017; Reshma & Mohanan, 2019). FCNPs (Wang *et al.*, 2013; Ding *et al.*, 2014; Goryacheva *et al.*, 2017*a*; Namdari *et al.*, 2017) and many non-cadmium SQDs (Li & Ruckenstein, 2004; He *et al.*, 2009; Xu *et al.*, 2016) are considered non-toxic. However, these implied cytotoxicity differences are not straightforward, because organisms' responses to Cd-QDs and other FNPs are highly context dependent, ranging from severe toxicity to unexpected positive effects (Hardman, 2006; Tsoi *et al.*, 2013; Wang & Tang, 2018). In the case of Cd-QDs, the addition of a ZnS shell can be effective in mitigating toxic responses (Chen *et al.*, 2012; Mei *et al.*, 2014; Modlitbová *et al.*, 2018*b*). On the contrary, double-shelled CdTe/CdS/ZnS nanoparticles were equally toxic to *Allium cepa* plants as were CdTe QDs, while single-shelled CdTe/ZnS QDs showed no toxicity (Modlitbová *et al.*, 2018*b*). However, in human erythroleukemia cells, CdTe/CdS/ZnS QDs were non-toxic up to 16 μM concentration, while CdTe QDs caused cell death at 0.75 μM (Chen *et al.*, 2012).

In addition to the shell, the coatings and conjugates added to FNPs can greatly affect their toxicity in both Cd-QDs (Galeone *et al.*, 2012; Hu *et al.*, 2017; Majumdar *et al.*, 2019) and FCNPs (Yang *et al.*, 2009; Chen *et al.*, 2015*a*; Qian *et al.*, 2018; Fan *et al.*, 2019) and some non-cadmium QDs (Marcon *et al.*, 2010; Bhattacharjee *et al.*, 2013). Fruit flies exposed to food incubated with CdSe/ZnS QDs with polymer coating (PC) or coated with mercaptoundecanoic acid (MUA) or PC-PEG exhibited signs of toxicity in all cases, with PC-PEG being the least harmful and MUA the most harmful (Galeone *et al.*, 2012). The capping agent may also play a role in toxicity: CdS QDs capped with polyvinylpyrrolidone (PVP) were more toxic than bare QDs or QDs capped with MPA, trioctylphosphine oxide (TOPO) or glycine (GLY) in soybean (*Glycine max*) plants (Majumdar *et al.*, 2019). However, all these QD treatments, especially QD-MAA and QD-GLY, resulted in changes to the amino acid composition of plants compared

to controls (Majumdar *et al.*, 2019). A toxicity test comparing nanodiamonds with carboxyl, hydroxyl and amino cappings revealed that carboxyl-capped NDs were the least toxic and amino-capped the most toxic to human embryonic kidney cells. However, for zebrafish embryos, the carboxyl-capped NDs were the most toxic (Marcon *et al.*, 2010). A study using 15 Si- or Ga-containing QDs confirmed that amino-capped particles are the most toxic to both rat and human cells (Bhattacharjee *et al.*, 2013).

Other factors to consider in toxicity tests are the FNP size, and the identity and concentration of elements in FCNPs. For the filamentous white-rot fungus *Phanerochaete chrysosporium*, carboxyl-capped CdSe/ZnS QDs were the least toxic, but smaller amino-capped CdSe/ZnS QDs were more toxic than larger amino-capped ones (Hu *et al.*, 2017). Smaller CQD particles also seem to be relatively more toxic, as across 35 CQDs, toxicity to human macrophages increased with the proportion of nitrogen in the dot core (Fan *et al.*, 2019). Likewise, CQDs doped with N or co-doped with N and S were more toxic to the microalga *Chlorella pyrenoidosa* than undoped CQDs (Xiao *et al.*, 2016). These findings are unfortunate, because N-doped CQDs exhibit the highest QYs [94% (Qu *et al.*, 2014); 94.5% (Liu *et al.*, 2018)] and smaller FNP size is more advantageous for research purposes due to more efficient uptake and translocation in tissues (Nordmann *et al.*, 2015).

A few studies have compared toxicity among different particle types (e.g. CQDs, CdTe QDs, CdS QDs). A comparative acute toxicity study in mice and human cells demonstrated that cell viability did not differ from control values for CQD concentrations up to 100 mg/l while CdTe QDs were toxic already at 0.2 mg/l (Navarro-Ruiz *et al.*, 2020). A comparison among three CQDs, CdTe QDs, CdS QDs and $CuInS_2$/ZnS QDs indicated that the non-cadmium SQDs were the least toxic to microalgae (*C. pyrenoidosa*), followed by CQDs and CdS QDs. The 50% lethality concentrations (LC50) for growth inhibition were 0.015 mg/l and 459.5 mg/l for CdTe QDs and $CuInS_2$/ZnS QDs, respectively, and 38.56–232.47 mg/l for various CQDs (Xiao *et al.*, 2016). Another study comparing the toxicities of CdTe QDs, CdSe/ZnS QDs and InP/ZnS QDs to the same microalgae revealed that CdTe QDs were the most toxic (cell viability affected at 50 nM), followed by InP/ZnS QDs (500 nM) and CdSe/ZnS QDs (1000–2000 nM) (Tang *et al.*, 2013). Conversely, a study comparing the toxicity of InP/ZnS QDs and CdSe/ZnS QDs to human cells and fruit flies found that InP/ZnS QDs were significantly less toxic than CdSe/ZnS QDs, which leached Cd^{2+} ions despite the ZnS shell (Brunetti *et al.*, 2013). These findings highlight the greater toxicity of unshelled Cd-containing QDs and potential issues with coatings.

Direct toxicity comparisons among studies are difficult because of differences in experimental approach, recorded parameters and high variability among organisms. For example, two long-term toxicity studies on rats reached contrasting conclusions: carboxyl-capped CdSe/ZnS QDs in one study caused no behavioural, physiological, or histological changes at 15 nM concentration 84 days post-injection (Hauck *et al.*, 2010), whereas three out of nine rats injected with a much lower 5 nM concentration died shortly after the injections (Yang *et al.*, 2018*a*). Similarly, while one study found a decrease in root elongation and biomass in thale cress at CQD concentrations above 0.125 mg/ml (Chen *et al.*, 2018), another found no toxicity with concentrations up to 2.24 mg/ml and reported that CQD concentrations up to 0.56 mg/ml enhanced growth (Li *et al.*, 2019*a*). Comparing separate studies, especially studies on CQDs and SQDs is further complicated because QD doses are typically reported as molar concentrations but CQD doses as mass per volume: the molecular weight for both of these is usually unknown. Molecular weight also varies greatly even within the same particle type. For example, the molecular weights of two different CdSe/ZnS nanoparticles have been calculated as 1100 and 85 kg/mol (Rosenthal *et al.*, 2011). Thus, there is a great need for more comparative studies that impose the same experimental parameters and report concentrations in comparable units.

Causes and mechanisms of FNP toxicity vary. For Cd-QDs, toxicity has commonly been attributed to the toxicity of Cd^{2+} ions leaching from the core (Mei *et al.*, 2014; Alaraby *et al.*, 2015; Modlitbová *et al.*, 2018*a*,*b*), but many studies comparing Cd-QDs and other Cd compounds have shown that toxicity cannot be explained by Cd^{2+} leaching alone (Ambrosone *et al.*, 2012; Chen *et al.*, 2012; Marmiroli *et al.*, 2020). Reported toxicity mechanisms include the production of ROS, inhibition of cell division, changes in enzyme concentrations, DNA breakage, increased apoptosis rates as well as changes in gene expression in both animal and plant systems (Galeone *et al.*, 2012; Marmiroli *et al.*, 2014, 2020; Tian *et al.*, 2017; Das, Bandyopadhyay & Pramanik, 2018; Lian *et al.*, 2019). The reported toxic responses to FCNPs (Chen *et al.*, 2016*a*; Chen *et al.*, 2018; Qian *et al.*, 2018; Zhang *et al.*, 2019*b*) and non-cadmium QDs (Xu *et al.*, 2016; Kolackova *et al.*, 2019; Yang *et al.*, 2019) are similar: oxidative stress, gene expression and growth inhibition. For some non-cadmium SQDs, there is some indication of toxicity caused by the core ions released due to dot degradation (Stern *et al.*, 2008; Tang *et al.*, 2013), but such degradation does not always induce significant toxicity (Veronesi *et al.*, 2019).

Taken together, FNP toxicity depends on a multitude of complex factors and can vary greatly even within the same particle type (Hardman, 2006; Tsoi *et al.*, 2013; Wang & Tang, 2018). Although it seems that Cd-QDs are relatively more toxic than other FNPs (Xiao *et al.*, 2016; Navarro-Ruiz *et al.*, 2020), this is not always evident. Given the high variation of responses among organisms and experimental conditions, toxicity has to be tested in a case-by-case manner before undertaking experiments utilising FNPs.

(*b*) Unexpected positive effects of FNPs

In striking contrast to toxicity, many studies have reported positive effects of FNPs, in particular FCNPs, on the

functioning and growth of various organisms. Growth enhancement of CQDs has been reported in microalgae, mung bean, wheat, thale cress and white clover (*Trifolium repens*) (Tripathi & Sarkar, 2015; Li *et al.*, 2016*b*; Wang *et al.*, 2018*b*; Zhang *et al.*, 2018; Li *et al.*, 2019*a*; Xue *et al.*, 2020). Additionally, pollen-based CQDs enhanced not only growth, but also potassium uptake of Chinese flowering cabbage (Zheng *et al.*, 2017). CQDs alleviated toxic effects of Cd^{2+} ions in grapefruit (*Citrus maxima*) seedlings and improved stress tolerance of peanut (*Arachis hypogaea*) plants (Su *et al.*, 2018; Li *et al.*, 2019*b*). Improved growth and disease resistance were observed in CQD-inoculated rice (Li *et al.*, 2018*c*). As reviewed by Li *et al.* (2020*b*), in most cases, growth induction is attributable to the enhancement of electron transfer or photosynthesis. Additionally, FCNPs may be degraded and used in plants for producing hormones or CO_2 for photosynthesis. FCNPs may also improve plant water and nutrient uptake by carrying water molecules or ions bound to their reactive surface groups from the substrate into the plants. The increased resistance to environmental stressors has been attributed mainly to the ROS scavenging activity of FCNPs, but also to FCNP-induced changes in gene expression (Li *et al.*, 2020*b*). The effective concentrations used in these examples are <1 mg/ml [but see Li *et al.* (2019*a*) and Xue *et al.* (2020)], but toxicity has also been observed at similar concentrations (Chen *et al.*, 2016*a*, 2018; Zhang *et al.*, 2019*b*).

In bacteria, CQDs promoted nitrogen fixation and growth of *Azotobacter chroococcum* by improving electron transfer in the nitrogenase enzyme responsible for transforming N_2 to NH_4 (Wang *et al.*, 2018*a*). CQDs have also been reported to increase the activity of other enzymes, such as laccase (Li *et al.*, 2015). However, much remains obscure in this area, as there are also reports of CQDs inhibiting enzyme activity (Zhang *et al.*, 2019*c*) and displaying antibacterial properties (Li *et al.*, 2018*d*,*e*).

Besides FCNPs, other FNPs may also generate positive effects. A recent study reported increased biomass production and water uptake of cucumber (*Cucumis sativus*) after inoculation with SiQDs in concentrations up to 0.3 mg/ml (Li *et al.*, 2019*c*). Similarly, UCNPs increased the growth of mung beans with concentrations up to 10 μg/ml, while concentrations equal to or larger than 100 μg/ml reduced growth (Peng *et al.*, 2012). Finally, a study on snow pea (*Pisum sativum*) revealed that Mn-doped CdS/ZnS QDs conjugated to N-acetyl cysteine improved growth at concentrations below 40 μg/ml, while larger concentrations inhibited seed germination (Das *et al.*, 2015). These studies indicate that for physiological experiments, considering such unexpected positive effects of FNPs is as important as toxicity.

(*c*) Pros and cons of FNP types

When selecting FNPs for experiments, researchers need to consider the chemical and physical properties of the particles as well as their potential side effects and availability. Cd-QDs generally exhibit the greatest brightness and fluorescence lifetimes, the most symmetric emission peaks, best commercial availability and accumulated technical and practical information (Drbohlavova *et al.*, 2009; Rosenthal *et al.*, 2011; Himmelstoß & Hirsch, 2019). However, in addition to toxicity, a major challenge with Cd-QDs is their proneness to 'blinking' – switching on and off fluorescence at ∼0.5 s intervals under continuous light exposure (Schiffman & Balakrishna, 2018). Blinking is thought to be caused by photoionisation of the core, which can be somewhat controlled by shells (Nirmal *et al.*, 1996). All dots need to be emissive simultaneously for accurate localisation and quantification (Whiteside *et al.*, 2012*a*).

The greatest advantages of FCNPs over Cd-QDs include lower cytotoxicity and relative ease of synthesis from natural ingredients or waste at low cost. FCNPs are also generally more photostable and are less prone to blinking, which renders them more suitable for long-term imaging experiments (Ding *et al.*, 2014; Lim *et al.*, 2015; Roy *et al.*, 2015; Das *et al.*, 2018; Zhang *et al.*, 2018*a*). In early FCNPs, the QY was insufficient, but doping with nitrogen is particularly promising for enhancing fluorescence intensity and QY (Wang *et al.*, 2015; Zheng *et al.*, 2015*b*). The FCNPs produced from non-standard materials contain abundant impurities, which disables reproducibility and biases assessment of their properties (Essner *et al.*, 2018; Ge *et al.*, 2018). Therefore, researchers should be cautious about the reported properties of FCNPs that have not been appropriately purified by dialysis or ultrafiltration. Additionally, most biological applications have utilised raw, unfunctionalised FCNPs, whose chemical properties are caused by unknown factors. Quite often, especially in chemical or ion sensors, sensing properties of FCNPs have not been pre-engineered. Instead, researchers have incubated synthesised FCNPs in solvents with potential sensing targets, searching for the one(s) that causes a detectable change in dot fluorescence. Therefore, it is difficult to determine the sensitive component in the dot. CPDs are little utilised in biological applications and there is limited toxicological information. The relative brightness of CPDs may be higher than that of other FNPs, which could markedly improve detection resolution (Wu & Chiu, 2013). However, the ∼0.6 ns fluorescence lifetime of the CPDs is shorter compared to other FNPs, which limits their utility for imaging applications (Wu & Chiu, 2013). The advantages of nanodiamonds include high chemical stability and good biocompatibility (Mohan *et al.*, 2010; Mochalin *et al.*, 2012; but see Marcon *et al.*, 2010; Zhang *et al.*, 2010), while the disadvantages include a high tendency for aggregation and uncertainty about particle structure and physicochemical properties (Mochalin *et al.*, 2012). Despite these shortcomings, intensive research efforts (Cayuela *et al.*, 2016; Essner *et al.*, 2018; Himmelstoß & Hirsch, 2019) and the yet largely unexplored possibilities of conjugating other molecules to FCNPs (Bhunia *et al.*, 2013) indicate that FCNPs are a rising star unlikely to dim soon.

Many non-cadmium SQDs are attractive alternatives to Cd-QDs due to lower toxicity and better resistance to degradation, plausibly as a result of covalent bonds in the core (Xu *et al.*, 2016). However, this group is highly

Table 2. Key properties of major fluorescent nanoparticle (FNP) types and fluorescent dyes. Values in parentheses indicate maximum values when outliers are included

Property	Traditional QD (Cd)	Carbon-based dot	Alternative FNP	Fluorescent dye
Ease of application	High	Medium	Low	Very high
Data availability	High	Medium	Low	Very high
Commercial availability	High	Medium	Low	Very high
Cost	High	Low	Low to high	Low
Difficulty of synthesis	High	Low to medium	Medium	Low
Quantum yield (%)	30–<100	0–<95	0–80	<90
Separation of spectra	High	Medium to high	Medium to high	Low
NIR suitability	High	Medium	Low to high	Low to medium
Fluorescence lifetime (ns)*	10–100	<100	Up to 200	1–10
Signal precision	High	High	ND	Low
Stability	High	High	ND	Low
Colour tunability	High	Medium	Medium	Not possible
Multimodality	Yes	Yes	Yes (theoretical)	No
Biocompatibility	Low	Medium to high	Low to high	High
Toxicity	High	Low to medium	Low to medium	Low to high
Water solubility	Low to medium	Medium to high	Low to medium	Low to high
Size (nm)	2–10(20)	<10(100)	1.4–25	∼0.5
Type-specific limitation	Blinking	Unreliability of existing data	Heterogeneity, lack of data	Sensitivity to microenvironment

ND, not experimentally determined; NIR, near-infrared; QD, quantum dot.
*Not taking into account afterglow particles.

heterogeneous, with limited applications in biology and scant toxicity information. Furthermore, as there is no general term to encompass these FNPs yet, the literature base is dispersed and the information difficult to find. SiQDs have generally lower toxicity and faster clearance from the body than Cd-QDs (Li & Ruckenstein, 2004; He *et al.*, 2009, but see Liu *et al.*, 2013), rendering SiQDs attractive options for drug-delivery purposes (Park *et al.*, 2009). However, preparing water-soluble SiQDs with good properties has limited their use in biological systems, but coatings might improve water solubility. Additionally, the synthesis of SiQDs often involves hazardous or expensive precursors such as nitric acid, hydrofluoric acid and (3-aminopropyl) triethoxysilane (APTES), rendering them less approachable than FCNPs (Chinnathambi *et al.*, 2014; Morozova *et al.*, 2020).

The improvement of the fluorescence signal of UCNPs requires careful selection of rare-earth dopants and optimisation of their concentrations; these should be as high as possible, although too high concentrations may cause a so-called 'concentration quenching' of the fluorescence (Wen *et al.*, 2018). This challenge has limited the use of UCNPs, but promising optimisation strategies include adding shells, increasing crystal size, and increasing the intensity of the excitation light, as well as evenly distributing ions in the particle (Wen *et al.*, 2018).

To summarise, Cd-QDs are easily accessible, quickly usable and there is a large body of available information about their properties. However, Cd-QDs are prone to blinking, relatively expensive and potentially toxic to living organisms. FCNPs entail the benefits of low toxicity and cost as well as high biocompatibility and adequate fluorescence properties. However, FCNPs have low commercial availability and their utilisation requires knowledge of optics, nanophysics and chemistry as well as a critical interpretation of literature. Non-cadmium SQDs represent an option intermediate between Cd-QDs and FCNPs – their fluorescent properties are generally comparable to those of other FNPs, whereas biocompatibility is better than in Cd-QDs but worse or equal to FCNPs. The lack of biological tests, heterogeneity of particle types, and low commercial availability all greatly reduce the applicability of non-cadmium SQDs.

While some research has compared the toxicity of different FNP types [mainly Cd-QDs compared to another type of FNP (Brunetti *et al.*, 2013; Tang *et al.*, 2013; Xiao *et al.*, 2016)], there are no experiments comparing the functionality of FNP types for biological use, except a few comparisons for differently coated, conjugated or doped FNPs of the same type. This lack of experimental comparison represents a major knowledge gap that should be addressed for selecting FNPs.

VI. RECOMMENDATIONS FOR FNP USERS AND DEVELOPERS

(1) Experimental considerations

In biological experiments, researchers have to consider abiotic and biotic factors related to the target system. For example, dosage and administration technique, surface charge, size, pH, species investigated and culture medium all affect aspects of FNP performance such as QY, uptake and toxicity

(Pang & Gong, 2019; Filali, Pirot & Miosse, 2020). Thus, preliminary performance and toxicity tests with the intended concentrations are necessary in the target system. Similarly, an FNP-free solvent addition treatment as an internal control should be considered. Although reference data are widely available especially for Cd-QDs, extrapolations of these even in the case of the same species are unreliable, because the responses are extremely complex and depend on multiple abiotic and biotic factors. Nearly as important as toxicity, growth-promoting side effects of FCNPs are of concern for ecological experiments. This warrants urgent attention because some of these side effects may question the biological relevance of the findings, depending on the hypotheses and controls. It is also advisable to establish controls with unconjugated dots and/or labelled FNPs with fluorescent dyes or relevant isotopes to account for possible confounding effects resulting from non-specific binding and the relatively large size of the dots (Jin *et al.*, 2018). In nutrient exchange studies, it is also important to quantify the nutrients that remain attached to FNPs at the end of the experiment. However, currently there is a lack of suitable approaches to achieve this (van't Padje *et al.*, 2020*b*).

It is necessary to address uptake and translocation of FNPs in the target system and to use relevant controls, because Cd-QDs sometimes fail to pass membranes of plant and animal cells (Al-Salim *et al.*, 2011; Navarro *et al.*, 2012; Li *et al.*, 2018*a*; Nastiti *et al.*, 2019). In animals, FNPs are commonly administered by injection or orally, but different administration techniques and injection sites may result in differential distribution of QDs (Huang *et al.*, 2013*b*). Furthermore, minor changes in the chemical components of the FNPs or their conjugates can result in their altered uptake and distribution (Choi *et al.*, 2009*a*; Martynenko *et al.*, 2016). Thus, batch effects and variation should be minimised by careful experimental design and relevant controls.

(2) Towards a standardised terminology

The rapid development of FNPs has led to the publication of a large number of mostly methodological papers, but standardised protocols and terminology development have lagged behind, pointing to limitations in the literature base. Inconsistent terminology, especially in carbon-based FNPs but also in some semiconductor QDs, has generated complications for research teams that are not experts in chemistry and physics. Thus, the popularity of Cd-containing QDs in biological research may partly stem from straightforward terminology. Therefore, we propose a universal, streamlined terminology for FNP types (Fig. 3). In addition to the main groupings presented above [semiconductor QDs, FCNPs and rare-earth doped nanoparticles (RENPs)], we classify FNPs into subcategories based on their elemental composition (SQDs), structure (FCNPs) or emission (RENPs).

For semiconductor QDs, we maintain the separation based on the groups of the periodic table as an official classification. Thus, group IV contains SQDs with Si or Ge cores, group III–V includes GaAs, InP, etc. cores, group II–VI represents CdSe, CdS, ZnS, etc. cores and group IV–VI includes SnS_2, PbSe, etc. cores. Furthermore, complex QDs include particles with group I–III–VI (e.g. $CuInS_2$) and group I–II–III–VI (e.g. $ZnCuInSe_2$) cores, as well as perovskites (e.g. $CsPbBr_3$). However, these groups are not practical in terms of retrieving biological research papers, as they are not routinely mentioned in biological papers, and are unnecessarily complicated for a biologist end user. Thus, we encourage authors to use the key words 'alternative quantum dots' in papers related to these particle types, to aid the retrieval of relevant papers. Finally, the key words 'fluorescent nanoparticles' should be added to all papers of this field, to facilitate retrieval of FNP-related research in general.

To reduce unnecessary complexity, we propose separation of carbon-based FNPs into four groups: carbon quantum dots (CQDs), graphene quantum dots (GQDs), carbonized polymer dots (CPDs) and nanodiamonds (NDs). Cayuela *et al.* (2016) advocated for the separation of CQDs and CNDs (carbon nanodots) based on structure and the presence of quantum confinement, and this terminology has gained some support (Xia *et al.*, 2019). However, this classification is impractical, because in most cases, the fluorescence mechanism of these particles is not known, and it does not even matter for their application. Furthermore, graphene QDs are not all quantum confined; yet this term has been preserved among classifications. In addition, the classification of polymer dots needs to be standardised to understand whether these are novel particle types or a subtype of carbon-based FNPs. In this respect, we advocate the inclusion of polymeric FNPs under FCNPs instead of the term polymer dot. The polymeric nature of the dot can then be further described with the term carbonized polymer dot (CPD) as recently suggested (Tao *et al.*, 2019). Accordingly, GQDs include all graphene-containing FNPs, and CPDs include all polymeric FNPs, whereas CQDs cover all carbon-based FNPs that do not belong to the other three categories. We recommend authors use the key words 'fluorescent carbon nanoparticles' in papers with some type of FCNPs.

We divide rare-earth doped FNPs into upconversion nanoparticles (UCNPs) and downconversion nanoparticles (DCNPs) depending on whether they exhibit fluorescent upconversion or traditional emission (i.e the emission peak is at a higher wavelength than the excitation peak).

(3) Towards comparability and reproducibility

For biological applications, Cd-QDs are usually purchased from a few major companies, which provide uniform and reliably determined particle properties and relatively high reproducibility, although batch effects may remain. By contrast, most other FNP types, especially FCNPs, are synthesised in-house or in different laboratories and companies from variable, often non-standard substrates, sometimes using poorly documented methodology, which severely limits data comparability and reproducibility. To minimise these issues, researchers should provide detailed protocols about

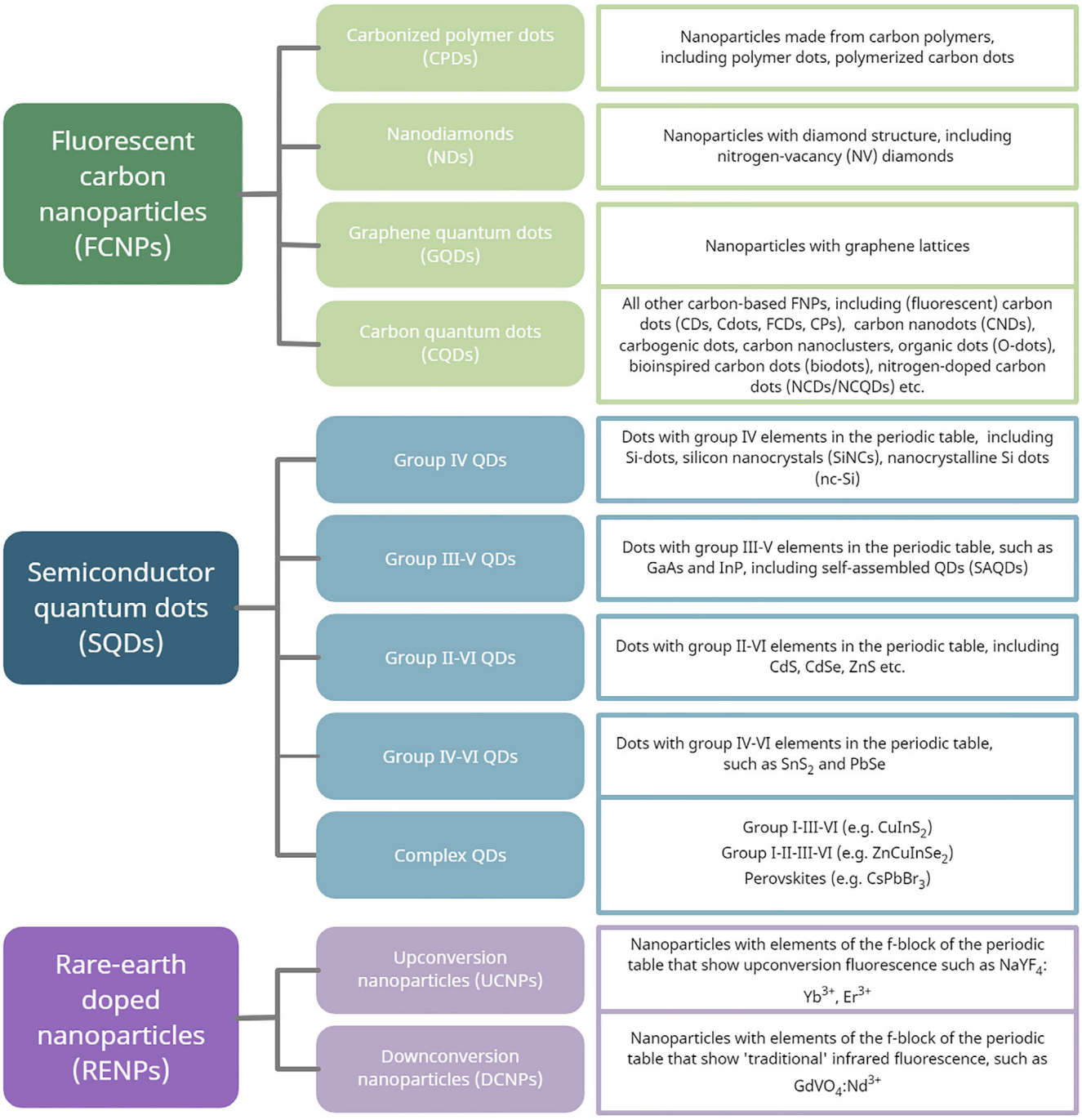

Fig. 3. Proposed classification of fluorescent nanoparticles (FNPs). The major FNP groups include fluorescent carbon nanoparticles (FCNPs), semiconductor quantum dots (SQDs) and rare-earth doped nanoparticles (RENPs). Their subgroups and information about previously used terminology are indicated.

FNP development, including synthesis, purification and the testing of structural and optical properties. Also, re-synthesis of previously developed FNPs, accompanied by detailed structural characterisation, may be necessary for comparing their properties. There is no overall agreement of minimum quality standards for FNPs, but FCNPs require purification by chromatographic techniques or dialysis through a <50 kDa membrane over at least 24 h (Essner *et al.*, 2018). Similarly, QY should be measured over a certain time in a standard solvent, because solvent properties affect QY markedly (Bhamore *et al.*, 2018), leading to incomparable data. From a biological perspective, reporting of QY in distilled

water is of particular importance but rarely practiced. Furthermore, QY should be compared and reported against a standard control such as quinine sulphate.

(4) Perspectives of FNPs in biological applications

Biologists have used only a fraction of available FNPs so far. Most biological experiments have been performed with commercial Cd-QDs, which are available with reactive groups, onto which the ligands of interest can be conjugated. However, given the toxicity issues with Cd-QDs, other types of FNPs have become increasingly utilised, but require rigorous testing for potential side effects. Nonetheless, FNPs offer a viable alternative to some more traditional methods such as labelling with fluorescent dyes or isotopes.

There is an enormous potential for the utilisation of FNPs in biological research, especially in ecology and physiology. Biosensing and tracking represent applications that could benefit from increased utilisation of FCNPs and non-cadmium QDs in particular. As medical research has shown, FCNPs and alternative FNPs can be utilised in more complex tracking, not just sensing of metal ions from liquids. Trophic transfer experiments have demonstrated the potential of FNP transfer between organisms (Bouldin *et al.*, 2008; Lewinski *et al.*, 2011; Koo *et al.*, 2015; Chae *et al.*, 2016), supporting their use in determining dietary preferences by using different-coloured FNPs added to nutrient sources. Furthermore, the pollen-labelling experiments of Minnaar & Anderson (2019) and Minnaar *et al.* (2019) could be extended to track the pollination routes and dispersal mechanisms of pollen, dust seeds and fungal spores. FNP-tagging of individual micro-organisms (Ekvall *et al.*, 2013; Hynson *et al.*, 2015) offers unique research avenues for tracking their movement and interactions with other organisms in response to environmental variables. Recent molecular tagging applications (Erland *et al.*, 2019; Whiteside *et al.*, 2019) suggest that FNPs may be useful for monitoring the movement and localisation of cells and biomolecules such as hormones, allelochemicals, enzymes and antioxidants, both within an individual and among conspecific or heterospecific organisms.

VII. CONCLUSIONS

(1) Fluorescent nanoparticles (FNPs) have been broadly utilised in technical and medical applications, but their use in biological systems lags far behind. A steadily increasing number of studies on tracking, sensing and imaging of small organisms, tissues, cells and biomolecules illustrates their promise for biological applications.

(2) Cadmium-containing semiconductor quantum dots (Cd-QDs) are an attractive option since their application requires little knowledge of chemistry and optics, and there is an adequate body of biological literature. However, toxicity of Cd-QDs, including forms with shells and coatings, remains problematic.

(3) Fluorescent carbon nanoparticles (FCNPs) represent a modern alternative that has remained underutilised in biology, mainly because navigating the different synthesis methodologies and existing literature is difficult without a strong chemical and physical background, and because FCNPs are largely unavailable in ready-to-use commercial packages.

(4) Cadmium-free semiconductor quantum dots and rare-earth doped nanoparticles urgently require biological exploration because of their excellent chemical and physical properties.

(5) Unifying terminology and developing common protocols for the synthesis, characterisation and utilisation of FNPs are urgently needed to ensure reproducibility and comparison of their physicochemical properties.

(6) Use of FNPs in bioapplications requires careful selection amongst available particles as well as preliminary toxicity tests and relevant experimental controls.

(7) FNPs facilitate testing multiple unique biological hypotheses in the fields of cell biology, physiology and ecology.

VIII. ACKNOWLEDGEMENTS

Research of S.M.A.F., U.M., R.J. and L.T. is supported by the Estonian Science Foundation grant PRG632 and EMP442. R.M.L. gratefully acknowledges support from the National Science Foundation under grant 011298. E.T.K was supported by European Research Council ERC grant 335542, HFSP grant RGP0029, and the Ammodo Foundation.

IX. REFERENCES

Afsari, H. S., Dos Santos, M. C., Lindén, S., Chen, T., Qiu, X., Van Bergen en Henegouwen, P. M. P., Jennings, T. L., Susumu, K., Medintz, I. L., Hildebrandt, N. & Miller, L. W. (2016). Time-gated FRET nanoassemblies for rapid and sensitive intra- and extracellular fluorescence imaging. *Science Advances* **2**, e1600265.

Alaraby, M., Demir, E., Hernández, A. & Marcos, R. (2015). Assessing potential harmful effects of CdSe quantum dots by using *Drosophila melanogaster* as in vivo model. *Science of the Total Environment* **530–531**, 66–75.

Alizadeh, N. & Salimi, A. (2019). Polymer dots as a novel probe for fluorescence sensing of dopamine and imaging in single living cell using droplet microfluidic platform. *Analytica Chimica Acta* **1091**, 40–49.

Alkahtani, M., Chen, Y., Pedraza, J. J., González, J. M., Parkinson, D. Y., Hemmer, P. R. & Liang, H. (2017). High resolution fluorescence bio-imaging upconversion nanoparticles in insects. *Optics Express* **25**, 1030–1039.

Al-Salim, N., Barraclough, E., Burgess, E., Clothier, B., Deurer, M., Green, S., Malone, L. & Weir, G. (2011). Quantum dot transport in soil, plants, and insects. *Science of the Total Environment* **409**, 3237–3248.

Álvarez-Diduk, R., Orozco, J. & Merkoçi, A. (2017). Paper strip-embedded graphene quantum dots: a screening device with a smartphone readout. *Scientific Reports* **7**, 976.

Ambrosone, A., Mattera, L., Marchesano, V., Quarta, A., Susha, A. S., Tino, A., Rogach, A. L. & Tortiglione, C. (2012). Mechanisms underlying toxicity induced by CdTe quantum dots determined in an invertebrate model organism. *Biomaterials* **33**, 1991–2000.

Anas, N. A. A., Fen, Y. W., Omar, N. A. S., Daniyal, W. M. E. M. M., Ramdzan, N. S. M. & Saleviter, S. (2019). Development of graphene quantum dots-based optical sensor for toxic metal ion detection. *Sensors (Switzerland)* **19**, 3850.

Asadian, E., Ghalkhani, M. & Shahrokhian, S. (2019). Electrochemical sensing based on carbon nanoparticles: a review. *Sensors and Actuators, B: Chemical* **293**, 183–209.

Baker, S. N. & Baker, G. A. (2010). Luminescent carbon nanodots: emergent nanolights. *Angewandte Chemie - International Edition* **49**, 6726–6744.

Ballou, B., Lagerholm, B. C., Ernst, L. A., Bruchez, M. P. & Waggoner, A. S. (2004). Noninvasive imaging of quantum dots in mice. *Bioconjugate Chemistry* **15**, 79–86.

Beloglazova, N. V., Speranskaya, E. S., De Saeger, S., Hens, Z., Abé, S. & Goryacheva, I. Y. (2012). Quantum dot based rapid tests for zearalenone detection. *Analytical and Bioanalytical Chemistry* **403**, 3013–3024.

Beloglazova, N. V., Speranskaya, E. S., Wu, A., Wang, Z., Sanders, M., Goftman, V. V., Zhang, D., Goryacheva, I. Y. & De Saeger, S. (2014). Novel multiplex fluorescent immunoassays based on quantum dot nanolabels for mycotoxins determination. *Biosensors and Bioelectronics* **62**, 59–65.

Bera, D., Qian, L., Tseng, T. K. & Holloway, P. H. (2010). Quantum dots and their multimodal applications: a review. *Materials* **3**, 2260–2345.

Bhamore, J. R., Jha, S., Park, T. J. & Kailasa, S. K. (2018). Fluorescence sensing of cu 2+ ion and imaging of fungal cell by ultra-small fluorescent carbon dots derived from *Acacia concinna* seeds. *Sensors and Actuators, B: Chemical* **277**, 47–54.

Bharali, D. J., Lucey, D. W., Jayakumar, H., Pudavar, H. E. & Prasad, P. N. (2005). Folate-receptor-mediated delivery of InP quantum dots for bioimaging using confocal and two-photon microscopy. *Journal of the American Chemical Society* **127**, 11364–11371.

Bhattacharjee, S., Rietjens, I. M. C. M., Singh, M. P., Atkins, T. M., Purkait, T. K., Xu, Z., Regli, S., Shukaliak, A., Clark, R. J., Mitchell, B. S., Alink, G. M., Marcelis, A. T. M., Fink, M. J., Veinot, J. G. C., Kauzlarich, S. M., et al. (2013). Cytotoxicity of surface-functionalized silicon and germanium nanoparticles: the dominant role of surface charges. *Nanoscale* **5**, 4870–4883.

Bhunia, S. K., Saha, A., Maity, A. R., Ray, S. C. & Jana, N. R. (2013). Carbon nanoparticle-based fluorescent bioimaging probes. *Scientific Reports* **3**, 1473.

Bian, S., Shen, C., Hua, H., Zhou, L., Zhu, H., Xi, F., Liu, J. & Dong, X. (2016). One-pot synthesis of sulfur-doped graphene quantum dots as a novel fluorescent probe for highly selective and sensitive detection of lead(II). *RSC Advances* **6**, 69977–69983.

Biju, V., Itoh, T. & Ishikawa, M. (2010). Delivering quantum dots to cells: bioconjugated quantum dots for targeted and nonspecific extracellular and intracellular imaging. *Chemical Society Reviews* **39**, 3031–3056.

Bondon, N., Raehm, L., Charnay, C., Boukherroub, R. & Durand, J. O. (2020). Nanodiamonds for bioapplications, recent developments. *Journal of Materials Chemistry B* **8**, 10878–10896.

Boschi, F. & de Sanctis, F. (2017). Overview of the optical properties of fluorescent nanoparticles for optical imaging. *European Journal of Histochemistry* **61**, 2830.

Bouldin, J. L., Ingle, T. M., Sengupta, A., Alexander, R., Hannigan, R. E. & Buchanan, R. A. (2008). Aqueous toxicity and food chain transfer of quantum dots™ in freshwater algae and *Ceriodaphnia dubia*. *Environmental Toxicology and Chemistry* **27**, 1958–1963.

Brandt, Y. I., Mitchell, T., Smolyakov, G. A., Osiński, M. & Hartley, R. S. (2015). Quantum dot assisted tracking of the intracellular protein Cyclin E in *Xenopus laevis* embryos. *Journal of Nanobiotechnology* **13**, 31.

Bruchez, M., Moronne, M., Gin, P., Weiss, S. & Alivisatos, A. P. (1998). Semiconductor nanocrystals as fluorescent biological labels. *Science* **281**, 2013–2016.

Brunetti, V., Chibli, H., Fiammengo, R., Galeone, A., Malvindi, M. A., Vecchio, G., Cingolani, R., Nadeau, J. L. & Pompa, P. P. (2013). InP/ZnS as a safer alternative to CdSe/ZnS core/shell quantum dots: in vitro and in vivo toxicity assessment. *Nanoscale* **5**, 307–317.

Brus, L. E. (1983). A simple model for the ionization potential, electron affinity, and aqueous redox potentials of small semiconductor crystallites. *The Journal of Chemical Physics* **79**, 5566–5571.

Bücking, H. & Heyser, W. (2001). Microautoradiographic localization of phosphate and carbohydrates in mycorrhizal roots of *Populus tremula* x *Populus alba* and the implications for transfer processes in e ectomycorrhizal associations. *Tree Physiology* **21**, 101–107.

Campos, B. B., Abellán, C., Zougagh, M., Jimenez-Jimenez, J., Rodríguez-Castellón, E., Esteves da Silva, J. C. G., Ríos, A. & Algarra, M. (2015). Fluorescent chemosensor for pyridine based on N-doped carbon dots. *Journal of Colloid and Interface Science* **458**, 209–216.

Canham, L. T. (1990). Silicon quantum wire array fabrication by electrochemical and chemical dissolution of wafers. *Applied Physics Letters* **57**, 1046–1048.

Carrillo-Carrión, C., Simonet, B. M. & Valcárcel, M. (2011). Rapid fluorescence determination of diquat herbicide in food grains using quantum dots as new reducing agent. *Analytica Chimica Acta* **692**, 103–108.

Cayuela, A., Laura Soriano, M. & Valcárcel, M. (2013). Strong luminescence of carbon dots induced by acetone passivation: efficient sensor for a rapid analysis of two different pollutants. *Analytica Chimica Acta* **804**, 246–251.

Cayuela, A., Soriano, M. L., Carrillo-Carrión, C. & Valcárcel, M. (2016). Semiconductor and carbon-based fluorescent nanodots: the need for consistency. *Chemical Communications* **52**, 1311–1326.

Cernusak, L. A., Tcherkez, G., Keitel, C., Cornwell, W. K., Santiago, L. S., Knohl, A., Barbour, M. M., Williams, D. G., Reich, P. B., Ellsworth, D. S., Dawson, T. E., Griffiths, H. G., Farquhar, G. D. & Wright, I. J. (2009). Why are non-photosynthetic tissues generally ^{13}C enriched compared with leaves in C3 plants? Review and synthesis of current hypotheses. *Functional Plant Biology* **36**, 199–213.

Chae, Y., Kim, S. W. & An, Y. J. (2016). In vivo visual evaluation of nanoparticle transfer in a three-species terrestrial food chain. *Chemosphere* **151**, 101–107.

Chan, W. C. W. & Nie, S. (1998). Quantum dot bioconjugates for ultrasensitive nonisotopic detection. *Science* **281**, 2016–2018.

Chang, B.-M., Lin, H.-H., Su, L.-J., Lin, W.-D., Lin, R.-J., Tzeng, Y.-K., Lee, R. T., Lee, Y. C., Yu, A. L. & Chang, H.-C. (2013). Highly fluorescent nanodiamonds protein-functionalized for cell labeling and targeting. *Advanced Functional Materials* **23**, 5737–5745.

Chang, L., He, X., Chen, L. & Zhang, Y. (2017). Mercaptophenylboronic acid-capped Mn-doped ZnS quantum dots for highly selective and sensitive fluorescence detection of glycoproteins. *Sensors and Actuators, B: Chemical* **243**, 72–77.

Chen, H., Li, W., Wang, Q., Jin, X., Nie, Z. & Yao, S. (2016). Nitrogen doped graphene quantum dots based single-luminophor generated dual-potential electrochemiluminescence system for ratiometric sensing of Co2+ ion. *Electrochimica Acta* **214**, 94–102.

Chen, J., Dou, R., Yang, Z., Wang, X., Mao, C., Gao, X. & Wang, L. (2016a). The effect and fate of water-soluble carbon nanodots in maize (*Zea mays* L.). *Nanotoxicology* **10**, 818–828.

Chen, J., Liu, B., Yang, Z., Qu, J., Xun, H., Dou, R., Gao, X. & Wang, L. (2018). Phenotypic, transcriptional, physiological and metabolic responses to carbon nanodot exposure in *Arabidopsis thaliana* (L.). *Environmental Science: Nano* **5**, 2672–2685.

Chen, J., Zhu, Y. & Zhang, Y. (2016b). Glutathione-capped Mn-doped ZnS quantum dots as a room-temperature phosphorescence sensor for the detection of Pb^{2+} ions. *Spectrochimica Acta - Part A: Molecular and Biomolecular Spectroscopy* **164**, 98–102.

Chen, J.-T., Sun, H.-Q., Wang, W.-L., Xu, W.-M., He, Q., Shen, S., Qian, J. & Gao, H.-L. (2015a). Polyethylene glycol modification decreases the cardiac toxicity of carbonaceous dots in mouse and zebrafish models. *Acta Pharmacologica Sinica* **36**, 1349–1355.

Chen, N., He, Y., Su, Y., Li, X., Huang, Q., Wang, H., Zhang, X., Tai, R. & Fan, C. (2012). The cytotoxicity of cadmium-based quantum dots. *Biomaterials* **33**, 1238–1244.

Chen, X., Gan, M., Xu, H., Chen, F., Ming, X., Xu, H., Wei, H., Xu, F. & Liu, C. (2014a). Development of a rapid and sensitive quantum dot-based immunochromatographic strip by double labeling PCR products for detection of *Staphylococcus aureus* in food. *Food Control* **46**, 225–232.

Chen, X., Jin, Q., Wu, L., Tung, C. H. & Tang, X. (2014b). Synthesis and unique photoluminescence properties of nitrogen-rich quantum dots and their applications. *Angewandte Chemie - International Edition* **53**, 12542–12547.

Chen, Y. & Rosenzweig, Z. (2002). Luminescent CdS quantum dots as selective ion probes. *Analytical Chemistry* **74**, 5132–5138.

Chen, Z., Wu, X., Hu, S., Hu, P., Yan, H., Tang, Z. & Liu, Y. (2015b). Upconversion $NaLuF_4$ fluorescent nanoprobes for jellyfish cell imaging and irritation assessment of organic dyes. *Journal of Materials Chemistry C* **3**, 6067–6076.

Cheng, X., Huang, Y., Li, D., Yuan, C., Li, Z. L., Sun, L., Jiang, H. & Ma, J. (2019). A sensitive polymer dots fluorescent sensor for determination of A-L-fucosidase activity in human serum. *Sensors and Actuators, B: Chemical* **288**, 38–43.

Chern, M., Kays, J. C., Bhuckory, S. & Dennis, A. M. (2019). Sensing with photoluminescent semiconductor quantum dots. *Methods and Applications in Fluorescence* **7**, 012005.

Chibli, H., Carlini, L., Park, S., Dimitrijevic, N. M. & Nadeau, J. L. (2011). Cytotoxicity of InP/ZnS quantum dots related to reactive oxygen species generation. *Nanoscale* **3**, 2552–2559.

Chinnathambi, S., Chen, S., Ganesan, S. & Hanagata, N. (2014). Silicon quantum dots for biological applications. *Advanced Healthcare Materials* **3**, 10–29.

Choi, H. S., Ipe, B. I., Misra, P., Lee, J. H., Bawendi, M. G. & Frangioni, J. V. (2009a). Tissue- and organ-selective biodistribution of NIR fluorescent quantum dots. *Nano Letters* **9**, 2354–2359.

Choi, Y., Kim, H. P., Hong, S. M., Ryu, J. Y., Han, S. J. & Song, R. (2009b). In situ visualization of gene expression using polymer-coated quantum-dot-DNA conjugates. *Small* **5**, 2085–2091.

Chou, K. F. & Dennis, A. M. (2015). Förster resonance energy transfer between quantum dot donors and quantum dot acceptors. *Sensors (Switzerland)* **15**, 13288–13325.

Chow, E. K., Zhang, X. Q., Chen, M., Lam, R., Robinson, E., Huang, H., Schaffer, D., Osawa, E., Goga, A. & Ho, D. (2011). Nanodiamond

therapeutic delivery agents mediate enhanced chemoresistant tumor treatment. *Science Translational Medicine* **3**, 73ra21.

Chung, I., Akita, R., Vandlen, R., Toomre, D., Schlessinger, J. & Mellman, I. (2010). Spatial control of EGF receptor activation by reversible dimerization on living cells. *Nature* **464**, 783–787.

Clarke, S. J., Hollmann, C. A., Zhang, Z., Suffern, D., Bradforth, S. E., Dimitrijevic, N. M., Minarik, W. G. & Nadeau, J. L. (2006). Photophysics of dopamine-modified quantum dots and effects on biological systems. *Nature Materials* **5**, 409–417.

Cui, D., Huang, J., Zhen, X., Li, J., Jiang, Y. & Pu, K. (2019). A semiconducting polymer nano-prodrug for hypoxia-activated photodynamic cancer therapy. *Angewandte Chemie - Internationhal Edition* **58**, 5920–5924.

Curri, M. L., Agostiano, A., Leo, G., Mallardi, A., Cosma, P. & Della Monica, M. (2002). Development of a novel enzyme/semiconductor nanoparticles system for biosensor applichyation. *Materials Science and Engineering C* **22**, 449–452.

Dahan, M., Lévi, S., Luccardini, C., Rostaing, P., Riveau, B. & Triller, A. (2003). Diffusion dynamics of Glycine receptors revealed by single-quantum dot tracking. *Science* **302**, 442–445.

D'Amora, M., Rodio, M., Sancataldo, G., Diaspro, A. & Intartaglia, R. (2019). Laser-fabricated fluorescent, ligand-free silicon nanoparticles: scale-up, biosafety, and 3D live imaging of zebrafish under development. *ACS Applied Bio Materials* **2**, 321–329.

Das, R., Bandyopadhyay, R. & Pramanik, P. (2018). Carbon quantum dots from natural resource: a review. *Materials Today Chemistry* **8**, 96–109.

Das, S., Wolfson, B. P., Tetard, L., Tharkur, J., Bazata, J. & Santra, S. (2015). Effect of N-acetyl cysteine coated CdS:Mn/ZnS quantum dots on seed germination and seedling growth of snow pea (*Pisum sativum* L.): imaging and spectroscopic studies. *Environmental Science: Nano* **2**, 203–212.

Desai, M. L., Deshmukh, B., Lenka, N., Haran, V., Jha, S., Basu, H., Singhal, R. K., Sharma, P. K., Kailasa, S. K. & Kim, K. H. (2019). Influence of doping ion, capping agent and pH on the fluorescence properties of zinc sulfide quantum dots: sensing of Cu^{2+} and Hg^{2+} ions and their biocompatibility with cancer and fungal cells. *Spectrochimica Acta - Part A: Molecular and Biomolecular Spectroscopy* **210**, 212–221.

Ding, C., Zhu, A. & Tian, Y. (2014). Functional surface engineering of C-dots for fluorescent biosensing and in vivo bioimaging. *Accounts of Chemical Research* **47**, 20–30.

Ding, X., Qu, L., Yang, R., Zhou, Y. & Li, J. (2015). A highly selective and simple fluorescent sensor for mercury (II) ion detection based on cysteamine-capped CdTe quantum dots synthesized by the reflux method. *Luminescence* **30**, 465–471.

Drbohlavova, J., Adam, V., Kizek, R. & Hubalek, J. (2009). Quantum dots - characterization, preparation and usage in biological systems. *International Journal of Molecular Sciences* **10**, 656–673.

Du, F., Zeng, F., Ming, Y. & Wu, S. (2013). Carbon dots-based fluorescent probes for sensitive and selective detection of iodide. *Microchimica Acta* **180**, 453–460.

Eggenberger, K., Merkulov, A., Darbandi, M., Nann, T. & Nick, P. (2007). Direct immunofluorescence of plant microtubules based on semiconductor nanocrystals. *Bioconjugate Chemistry* **18**, 1879–1886.

Ekvall, M. T., Bianco, G., Linse, S., Linke, H., Bäckman, J. & Hansson, L. A. (2013). Three-dimensional tracking of small aquatic organisms using fluorescent nanoparticles. *PLoS One* **8**, e78498.

Ekvall, M. T., Sha, Y., Palmér, T., Bianco, G., Bäckman, J., Åström, K. & Hansson, L. A. (2020). Behavioural responses to co-occurring threats of predation and ultraviolet radiation in *Daphnia*. *Freshwater Biology* **65**, 1509–1517.

Erland, L. A. E., Yasunaga, A., Li, I. T. S., Murch, S. J. & Saxena, P. K. (2019). Direct visualization of location and uptake of applied melatonin and serotonin in living tissues and their redistribution in plants in response to thermal stress. *Journal of Pineal Research* **66**, e12527.

Erogbogbo, F., Yong, K. T., Roy, I., Hu, R., Law, W. C., Zhao, W., Ding, H., Wu, F., Kumar, R., Swihart, M. T. & Prasad, P. N. (2011). In vivo targeted cancer imaging, sentinel lymph node mapping and multi-channel imaging with biocompatible silicon nanocrystals. *ACS Nano* **5**, 413–423.

Erogbogbo, F., Yong, K. T., Roy, I., Xu, G. X., Prasad, P. N. & Swihart, M. T. (2008). Biocompatible luminescent silicon quantum dots for imaging of cancer cells. *ACS Nano* **2**, 873–878.

Essner, J. B., Kist, J. A., Polo-Parada, L. & Baker, G. A. (2018). Artifacts and errors associated with the ubiquitous presence of fluorescent impurities in carbon nanodots. *Chemistry of Materials* **30**, 1878–1887.

Fan, J., Claudel, M., Ronzani, C., Arezki, Y., Lebeau, L. & Pons, F. (2019). Physicochemical characteristics that affect carbon dot safety: lessons from a comprehensive study on a nanoparticle library. *International Journal of Pharmaceutics* **569**, 118521.

Fan, Z., Li, Y., Li, X., Fan, L., Zhou, S., Fang, D. & Yang, S. (2014). Surrounding media sensitive photoluminescence of boron-doped graphene quantum dots for highly fluorescent dye crystals, chemical sensing and bioimaging. *Carbon* **70**, 149–156.

Feng, T., Ai, X., An, G., Yang, P. & Zhao, Y. (2016). Charge-convertible carbon dots for imaging-guided drug delivery with enhanced in vivo cancer therapeutic efficiency. *ACS Nano* **10**, 4410–4420.

Feugang, J. M., Youngblood, R. C., Greene, J. M., Willard, S. T. & Ryan, P. L. (2015). Self-illuminating quantum dots for non-invasive bioluminescence imaging of mammalian gametes. *Journal of Nanobiotechnology* **13**, 38.

Filali, S., Pirot, F. & Miossec, P. (2020). Biological applications and toxicity minimization of semiconductor quantum dots. *Trends in Biotechnology* **38**, 163–177.

Galeone, A., Vecchio, G., Malvindi, M. A., Brunetti, V., Cingolani, R. & Pompa, P. P. (2012). In vivo assessment of CdSe-ZnS quantum dots: coating dependent bioaccumulation and genotoxicity. *Nanoscale* **4**, 6401–6407.

Gao, W., Song, H., Wang, X., Liu, X., Pang, X., Zhou, Y., Gao, B. & Peng, X. (2018). Carbon dots with red mission for sensing of Pt^{2+}, Au^{3+}, and Pd^{2+} and their bioapplications in vitro and in vivo. *ACS Applied Materials and Interfaces* **10**, 1147–1154.

Gao, Z., Yang, D., Wan, Y. & Yang, Y. (2020). One-step synthesis of carbon dots for selective bacterial inactivation and bacterial differentiation. *Analytical and Bioanalytical Chemistry* **412**, 871–880.

García-Cortés, M., Fernández-Argüelles, M. T., Costa-Fernández, J. M. & Sanz-Medel, A. (2017). Sensitive prostate specific antigen quantification using dihydrolipoic acid surface-functionalized phosphorescent quantum dots. *Analytica Chimica Acta* **987**, 118–126.

Ge, L., Pan, N., Jin, J., Wang, P., Lecroy, G. E., Liang, W., Yang, L., Teisl, L. R., Tang, Y. & Sun, Y. P. (2018). Systematic comparison of carbon dots from different preparations - consistent optical properties and photoinduced redox characteristics in visible spectrum and structural and mechanistic implications. *Journal of Physical Chemistry C* **122**, 21667–21676.

Gismondi, A., Reina, G., Orlanducci, S., Mizzoni, F., Gay, S., Terranova, M. L. & Canini, A. (2015). Nanodiamonds coupled with plant bioactive metabolites: a nanotech approach for cancer therapy. *Biomaterials* **38**, 22–35.

Goldman, E. R., Clapp, A. R., Anderson, G. P., Uyeda, H. T., Mauro, J. M., Medintz, I. L. & Mattoussi, H. (2004). Multiplexed toxin analysis using four colors of quantum dot fluororeagents. *Analytical Chemistry* **76**, 684–688.

Goldman, E. R., Medintz, I. L., Whitley, J. L., Hayhurst, A., Clapp, A. R., Uyeda, H. T., Deschamps, J. R., Lassman, M. E. & Mattoussi, H. (2005). A hybrid quantum dot - antibody fragment fluorescence resonance energy transfer-based TNT sensor. *Journal of the American Chemical Society* **127**, 6744–6751.

Gorshkov, K., Susumu, K., Chen, J., Xu, M., Pradhan, M., Zhu, W., Hu, X., Breger, J. C., Wolak, M. & Oh, E. (2020). Quantum dot-conjugated SARS-CoV-2 spike pseudo-virions enable tracking of angiotensin converting enzyme 2 binding and endocytosis. *ACS Nano* **14**, 12234–12247.

Goryacheva, I. Y., Sapelkin, A. V. & Sukhorukov, G. B. (2017a). Carbon nanodots: mechanisms of photoluminescence and principles of application. *Trends in Analytical Chemistry* **90**, 27–37.

Goryacheva, O. A., Beloglazova, N. V., Vostrikova, A. M., Pozharov, M. V., Sobolev, A. M. & Goryacheva, I. Y. (2017b). Lanthanide-to-quantum dot Förster resonance energy transfer (FRET): application for immunoassay. *Talanta* **164**, 377–385.

Green, M. (2010). The nature of quantum dot capping ligands. *Journal of Materials Chemistry* **20**, 5797–5809.

Guo, X., Zhang, L., Wang, Z., Sun, Y., Liu, Q., Dong, W. & Hao, A. (2019). Fluorescent carbon dots based sensing system for detection of enrofloxacin in water solutions. *Spectrochimica Acta - Part A: Molecular and Biomolecular Spectroscopy* **219**, 15–22.

Gupta, G. S., Kumar, A., Senapati, V. A., Pandey, A. K., Shanker, R. & Dhawan, A. (2017). Laboratory scale microbial food chain to study bioaccumulation, biomagnification, and ecotoxicity of cadmium telluride quantum dots. *Environmental Science and Technology* **51**, 1695–1706.

Gurdasani, K., Li, L., Rafter, M. A., Daglish, G. J. & Walter, G. H. (2021). Nanoparticles as potential external markers for mark–release–recapture studies on *Tribolium castaneum*. *Entomologia Experimentalis et Applicata* **169**, 575–581.

Gustafsson, F. S., Whiteside, M. D., Jiranek, V. & Durall, D. M. (2014). Development and use of a quantum dot probe to track multiple yeast strains in mixed culture. *Scientific Reports* **4**, 6971.

Han, M., Gao, X., Su, J. Z. & Nie, S. (2001). Quantum-dot-tagged microbeads for multiplexed optical coding of biomolecules. *Nanomaterials* **7**, 176.

Han, S., Chang, T., Zhao, H., Du, H., Liu, S., Wu, B. & Qin, S. (2017). Cultivating fluorescent flowers with highly luminescent carbon dots fabricated by a double passivation method. *Nanomaterials* **7**, 176.

Hardman, R. (2006). A toxicologic review of quantum dots: toxicity depends on physicochemical and environmental factors. *Environmental Health Perspectives* **114**, 165–172.

Hauck, T. S., Anderson, R. E., Fischer, H. C., Newbigging, S. & Chan, W. C. W. (2010). In vivo quantum-dot toxicity assessment. *Small* **6**, 138–144.

He, Y., Hu, X., Gong, Z., Chen, S. & Yuan, R. (2020). A novel electrochemiluminescence biosensor based on the self-ECL emission of conjugated polymer dots for lead ion detection. *Microchimica Acta* **187**, 237.

He, Y., Kang, Z. H., Li, Q. S., Tsang, C. H. A., Fan, C. H. & Lee, S. T. (2009). Ultrastable, highly fluorescent, and water-dispersed silicon-based nanospheres as cellular probes. *Angewandte Chemie - International Edition* **48**, 128–132.

Heuschele, J., Ekvall, M. T., Bianco, G., Hylander, S. & Hansson, L.-A. (2017). Context-dependent individual behavioral consistency in *Daphnia*. *Ecosphere* **8**, e01679.

Hevesy, G. (1939). Application of isotopes in biology. *Journal of the Chemical Society (Resumed)* 1213–1223. https://doi.org/10.1039/JR9390001213.

Hezinger, A. F. E., Tessmar, J. & Göpferich, A. (2008). Polymer coating of quantum dots - a powerful tool toward diagnostics and sensorics. *European Journal of Pharmaceutics and Biopharmaceutics* **68**, 138–152.

Himmelstoss, S. F. & Hirsch, T. (2019). A critical comparison of lanthanide based upconversion nanoparticles to fluorescent proteins, semiconductor quantum dots, and carbon dots for use in optical sensing and imaging. *Methods and Applications in Fluorescence* **7**, 22002.

Hischemöller, A., Nordmann, J., Ptacek, P., Mummenhoff, K. & Haase, M. (2009). In-vivo imaging of the uptake of upconversion nanoparticles by plant roots. *Journal of Biomedical Nanotechnology* **5**, 278–284.

Holbrook, R. D., Murphy, K. E., Morrow, J. B. & Cole, K. D. (2008). Trophic transfer of nanoparticles in a simplified invertebrate food web. *Nature Nanotechnology* **3**, 352–355.

Hoy, J., Morrison, P. J., Steinberg, L. K., Buhro, W. E. & Loomis, R. A. (2013). Excitation energy dependence of the photoluminescence quantum yields of core and core/shell quantum dots. *Journal of Physical Chemistry Letters* **4**, 2053–2060.

Hsu, C. Y., Chen, C. W., Yu, H. P., Lin, Y. F. & Lai, P. S. (2013). Bioluminescence resonance energy transfer using luciferase-immobilized quantum dots for self-illuminated photodynamic therapy. *Biomaterials* **34**, 1204–1212.

Hu, J., Zhan, S., Fu, H., Nie, G., Hu, S., Wu, S., Shi, L., Wu, X. & Liu, Y. (2019). Dye-sensitized core/shell upconversion nanoparticles for detecting nitrites in plant cells. *Particle and Particle Systems Characterization* **36**, 1900014.

Hu, L., Zeng, G., Chen, G., Huang, Z., Wan, J., Chen, A., Yu, Z., Yang, J., He, K. & Qin, L. (2017). Bioaccumulation and toxicity of CdSe/ZnS quantum dots in *Phanerochaete chrysosporium*. *Colloids and Surfaces B: Biointerfaces* **159**, 303–311.

Hu, X. & Gao, X. (2010). Silica-polymer dual layer-encapsulated quantum dots with remarkable stability. *ACS Nano* **4**, 6080–6086.

Hu, Y., Fu, A., Miao, Z., Zhang, X., Wang, T., Kang, A., Shan, J., Zhu, D. & Li, W. (2018). Fluorescent ligand fishing combination with in-situ imaging and characterizing to screen Hsp 90 inhibitors from *Curcuma longa* L. based on InP/ZnS quantum dots embedded mesoporous nanoparticles. *Talanta* **178**, 258–267.

Huang, H., Liao, L., Xu, X., Zou, M., Liu, F. & Li, N. (2013a). The electron-transfer based interaction between transition metal ions and photoluminescent graphene quantum dots (GQDs): a platform for metal ion sensing. *Talanta* **117**, 152–157.

Huang, X., Zhang, F., Zhu, L., Choi, K. Y., Guo, N., Guo, J., Tackett, K., Anilkumar, P., Liu, G., Quan, Q., Choi, H. S., Niu, G., Sun, Y. P., Lee, S. & Chen, X. (2013b). Effect of injection routes on the biodistribution, clearance, and tumor uptake of carbon dots. *ACS Nano* **7**, 5684–5693.

Hylander, S., Ekvall, M. T., Bianco, G., Yang, X. & Hansson, L. A. (2014). Induced tolerance expressed as relaxed behavioural threat response in millimetresized aquatic organisms. *Proceedings of the Royal Society B: Biological Sciences* **281**, 20140364.

Hynson, N. A., Allison, S. D. & Treseder, K. K. (2015). Quantum dots reveal shifts in organic nitrogen uptake by fungi exposed to long-term nitrogen enrichment. *PLoS One* **10**, 1–13.

Idris, N. M., Li, Z., Ye, L., Wei Sim, E. K., Mahendran, R., Ho, P. C. L. & Zhang, Y. (2009). Tracking transplanted cells in live animal using upconversion fluorescent nanoparticles. *Biomaterials* **30**, 5104–5113.

Jackson, B. P., Bugge, D., Ranville, J. F. & Chen, C. Y. (2012). Bioavailability, toxicity, and bioaccumulation of quantum dot nanoparticles to the amphipod *Leptocheirus plumulosus*. *Environmental Science and Technology* **46**, 5550–5556.

Jaiswal, J. K., Mattoussi, H., Mauro, J. M. & Simon, S. M. (2003). Long-term multiple color imaging of live cells using quantum dot bioconjugates. *Nature Biotechnology* **21**, 47–51.

Jiang, S., Zhang, Y., Lim, K. M., Sim, E. K. W. & Ye, L. (2009). NIR-to-visible upconversion nanoparticles for fluorescent labeling and targeted delivery of siRNA. *Nanotechnology* **20**, 155101.

Jin, D., Xi, P., Wang, B., Zhang, L., Enderlein, J. & Van Oijen, A. M. (2018). Nanoparticles for super-resolution microscopy and single-molecule tracking. *Nature Methods* **15**, 415–423.

Jinadasa, K. K., Peña-Vázquez, E., Bermejo-Barrera, P. & Moreda-Piñeiro, A. (2020). Synthesis and application of a surface ionic imprinting polymer on silica-coated Mn-doped ZnS quantum dots as a chemosensor for the selective quantification of inorganic arsenic in fish. *Analytical and Bioanalytical Chemistry* **412**, 1663–1673.

Kasibabu, B. S. B., D'Souza, S. L., Jha, S. & Kailasa, S. K. (2015a). Imaging of bacterial and fungal cells using fluorescent carbon dots prepared from *Carica papaya* juice. *Journal of Fluorescence* **25**, 803–810.

Kasibabu, B. S. B., D'souza, S. L., Jha, S., Singhal, R. K., Basu, H. & Kailasa, S. K. (2015b). One-step synthesis of fluorescent carbon dots for imaging bacterial and fungal cells. *Analytical Methods* **7**, 2373–2378.

Khan, M. S., Bhaisare, M. L., Pandey, S., Talib, A., Wu, S. M., Kailasa, S. K. & Wu, H. F. (2015). Exploring the ability of water soluble carbon dots as matrix for detecting neurological disorders using MALDI-TOF MS. *International Journal of Mass Spectrometry* **393**, 25–33.

Kim, D., Lee, Y. D., Jo, S., Kim, S. & Lee, T. S. (2020). Detection and imaging of cathepsin L in cancer cells using the aggregation of conjugated polymer dots and magnetic nanoparticles. *Sensors and Actuators, B: Chemical* **307**, 127641.

Kim, S. W., Kwak, J. I. & An, Y. J. (2016). Fluorescent approach for visually observing quantum dot uptake in living organisms. *Chemosphere* **144**, 1763–1770.

Klein, S., Zolk, O., Fromm, M. F., Schrödl, F., Neuhuber, W. & Kryschi, C. (2009). Functionalized silicon quantum dots tailored for targeted siRNA delivery. *Biochemical and Biophysical Research Communications* **387**, 164–168.

Kolackova, M., Moulick, A., Kopel, P., Dvorak, M., Adam, V., Klejdus, B. & Huska, D. (2019). Antioxidant, gene expression and metabolomics fingerprint analysis of *Arabidopsis thaliana* treated by foliar spraying of ZnSe quantum dots and their growth inhibition of *Agrobacterium tumefaciens*. *Journal of Hazardous Materials* **365**, 932–941.

Koo, Y., Wang, J., Zhang, Q., Zhu, H., Chehab, E. W., Colvin, V. L., Alvarez, P. J. J. & Braam, J. (2015). Fluorescence reports intact quantum dot uptake into roots and translocation to leaves of *Arabidopsis thaliana* and subsequent ingestion by insect herbivores. *Environmental Science and Technology* **49**, 626–632.

Landfester, K., Montenegro, R., Scherf, U., Güntner, R., Asawapirom, U., Patil, S., Neher, D. & Kietzke, T. (2002). Semiconducting polymer nanospheres in aqueous dispersion prepared by a miniemulsion process. *Advanced Materials* **14**, 651–655.

Langer, S. M., Weiss, L. C., Ekvall, M. T., Bianco, G., Hansson, L. A. & Tollrian, R. (2019). A three-dimensional perspective of Daphnia's swimming behavior with and without predator cues. *Limnology and Oceanography* **64**, 1515–1525.

Lee, W. M. & An, Y. J. (2015). Evidence of three-level trophic transfer of quantum dots in an aquatic food chain by using bioimaging. *Nanotoxicology* **9**, 407–412.

Lei, Y. M., Zhou, J., Chai, Y. Q., Zhuo, Y. & Yuan, R. (2018). SnS_2 quantum dots as new emitters with strong electrochemiluminescence for ultrasensitive antibody detection. *Analytical Chemistry* **90**, 12270–12277.

Lewinski, N. A., Zhu, H., Jo, H. J. E., Pham, D., Kamath, R. R., Ouyang, C. R., Vulpe, C. D., Colvin, V. L. & Drezek, R. A. (2010). Quantification of water solubilized CdSe/ZnS quantum dots in *Daphnia magna*. *Environmental Science and Technology* **44**, 1841–1846.

Lewinski, N. A., Zhu, H., Ouyang, C. R., Conner, G. P., Wagner, D. S., Colvin, V. L. & Drezek, R. A. (2011). Trophic transfer of amphiphilic polymer coated CdSe/ZnS quantum dots to *Danio rerio*. *Nanoscale* **3**, 3080–3083.

Li, D., Sun, Y., Shen, Q., Zhang, Q., Huang, W., Kang, Q. & Shen, D. (2020a). Smartphone-based three-channel ratiometric fluorescent device and application in filed analysis of Hg^{2+}, $^{Fe3+}$ and Cu^{2+} in water samples. *Microchemical Journal* **152**, 104423.

Li, H., Guo, S., Li, C., Huang, H., Liu, Y. & Kang, Z. (2015). Tuning laccase catalytic activity with phosphate functionalized carbon dots by visible light. *ACS Applied Materials and Interfaces* **7**, 10004–10012.

Li, H., Huang, J., Liu, Y., Lu, F., Zhong, J., Wang, Y., Li, S., Lifshitz, Y., Lee, S. T. & Kang, Z. (2019a). Enhanced RuBisCO activity and promoted dicotyledons growth with degradable carbon dots. *Nano Research* **12**, 1585–1593.

Li, H., Huang, J., Lu, F., Liu, Y., Song, Y., Sun, Y., Zhong, J., Huang, H., Wang, Y., Li, S., Lifshitz, Y., Lee, S. T. & Kang, Z. (2018c). Impacts of carbon dots on rice plants: boosting the growth and improving the disease resistance. *ACS Applied Bio Materials* **1**, 663–672.

Li, H., Huang, J., Song, Y., Zhang, M., Wang, H., Lu, F., Huang, H., Liu, Y., Dai, X., Gu, Z., Yang, Z., Zhou, R. & Kang, Z. (2018d). Degradable carbon dots with broad-spectrum antibacterial activity. *ACS Applied Materials and Interfaces* **10**, 26936–26946.

Li, H., Zhang, M., Song, Y., Wang, H., Liu, C., Fu, Y., Huang, H., Liu, Y. & Kang, Z. (2018e). Multifunctional carbon dot for lifetime thermal sensing, nucleolus imaging and antialgal activity. *Journal of Materials Chemistry B* **6**, 5708–5717.

Li, J., Xiao, L., Cheng, Y., Cheng, Y., Wang, Y., Wang, X. & Ding, L. (2019b). Applications of carbon quantum dots to alleviate Cd^{2+} phytotoxicity in *Citrus maxima* seedlings. *Chemosphere* **236**, 124385.

Li, L. L., Ji, J., Fei, R., Wang, C. Z., Lu, Q., Zhang, J. R., Jiang, L. P. & Zhu, J. J. (2012). A facile microwave avenue to electrochemiluminescent two-color graphene quantum dots. *Advanced Functional Materials* **22**, 2971–2979.

Li, R., Sun, H., Wang, S., Wang, Y. & Yu, K. (2018a). Retention of CdS/ZnS quantum dots (QDs) on the root epidermis of woody plant and its implications by benzo[a]pyrene: evidence from the in situ synchronous nanosecond time-resolved fluorescence spectra method. *Journal of Agricultural and Food Chemistry* **66**, 814–821.

Li, S., Peng, Z., Dallman, J., Baker, J., Othman, A. M., Blackwelder, P. L. & Leblanc, R. M. (2016a). Crossing the blood-brain-barrier with transferrin conjugated carbon dots: a zebrafish model study. *Colloids and Surfaces B: Biointerfaces* **145**, 251–256.

Li, S., Wang, J., Sheng, W., Wen, W., Gu, Y. & Wang, S. (2018b). Fluorometric lateral flow immunochromatographic zearalenone assay by exploiting a quencher system composed of carbon dots and silver nanoparticles. *Microchimica Acta* **185**, 388.

Li, W., Zhang, H., Zheng, Y., Chen, S., Liu, Y., Zhuang, J., Liu, W. R. & Lei, B. (2017). Multifunctional carbon dots for highly luminescent orange-emissive cellulose based composite phosphor construction and plant tissue imaging. *Nanoscale* **9**, 12976–12983.

Li, W., Zheng, Y., Zhang, H., Liu, Z., Su, W., Chen, S., Liu, Y., Zhuang, J. & Lei, B. (2016b). Phytotoxicity, uptake, and translocation of fluorescent carbon dots in mung bean plants. *ACS Applied Materials and Interfaces* **8**, 19939–19945.

Li, Y., Li, W., Zhang, H., Dong, R., Li, D., Liu, Y., Huang, L. & Lei, B. (2019c). Biomimetic preparation of silicon quantum dots and their phytophysiology effect on cucumber seedlings. *Journal of Materials Chemistry B* **7**, 1107–1115.

Li, Y., Xu, X., Wu, Y., Zhuang, J., Zhang, X., Zhang, H., Lei, B., Hu, C. & Liu, Y. (2020b). A review on the effects of carbon dots in plant systems. *Materials Chemistry Frontiers* **4**, 437–448.

Li, Z., Wang, Y., Wang, J., Tang, Z., Pounds, J. G. & Lin, Y. (2010). Rapid and sensitive detection of protein biomarker using a portable fluorescence biosensor based on quantum dots and a lateral flow test strip. *Analytical Chemistry* **82**, 7008–7014.

Li, Z. F. & Ruckenstein, E. (2004). Water-soluble poly(acrylic acid) grafted luminescent silicon nanoparticles and their use as fluorescent biological staining labels. *Nano Letters* **4**, 1463–1467.

Lian, F., Wang, C. C., Wang, C. C., Gu, S. & Cao, X. (2019). Variety-dependent responses of rice plants with differential cadmium accumulating capacity to cadmium telluride quantum dots (CdTe QDs): cadmium uptake, antioxidative enzyme activity, and gene expression. *Science of the Total Environment* **697**, 134083.

Liang, R. Q., Li, W., Li, Y., Tan, C. Y., Li, J. X., Jin, Y. X. & Ruan, K. C. (2005). An oligonucleotide microarray for microRNA expression analysis based on labeling RNA with quantum dot and nanogold probe. *Nucleic Acids Research* **33**, e17.

Lim, M. E., Lee, Y. L., Zhang, Y. & Chu, J. J. H. (2012). Photodynamic inactivation of viruses using upconversion nanoparticles. *Biomaterials* **33**, 1912–1920.

Lim, S. Y., Shen, W. & Gao, Z. (2015). Carbon quantum dots and their applications. *Chemical Society Reviews* **44**, 362–381.

Lin, B., Yu, Y., Liu, F., Cao, Y. & Guo, M. (2017). Tunable and nontoxic fluorescent probes based on carbon dots for imaging of indole propionic acid receptor in plant tissues in situ. *Journal of Fluorescence* **27**, 1495–1503.

Lin, F., Bao, Y.-W. & Wu, F.-G. (2019). Carbon dots for sensing and killing microorganisms. *C—Journal of Carbon Research* **5**, 33.

Linehan, K., Carolan, D. & Doyle, H. (2019). Highly selective optical detection of Fe^{3+} ions in aqueous solution using label-free silicon nanocrystals. *Particle and Particle Systems Characterization* **36**, 1900034.

Liu, C., Mao, G., Su, C., Ji, X., Chen, Z. & He, Z. (2015). Aptamer-functionalized CdTe:Zn^{2+} quantum dots for the detection of tomato systemin. *Analytical Methods* **7**, 7748–7752.

Liu, C., Zhang, P., Zhai, X., Tian, F., Li, W., Yang, J., Liu, Y., Wang, H., Wang, W. & Liu, W. (2012). Nano-carrier for gene delivery and bioimaging based on carbon dots with PEI-passivation enhanced fluorescence. *Biomaterials* **33**, 3604–3613.

Liu, H., Li, Z., Sun, Y., Geng, X., Hu, Y., Meng, H., Ge, J. & Qu, L. (2018). Synthesis of luminescent carbon dots with ultrahigh quantum yield and inherent folate receptor-positive cancer cell targetability. *Scientific Reports* **8**, 1086.

Liu, H., Zhang, X., Xing, B., Han, P., Gambhir, S. S. & Cheng, Z. (2010). Radiation-luminescence-excited quantum dots for in vivo multiplexed optical imaging. *Small* **6**, 1087–1091.

Liu, J., Erogbogbo, F., Yong, K. T., Ye, L., Liu, J., Hu, R., Chen, H., Hu, Y., Yang, Y., Yang, J., Roy, I., Karker, N. A., Swihart, M. T. & Prasad, P. N. (2013). Assessing clinical prospects of silicon quantum dots: studies in mice and monkeys. *ACS Nano* **7**, 7303–7310.

Liu, S. L., Wang, Z. G., Zhang, Z. L. & Pang, D. W. (2016a). Tracking single viruses infecting their host cells using quantum dots. *Chemical Society Reviews* **45**, 1211–1224.

Liu, X., Braun, G. B., Zhong, H., Hall, D. J., Han, W., Qin, M., Zhao, C., Wang, M., She, Z. G., Cao, C., Sailor, M. J., Stallcup, W. B., Ruoslahti, E. & Sugahara, K. N. (2016b). Tumor-targeted multimodal optical imaging with versatile cadmium-free quantum dots. *Advanced Functional Materials* **26**, 267–276.

Liu, Y., Zhao, Y., Zhang, T., Chang, Y., Wang, S., Zou, R., Zhu, G., Shen, L. & Guo, Y. (2019). Quantum dots-based immunochromatographic strip for rapid and sensitive detection of acetamiprid in agricultural products. *Frontiers in Chemistry* **7**, 76.

Liu, Y.-Y., Chang, B.-M. & Chang, H.-C. (2020). Nanodiamond-enabled biomedical imaging. *Nanomedicine* **15**, 1599–1616.

Lu, W., Qin, X., Liu, S., Chang, G., Zhang, Y., Luo, Y., Asiri, A. M., Al-Youbi, A. O. & Sun, X. (2012). Economical, green synthesis of fluorescent carbon nanoparticles and their use as probes for sensitive and selective detection of mercury(II) ions. *Analytical Chemistry* **84**, 5351–5357.

Luo, J. H., Li, Q., Chen, S. H. & Yuan, R. (2019). Coreactant-free dual amplified electrochemiluminescent biosensor based on conjugated polymer dots for the ultrasensitive detection of microRNA. *ACS Applied Materials and Interfaces* **11**, 27363–27370.

Ma, L., Wu, S. M., Huang, J., Ding, Y., Pang, D. W. & Li, L. (2008). Fluorescence in situ hybridization (FISH) on maize metaphase chromosomes with quantum dot-labeled DNA conjugates. *Chromosoma* **117**, 181–187.

Majumdar, S., Ma, C., Villani, M., Zuverza-Mena, N., Pagano, L., Huang, Y., Zappettini, A., Keller, A. A., Marmiroli, N., Dhankher, O. P. & White, J. C. (2019). Surface coating determines the response of soybean plants to cadmium sulfide quantum dots. *NanoImpact* **14**, 10015.

Malik, M. A., O'Brien, P. & Revaprasadu, N. (1999). A novel route for the preparation of CuSe and CuInSe2 nanoparticles. *Advanced Materials* **11**, 1441–1444.

Mandal, G., Darragh, M., Wang, Y. A. & Heyes, C. D. (2013). Cadmium-free quantum dots as time-gated bioimaging probes in highly-autofluorescent human breast cancer cells. *Chemical Communications* **49**, 624–626.

Marcon, L., Riquet, F., Vicogne, D., Szunerits, S., Bodart, J. F. & Boukherroub, R. (2010). Cellular and in vivo toxicity of functionalized nanodiamond in *Xenopus* embryos. *Journal of Materials Chemistry* **20**, 8064–8069.

Marmiroli, M., Mussi, F., Pagano, L., Imperiale, D., Lencioni, G., Villani, M., Zappettini, A., White, J. C. & Marmiroli, N. (2020). Cadmium sulfide quantum dots impact *Arabidopsis thaliana* physiology and morphology. *Chemosphere* **240**, 124856.

Marmiroli, M., Pagano, L., Savo Sardaro, M. L., Villani, M. & Marmiroli, N. (2014). Genome-wide approach in *Arabidopsis thaliana* to assess the toxicity of cadmium sulfide quantum dots. *Environmental Science and Technology* **48**, 5902–5909.

Martynenko, I. V., Kuznetsova, V. A., Litvinov, I. K., Orlova, A. O., Maslov, V. G., Fedorov, A. V., Dubavik, A., Purcell-Milton, F., Gun'ko, Y. K. & Baranov, A. V. (2016). Enantioselective cellular uptake of chiral semiconductor nanocrystals. *Nanotechnology* **27**, 075102.

Martynenko, I. V., Litvin, A. P., Purcell-Milton, F., Baranov, A. V., Fedorov, A. V. & Gun'Ko, Y. K. (2017). Application of semiconductor quantum dots in bioimaging and biosensing. *Journal of Materials Chemistry B* **5**, 6701–6727.

Massey, M., Wu, M., Conroy, E. M. & Algar, W. R. (2015). Mind your P's and Q's: the coming of age of semiconducting polymer dots and semiconductor quantum dots in biological applications. *Current Opinion in Biotechnology* **34**, 30–40.

Mattoussi, H., Matthew Mauro, J., Goldman, E. R., Anderson, G. P., Sundar, V. C., Mikulec, F. V. & Bawendi, M. G. (2000). Self-assembly of CdSe-ZnS quantum dot bioconjugates using an engineered recombinant protein. *Journal of the American Chemical Society* **122**, 12142–12150.

McVey, B. F. P. & Tilley, R. D. (2014). Solution synthesis, optical properties, and bioimaging applications of silicon nanocrystals. *Accounts of Chemical Research* **47**, 3045–3051.

Medintz, I. L., Clapp, A. R., Brunel, F. M., Tiefenbrunn, T., Tetsuo Uyeda, H., Chang, E. L., Deschamps, J. R., Dawson, P. E. & Mattoussi, H. (2006). Proteolytic activity monitored by fluorescence resonance energy transfer through quantum-dot-peptide conjugates. *Nature Materials* **5**, 581–589.

Medintz, I. L., Stewart, M. H., Trammell, S. A., Susumu, K., Delehanty, J. B., Mei, B. C., Melinger, J. S., Blanco-Canosa, J. B., Dawson, P. E. & Mattoussi, H. (2010). Quantum-dot/dopamine bioconjugates function as redox coupled assemblies for in vitro and intracellular pH sensing. *Nature Materials* **9**, 676–684.

Mehta, V. N., Jha, S., Basu, H., Singhal, R. K. & Kailasa, S. K. (2015). One-step hydrothermal approach to fabricate carbon dots from apple juice for imaging of mycobacterium and fungal cells. *Sensors and Actuators, B: Chemical* **213**, 434–443.

Mei, J., Yang, L. Y., Lai, L., Xu, Z. Q., Wang, C., Zhao, J., Jin, J. C., Jiang, F. L. & Liu, Y. (2014). The interactions between CdSe quantum dots and yeast *Saccharomyces cerevisiae*: adhesion of quantum dots to the cell surface and the protection effect of ZnS shell. *Chemosphere* **112**, 92–99.

Merkl, J. P., Wolter, C., Flessau, S., Schmidtke, C., Ostermann, J., Feld, A., Mews, A. & Weller, H. (2016). Investigations of ion transport through nanoscale polymer membranes by fluorescence quenching of CdSe/CdS quantum dot/quantum rods. *Nanoscale* **8**, 7402–7407.

Mićić, O. I., Sprague, J., Lu, Z. & Nozik, A. J. (1996). Highly efficient band-edge emission from InP quantum dots. *Applied Physics Letters* **68**, 3150–3152.

Minnaar, C. & Anderson, B. (2019). Using quantum dots as pollen labels to track the fates of individual pollen grains. *Methods in Ecology and Evolution* **10**, 604–614.

Minnaar, C., de Jager, M. L. & Anderson, B. (2019). Intraspecific divergence in floral-tube length promotes asymmetric pollen movement and reproductive isolation. *New Phytologist* **224**, 1160–1170.

Mochalin, V. N., Shenderova, O., Ho, D. & Gogotsi, Y. (2012). The properties and applications of nanodiamonds. *Nature Nanotechnology* **7**, 11–23.

Modlitbová, P., Hlaváček, A., Švestková, T., Poříźka, P., Šimoníková, L., Novotný, K. & Kaiser, J. (2019). The effects of photon-upconversion nanoparticles on the growth of radish and duckweed: bioaccumulation, imaging, and spectroscopic studies. *Chemosphere* **225**, 723–734.

Modlitbová, P., Novotný, K., Poříźka, P., Klus, J., Lubal, P., Zlámalová-Gargošová, H. & Kaiser, J. (2018a). Comparative investigation of toxicity and bioaccumulation of cd-based quantum dots and cd salt in freshwater plant *Lemna minor* L. *Ecotoxicology and Environmental Safety* **147**, 334–341.

Modlitbová, P., Poříźka, P., Novotný, K., Drbohlavová, J., Chamradová, I., Farka, Z., Zlámalová-Gargošová, H., Romih, T. & Kaiser, J. (2018b). Short-term assessment of cadmium toxicity and uptake from different types of cd-based quantum dots in the model plant *Allium cepa* L. *Ecotoxicology and Environmental Safety* **153**, 23–31.

Mohan, N., Chen, C. S., Hsieh, H. H., Wu, Y. C. & Chang, H. C. (2010). In vivo imaging and toxicity assessments of fluorescent nanodiamonds in *Caenorhabditis elegans*. *Nano Letters* **10**, 3692–3699.

Morozova, S., Alikina, M., Vinogradov, A. & Pagliaro, M. (2020). Silicon quantum dots: synthesis, encapsulation, and epplication in light-emitting diodes. *Frontiers in Chemistry* **8**, 191.

Müller, F., Houben, A., Barker, P. E., Xiao, Y., Käs, J. A. & Melzer, M. (2006). Quantum dots - a versatile tool in plant science? *Journal of Nanobiotechnology* **4**, 5.

Nair, R., Poulose, A. C., Nagaoka, Y., Yoshida, Y., Maekawa, T. & Kumar, D. S. (2011). Uptake of FITC labeled silica nanoparticles and quantum dots by rice seedlings: effects on seed germination and their potential as biolabels for plants. *Journal of Fluorescence* **21**, 2057–2068.

Namdari, P., Negahdari, B. & Eatemadi, A. (2017). Synthesis, properties and biomedical applications of carbon-based quantum dots: An updated review. *Biomedicine and Pharmacotherapy* **87**, 209–222.

Nastiti, C. M. R. R., Mohammed, Y., Telaprolu, K. C., Liang, X., Grice, J. E., Roberts, M. S. & Benson, H. A. E. (2019). Evaluation of quantum dot skin penetration in porcine skin: effect of age and anatomical site of topical application. *Skin Pharmacology and Physiology* **32**, 182–191.

Navarro, D. A., Bisson, M. A. & Aga, D. S. (2012). Investigating uptake of water-dispersible CdSe/ZnS quantum dot nanoparticles by *Arabidopsis thaliana* plants. *Journal of Hazardous Materials* **211–212**, 427–435.

Navarro-Ruiz, M. C., Cayuela, A., Soriano, M. L., Guzm, R., Malag, M. M. & Valc, M. (2020). A systematic comparative study of the toxicity of semiconductor and graphitic carbon-based quantum dots using in vitro cell models. *Applied Sciences* **10**, 8845.

Newsome, S. D., Martinez del Rio, C., Bearhop, S. & Phillips, D. L. (2007). A niche for isotopic ecology. *Frontiers in Ecology and the Environment* **5**, 429–436.

Nirmal, M., Dabbousi, B. O., Bawendi, M. G., Macklin, J. J., Trautman, J. K., Harris, T. D. & Brus, L. E. (1996). Fluorescence intermittency in single cadmium selenide nanocrystals. *Nature* **383**, 802–804.

Nishimura, H., Ritchie, K., Kasai, R. S., Goto, M., Morone, N., Sugimura, H., Tanaka, K., Sase, I., Yoshimura, A., Nakano, Y., Fujiwara, T. K. & Kusumi, A. (2013). Biocompatible fluorescent silicon nanocrystals for single-molecule tracking and fluorescence imaging. *Journal of Cell Biology* **202**, 967–983.

Nordmann, J., Buczka, S., Voss, B., Haase, M. & Mummenhoff, K. (2015). In vivo analysis of the size- and time-dependent uptake of $NaYF_4$:Yb,Er upconversion nanocrystals by pumpkin seedlings. *Journal of Materials Chemistry B* **3**, 144–150.

Pan, D., Zhang, J., Li, Z. & Wu, M. (2010). Hydrothermal route for cutting graphene sheets into blue-luminescent graphene quantum dots. *Advanced Materials* **22**, 734–738.

Pan, L., Sun, S., Zhang, A., Jiang, K., Zhang, L., Dong, C., Huang, Q., Wu, A. & Lin, H. (2015). Truly fluorescent excitation-dependent carbon dots and their applications in multicolor cellular imaging and multidimensional sensing. *Advanced Materials* **27**, 7782–7787.

Pang, C. & Gong, Y. (2019). Current status and future prospects of semiconductor quantum dots in botany. *Journal of Agricultural and Food Chemistry* **67**, 7561–7568.

Park, J. H., Gu, L., Von Maltzahn, G., Ruoslahti, E., Bhatia, S. N. & Sailor, M. J. (2009). Biodegradable luminescent porous silicon nanoparticles for in vivo applications. *Nature Materials* **8**, 331–336.

Park, Y., Yoo, J., Lim, B., Kwon, W. & Rhee, S. W. (2016). Improving the functionality of carbon nanodots: doping and surface functionalization. *Journal of Materials Chemistry A* **4**, 11582–11603.

Parvizi, R., Azad, S., Dashtian, K., Ghaedi, M. & Heidari, H. (2019). Natural source-based graphene as sensitising agents for air quality monitoring. *Scientific Reports* **9**, 3798.

Pelley, J. L., Daar, A. S. & Saner, M. A. (2009). State of academic knowledge on toxicity and biological fate of quantum dots. *Toxicological Sciences* **112**, 276–296.

Peng, J., Sun, Y., Liu, Q., Yang, Y., Zhou, J., Feng, W., Zhang, X. & Li, F. (2012). Upconversion nanoparticles dramatically promote plant growth without toxicity. *Nano Research* **5**, 770–782.

Peng, Z., Miyanji, E. H., Zhou, Y., Pardo, J., Hettiarachchi, S. D., Li, S., Blackwelder, P. L., Skromne, I. & Leblanc, R. M. (2017). Carbon dots: promising biomaterials for bone-specific imaging and drug delivery. *Nanoscale* **9**, 17533–17543.

Plácido, J., Bustamante-López, S., Meissner, K. E., Kelly, D. E. & Kelly, S. L. (2019). Microalgae biochar-derived carbon dots and their application in heavy metal sensing in aqueous systems. *Science of the Total Environment* **656**, 531–539.

Pradhan, N., Battaglia, D. M., Liu, Y. & Peng, X. (2007). Efficient, stable, small, and water-soluble doped ZnSe nanocrystal emitters as non-cadmium biomedical labels. *Nano Letters* **7**, 312–317.

Pramanik, A., Kole, A. K., Krishnaraj, R. N., Biswas, S., Tiwary, C. S., Varalakshmi, P., Rai, S. K., Kumar, B. A. & Kumbhakar, P. (2016). A novel technique of synthesis of highly fluorescent carbon nanoparticles from broth constituent and in-vivo bioimaging of *C. elegans*. *Journal of Fluorescence* **26**, 1541–1548.

Qi, B. P., Bao, L., Zhang, Z. L. & Pang, D. W. (2016). Electrochemical methods to study photoluminescent carbon nanodots: preparation, photoluminescence mechanism and sensing. *ACS Applied Materials and Interfaces* **8**, 28372–28382.

Qian, K., Guo, H., Chen, G., Ma, C. & Xing, B. (2018). Distribution of different surface modified carbon dots in pumpkin seedlings. *Scientific Reports* **8**, 7991.

Qu, D., Zheng, M., Zhang, L., Zhao, H., Xie, Z., Jing, X., Haddad, R. E., Fan, H. & Sun, Z. (2014). Formation mechanism and optimization of highly luminescent N-doped graphene quantum dots. *Scientific Reports* **4**, 5294.

Ravindran, S., Kim, S., Martin, R., Lord, E. M. & Ozkan, C. S. (2005). Quantum dots as bio-labels for the localization of a small plant adhesion protein. *Nanotechnology* **16**, 1–4.

Reed, M. A., Bate, R. T., Bradshaw, K., Duncan, W. M., Frensley, W. R., Lee, J. W. & Shih, H. D. (1986). Spatial quantization in GaAs-AlGaAs multiple quantum dots. *Journal of Vacuum Science and Technology B: Microelectronics and Nanometer Structures* **4**, 358–360.

Resch-Genger, U., Grabolle, M., Cavaliere-Jaricot, S., Nitschke, R. & Nann, T. (2008). Quantum dots versus organic dyes as fluorescent labels. *Nature Methods* **5**, 763–775.

Reshma, V. G. & Mohanan, P. V. (2019). Quantum dots: applications and safety consequences. *Journal of Luminescence* **205**, 287–298.

Rieger, S., Kulkarni, R. P., Darcy, D., Fraser, S. E. & Köster, R. W. (2005). Quantum dots are powerful multipurpose vital labeling agents in zebrafish embryos. *Developmental Dynamics* **234**, 670–681.

Ristic, B. Z., Milenkovic, M. M., Dakic, I. R., Todorovic-Markovic, B. M., Milosavljevic, M. S., Budimir, M. D., Paunovic, V. G., Dramicanin, M. D., Markovic, Z. M. & Trajkovic, V. S. (2014). Photodynamic antibacterial effect of graphene quantum dots. *Biomaterials* **35**, 4428–4435.

Ritenberg, M., Nandi, S., Kolusheva, S., Dandela, R., Meijler, M. M. & Jelinek, R. (2016). Imaging *Pseudomonas aeruginosa* biofilm extracellular polymer scaffolds with amphiphilic carbon dots. *ACS Chemical Biology* **11**, 1265–1270.

Rocha, T. L., Mestre, N. C., Sabóia-Morais, S. M. T. & Bebianno, M. J. (2017). Environmental behaviour and ecotoxicity of quantum dots at various trophic levels: a review. *Environment International* **98**, 1–17.

Rosenthal, S. J., Chang, J. C., Kovtun, O., McBride, J. R. & Tomlinson, I. D. (2011). Biocompatible quantum dots for biological applications. *Chemistry and Biology* **18**, 10–24.

Rossetti, R., Nakahara, S. & Brus, L. E. (1983). Quantum size effects in the redox potentials, resonance Raman spectra, and electronic spectra of CdS crystallites in aqueous solution. *The Journal of Chemical Physics* **79**, 1086–1088.

Roy, P., Chen, P. C., Periasamy, A. P., Chen, Y. N. & Chang, H. T. (2015). Photoluminescent carbon nanodots: synthesis, physicochemical properties and analytical applications. *Materials Today* **18**, 447–458.

Safarpour, H., Safarnejad, M. R., Tabatabaei, M., Mohsenifar, A., Rad, F., Basirat, M., Shahryari, F. & Hasanzadeh, F. (2012). Development of a quantum dots FRET-based biosensor for efficient detection of *Polymyxa betae*. *Canadian Journal of Plant Pathology* **34**, 507–515.

Schiffman, J. D. & Balakrishna, R. G. (2018). Quantum dots as fluorescent probes: synthesis, surface chemistry, energy transfer mechanisms, and applications. *Sensors and Actuators, B: Chemical* **258**, 1191–1214.

Selvan, S. T., Tan, T. T. & Ying, J. Y. (2005). Robust, non-cytotoxic, silica-coated CdSe quantum dots with efficient photoluminescence. *Advanced Materials* **17**, 1620–1625.

Sha, R., Jones, S. S., Vishnu, N., Soundiraraju, B. & Badhulika, S. (2018). A novel biomass derived carbon quantum dots for highly sensitive and selective detection of hydrazine. *Electroanalysis* **30**, 2228–2232.

Shamsipur, M., Chabok, A., Molaabasi, F., Seyfoori, A., Hajipour-Verdom, B., Shojaedin-Givi, B., Sedghi, M., Naderi-Manesh, H. & Yeganeh-Faal, A. (2019). Label free phosphate functionalized semiconducting polymer dots for detection of iron(III) and cytochrome c with application to apoptosis imaging. *Biosensors and Bioelectronics* **141**, 111337.

Sharma, V. K., McDonald, T. J., Sohn, M., Anquandah, G. A. K., Pettine, M. & Zboril, R. (2017). Assessment of toxicity of selenium and cadmium selenium quantum dots: a review. *Chemosphere* **188**, 403–413.

Shen, C., Ge, S., Pang, Y., Xi, F., Liu, J., Dong, X. & Chen, P. (2017). Facile and scalable preparation of highly luminescent N,S co-doped graphene quantum dots and their application for parallel detection of multiple metal ions. *Journal of Materials Chemistry B* **5**, 6593–6600.

Sheng, L., Huangfu, B., Xu, Q., Tian, W., Li, Z., Meng, A. & Tan, S. (2020). A highly selective and sensitive fluorescent probe for detecting Cr(VI) and cell imaging based on nitrogen-doped graphene quantum dots. *Journal of Alloys and Compounds* **820**, 153191.

Shi, B., Su, Y., Zhang, L., Huang, M., Liu, R. & Zhao, S. (2016). Nitrogen and phosphorus co-doped carbon nanodots as a novel fluorescent probe for highly sensitive detection of Fe^{3+} in human serum and living cells. *ACS Applied Materials and Interfaces* **8**, 10717–10725.

Shi, B., Zhang, L., Lan, C., Zhao, J., Su, Y. & Zhao, S. (2015). One-pot green synthesis of oxygen-rich nitrogen-doped graphene quantum dots and their potential application in pH-sensitive photoluminescence and detection of mercury(II) ions. *Talanta* **142**, 131–139.

Shojaei, T. R., Salleh, M. A. M., Sijam, K., Rahim, R. A., Mohsenifar, A., Safarnejad, R. & Tabatabaei, M. (2016). Fluorometric immunoassay for detecting the plant virus *Citrus tristeza* using carbon nanoparticles acting as quenchers and antibodies labeled with CdTe quantum dots. *Microchimica Acta* **183**, 2277–2287.

So, M. K., Xu, C., Loening, A. M., Gambhir, S. S. & Rao, J. (2006). Self-illuminating quantum dot conjugates for in vivo imaging. *Nature Biotechnology* **24**, 339–343.

Sooklal, K., Cullum, B. S., Angel, S. M. & Murphy, C. J. (1996). Photophysical properties of ZnS nanoclusters with spatially localized Mn^{2+}. *Journal of Physical Chemistry* **100**, 4551–4555.

Srivastava, R. R., Singh, V. K. & Srivastava, A. (2020). Facile synthesis of highly fluorescent water-soluble SnS_2 QDs for effective detection of Fe^{3+} and unveiling its fluorescence quenching mechanism. *Optical Materials* **109**, 110337.

Stern, S. T., Zolnik, B. S., McLeland, C. B., Clogston, J., Zheng, J. & McNeil, S. E. (2008). Induction of autophagy in porcine kidney cells by quantum dots: a common cellular response to nanomaterials? *Toxicological Sciences* **106**, 140–152.

Su, L. X., Ma, X. L., Zhao, K. K., Shen, C. L., Lou, Q., Yin, D. M. & Shan, C. X. (2018). Carbon nanodots for enhancing the stress resistance of peanut plants. *ACS Omega* **3**, 17770–17777.

Sun, H., Gao, N., Dong, K., Ren, J. & Qu, X. (2014). Graphene quantum dots-band-aids used for wound disinfection. *ACS Nano* **8**, 6202–6210.

Sun, J., Ling, P. & Gao, F. (2017). A mitochondria-targeted Ratiometric biosensor for pH monitoring and imaging in living cells with Congo-red-functionalized dual-emission semiconducting polymer dots. *Analytical Chemistry* **89**, 11703–11710.

Swift, T. A., Fagan, D., Benito-Alifonso, D., Hill, S. A., Yallop, M. L., Oliver, T. A. A., Lawson, T., Galan, M. C. & Whitney, H. M. (2021). Photosynthesis and crop productivity are enhanced by glucose-functionalised carbon dots. *New Phytologist* **229**, 783–790.

Tan, X., Li, Q. & Yang, J. (2020). CdTe QDs based fluorescent sensor for the determination of gallic acid in tea. *Spectrochimica Acta - Part A: Molecular and Biomolecular Spectroscopy* **224**, 117356.

Tang, S., Allagadda, V., Chibli, H., Nadeau, J. L. & Mayer, G. D. (2013). Comparison of cytotoxicity and expression of metal regulatory genes in zebrafish (*Danio rerio*) liver cells exposed to cadmium sulfate, zinc sulfate and quantum dots. *Metallomics* **5**, 1411–1422.

Tao, S., Feng, T., Zheng, C., Zhu, S. & Yang, B. (2019). Carbonized polymer dots: a brand new perspective to recognize luminescent carbon-based nanomaterials. *Journal of Physical Chemistry Letters* **10**, 5182–5188.

Taranova, N. A., Berlina, A. N., Zherdev, A. V. & Dzantiev, B. B. (2015). 'Traffic light' immunochromatographic test based on multicolor quantum dots for the simultaneous detection of several antibiotics in milk. *Biosensors and Bioelectronics* **63**, 255–261.

Tian, L. J., Peng, Y., Chen, D. L., Ma, J. Y., Yu, H. Q. & Li, W. W. (2017). Spectral insights into the transformation and distribution of CdSe quantum dots in microorganisms during food-chain transport. *Scientific Reports* **7**, 4370.

Tian, P., Tang, L., Teng, K. S. & Lau, S. P. (2018). Graphene quantum dots from chemistry to applications. *Materials Today Chemistry* **10**, 221–258.

Tripathi, S. & Sarkar, S. (2015). Influence of water soluble carbon dots on the growth of wheat plant. *Applied Nanoscience (Switzerland)* **5**, 609–616.

Tsoi, K. M., Dai, Q., Alman, B. A. & Chan, W. C. W. (2013). Are quantum dots toxic? Exploring the discrepancy between cell culture and animal studies. *Accounts of Chemical Research* **46**, 662–671.

van't Padje, A., Bonfante, P., Ciampi, L. T. & Kiers, E. T. (2021). Quantifying nutrient trade in the arbuscular mycorrhizal symbiosis under extreme weather events using quantum-dot tagged phosphorus. *Frontiers in Ecology and Evolution* **9**, 153.

van't Padje, A., Oyarte Galvez, L., Klein, M., Hink, M. A., Postma, M., Shimizu, T. & Kiers, E. T. (2020a). Temporal tracking of quantum-dot apatite across in vitro mycorrhizal networks shows how host demand can influence fungal nutrient transfer strategies. *ISME Journal* **15**, 435–449.

van't Padje, A., Werner, G. D. A. & Kiers, E. T. (2020b). Mycorrhizal fungi control phosphorus value in trade symbiosis with host roots when exposed to abrupt 'crashes' and 'booms' of resource availability. *New Phytologist* **229**, 2933–2944.

Vastarella, W. & Nicastri, R. (2005). Enzyme/semiconductor nanoclusters combined systems for novel amperometric biosensors. *Talanta* **66**, 627–633.

Vaz, R., Bettini, J., Júnior, J. G. F., Lima, E. D. S., Botero, W. G., Santos, J. C. C. & Schiavon, M. A. (2017). High luminescent carbon dots as an eco-friendly fluorescence sensor for Cr(VI) determination in water and soil samples. *Journal of Photochemistry and Photobiology A: Chemistry* **346**, 502–511.

Veronesi, G., Moros, M., Castillo-Michel, H., Mattera, L., Onorato, G., Wegner, K. D., Ling, W. L., Reiss, P. & Tortiglione, C. (2019). In vivo biotransformations of indium phosphide quantum dots revealed by x-ray microspectroscopy. *ACS Applied Materials & Interfaces* **11**, 35630–35640.

Wagner, A. M., Knipe, J. M., Orive, G. & Peppas, N. A. (2019). Quantum dots in biomedical applications. *Acta Biomaterialia* **94**, 44–63.

Wang, C., Tao, H., Cheng, L. & Liu, Z. (2011). Near-infrared light induced in vivo photodynamic therapy of cancer based on upconversion nanoparticles. *Biomaterials* **32**, 6145–6154.

Wang, C. Z. & He, X. P. (2018). Supramolecular glycorhodamine-polymer dot ensembles for the homogeneous, fluorogenic analysis of lectins. *Carbohydrate Research* **455**, 1–4.

Wang, D., Lin, B., Cao, Y., Guo, M. & Yu, Y. (2016). A highly selective and sensitive fluorescence detection method of glyphosate based on an immune reaction strategy of carbon dot labeled antibody and antigen magnetic beads. *Journal of Agricultural and Food Chemistry* **64**, 6042–6050.

Wang, H., Li, H., Zhang, M., Song, Y., Huang, J., Huang, H., Shao, M., Liu, Y. & Kang, Z. (2018a). Carbon dots enhance the nitrogen fixation activity of *Azotobacter chroococcum*. *ACS Applied Materials and Interfaces* **10**, 16308–16314.

Wang, H., Zhang, M., Song, Y., Li, H., Huang, H., Shao, M., Li, Y. & Kang, Z. (2018b). Carbon dots promote the growth and photosynthesis of mung bean sprouts. *Carbon* **136**, 94–102.

Wang, J., Yang, Y., Zhu, H., Braam, J., Schnoor, J. L. & Alvarez, P. J. J. (2014). Uptake, translocation, and transformation of quantum dots with cationic versus anionic coatings by *Populus deltoides* × nigra cuttings. *Environmental Science and Technology* **48**, 6754–6762.

Wang, J., Zhang, P., Huang, C., Liu, G., Leung, K. C. F. & Wáng, Y. X. J. (2015). High performance photoluminescent carbon dots for in vitro and in vivo bioimaging: effect of nitrogen doping ratios. *Langmuir* **31**, 8063–8073.

Wang, K., Gao, Z., Gao, G., Wo, Y., Wang, Y., Shen, G. & Cui, D. (2013). Systematic safety evaluation on photoluminescent carbon dots. *Nanoscale Research Letters* **8**, 122.

Wang, S., Liu, Y., Jiao, S., Zhao, Y., Guo, Y., Wang, M. & Zhu, G. (2017). Quantum-dot-based lateral flow immunoassay for detection of neonicotinoid residues in tea leaves. *Journal of Agricultural and Food Chemistry* **65**, 10107–10114.

Wang, W., Zhang, Y., Liu, Y. & He, Y. (2019). Highly selective and sensitive ratiometric fluorescent polymer dots for detecting hypochlorite in 100% aqueous media. *Spectrochimica Acta - Part A: Molecular and Biomolecular Spectroscopy* **207**, 73–78.

Wang, Y. & Tang, M. (2018). Review of in vitro toxicological research of quantum dot and potentially involved mechanisms. *Science of the Total Environment.* **625**, 940–962.

Wang, Y., Zhou, Y., Xu, L., Han, Z., Yin, H. & Ai, S. (2018). Photoelectrochemical apta-biosensor for zeatin detection based on graphene quantum dots improved photoactivity of graphite-like carbon nitride and streptavidin induced signal inhibition. *Sensors and Actuators, B: Chemical* **257**, 237–244.

Wen, S., Zhou, J., Zheng, K., Bednarkiewicz, A., Liu, X. & Jin, D. (2018). Advances in highly doped upconversion nanoparticles. *Nature Communications* **9**, 2415.

Werlin, R., Priester, J. H., Mielke, R. E., Krämer, S., Jackson, S., Stoimenov, P. K., Stucky, G. D., Cherr, G. N., Orias, E. & Holden, P. A. (2011). Biomagnification of cadmium selenide quantum dots in a simple experimental microbial food chain. *Nature Nanotechnology* **6**, 65–71.

Whiteside, M. D., Digman, M. A., Gratton, E. & Treseder, K. K. (2012a). Organic nitrogen uptake by arbuscular mycorrhizal fungi in a boreal forest. *Soil Biology and Biochemistry* **55**, 7–13.

Whiteside, M. D., Garcia, M. O. & Treseder, K. K. (2012b). Amino acid uptake in arbuscular mycorrhizal plants. *PLoS One* **7**, 8–11.

Whiteside, M. D., Treseder, K. K. & Atsatt, P. R. (2009). The brighter side of soils: quantum dots track organic nitrogen through fungi and plants. *Ecology* **90**, 100–108.

Whiteside, M. D., Werner, G. D. A., Caldas, V. E. A., van't Padje, A., Dupin, S. E., Elbers, B., Bakker, M., Wyatt, G. A. K., Klein, M., Hink, M. A., Postma, M., Vaitla, B., Noë, R., Shimizu, T. S., West, S. A., et al. (2019). Mycorrhizal fungi respond to resource inequality by moving phosphorus from rich to poor patches across networks. *Current Biology* **29**, 2043–2050.

Willner, I., Patolsky, F. & Wasserman, J. (2001). Photoelectrochemistry with controlled DNA-cross-linked CdS nanoparticle arrays. *Angewandte Chemie - International Edition* **40**, 1861–1864.

Winnik, F. M. & Maysinger, D. (2013). Quantum dot cytotoxicity and ways to reduce it. *Accounts of Chemical Research* **46**, 672–680.

Wu, C., Bull, B., Szymanski, C., Christensen, K. & McNeill, J. (2008). Multicolor conjugated polymer dots for biological fluorescence imaging. *ACS Nano* **2**, 2415–2423.

Wu, C. & Chiu, D. T. (2013). Highly fluorescent semiconducting polymer dots for biology and medicine. *Angewandte Chemie - International Edition* **52**, 3086–3109.

Wu, J. K., Ma, J. W., Wang, H., Qin, D. M., An, L., Ma, Y., Zheng, Z. T., De Hua, X., Wang, T. L. & Wu, X. J. (2019). Rapid and visual detection of benzothiostrobin residue in strawberry using quantum dot-based lateral flow test strip. *Sensors and Actuators, B: Chemical* **283**, 222–229.

Wu, P., Li, Y. & Yan, X. P. (2009). CdTe quantum dots (QDs) based kinetic discrimination of Fe^{2+} and Fe^{3+}, and CdTe QDs-Fenton hybrid system for sensitive photoluminescent detection of Fe^{2+}. *Analytical Chemistry* **81**, 6252–6257.

Wu, P. & Yan, X. P. (2010). Ni^{2+}-modulated homocysteine-capped CdTe quantum dots as a turn-on photoluminescent sensor for detecting histidine in biological fluids. *Biosensors and Bioelectronics* **26**, 485–490.

Wu, S., Zhang, H., Shi, Z., Duan, N., Fang, C. C., Dai, S. & Wang, Z. (2015). Aptamer-based fluorescence biosensor for chloramphenicol determination using upconversion nanoparticles. *Food Control* **50**, 597–604.

Xia, C., Zhu, S., Feng, T., Yang, M. & Yang, B. (2019). Evolution and synthesis of carbon dots: from carbon dots to carbonized polymer dots. *Advanced Science* **6**, 1901316.

Xiao, A., Wang, C., Chen, J., Guo, R., Yan, Z. & Chen, J. (2016). Carbon and metal quantum dots toxicity on the microalgae *Chlorella pyrenoidosa*. *Ecotoxicology and Environmental Safety* **133**, 211–217.

Xie, W. Y., Huang, W. T., Luo, H. Q. & Li, N. B. (2012). CTAB-capped Mn-doped ZnS quantum dots and label-free aptamer for room-temperature phosphorescence detection of mercury ions. *Analyst* **137**, 4651–4653.

Xu, G., Zeng, S., Zhang, B., Swihart, M. T., Yong, K. T. & Prasad, P. N. (2016). New generation cadmium-free quantum dots for biophotonics and nanomedicine. *Chemical Reviews* **116**, 12234–12327.

Xu, J., Jie, X., Xie, F., Yang, H., Wei, W. & Xia, Z. (2018). Flavonoid moiety-incorporated carbon dots for ultrasensitive and highly selective fluorescence detection and removal of Pb^{2+}. *Nano Research* **11**, 3648–3657.

Xu, X., Ray, R., Gu, Y., Ploehn, H. J., Gearheart, L., Raker, K. & Scrivens, W. A. (2004). Electrophoretic analysis and purification of fluorescent single-walled carbon nanotube fragments. *Journal of the American Chemical Society* **126**, 12736–12737.

Xue, R., Fu, L., Dong, S., Yang, H. & Zhou, D. (2020). Promoting *Chlorella* photosynthesis and bioresource production using directionally prepared carbon dots with tunable emission. *Journal of Colloid and Interface Science* **569**, 195–203.

Yadav, P., Nishanthi, S. T., Purohit, B., Shanavas, A. & Kailasam, K. (2019). Metal free visible light photocatalytic carbon nitride quantum dots as efficient antibacterial agents: An insight study. *Carbon* **152**, 587–597.

Yaghini, E., Turner, H. D., Le Marois, A. M., Suhling, K., Naasani, I. & MacRobert, A. J. (2016). In vivo biodistribution studies and ex vivo lymph node imaging using heavy metal-free quantum dots. *Biomaterials* **104**, 182–191.

Yan, S., Zeng, X., Tang, Y., Liu, B., Wang, Y. & Liu, X. (2019). Activating antitumor immunity and antimetastatic effect through polydopamine-encapsulated core–shell upconversion nanoparticles. *Advanced Materials* **31**, 1905825.

Yang, L., Kuang, H., Zhang, W., Wei, H. & Xu, H. (2018a). Quantum dots cause acute systemic toxicity in lactating rats and growth restriction of offspring. *Nanoscale* **10**, 11564–11577.

Yang, S. T., Wang, X., Wang, H., Lu, F., Luo, P. G., Cao, L., Meziani, M. J., Liu, J. H., Liu, Y., Chen, M., Huang, Y. & Sun, Y. P. (2009). Carbon dots as nontoxic and high-performance fluorescence imaging agents. *Journal of Physical Chemistry C* **113**, 18110–18114.

Yang, Y., Huo, D., Wu, H., Wang, X., Yang, J., Bian, M., Ma, Y. & Hou, C. (2018b). N, P-doped carbon quantum dots as a fluorescent sensing platform for carbendazim detection based on fluorescence resonance energy transfer. *Sensors and Actuators, B: Chemical* **274**, 296–303.

Yang, Y., Lv, S., Wang, F., An, Y., Fang, N., Zhang, W., Zhao, W., Guo, X. & Ji, S. (2019). Toxicity and serum metabolomics investigation of Mn-doped ZnS quantum dots in mice. *International Journal of Nanomedicine* **14**, 6297–6311.

Yang, Z., Loh, K. Y., Te Chu, Y., Feng, R., Satyavolu, N. S. R., Xiong, M., Nakamata Huynh, S. M., Hwang, K., Li, L., Xing, H., Zhang, X., Chemla, Y. R., Gruebele, M. & Lu, Y. (2018c). Optical control of metal ion probes in cells and zebrafish using highly selective DNAzymes conjugated to upconversion nanoparticles. *Journal of the American Chemical Society* **140**, 17656–17665.

Yao, J., Yang, M. & Duan, Y. (2014). Chemistry, biology, and medicine of fluorescent nanomaterials and related systems: new insights into biosensing, bioimaging, genomics, diagnostics, and therapy. *Chemical Reviews* **144**, 6130–6178.

Yi, Y., Zhu, G., Liu, C., Huang, Y., Zhang, Y., Li, H., Zhao, J. & Yao, S. (2013). A label-free silicon quantum dots-based photoluminescence sensor for ultrasensitive detection of pesticides. *Analytical Chemistry* **85**, 11464–11470.

Yong, K. T., Ding, H., Roy, I., Law, W. C., Bergey, E. J., Maitra, A. & Prasad, P. N. (2009). Imaging pancreatic cancer using bioconjugated InP quantum dots. *ACS Nano* **3**, 502–510.

Yu, G., Liang, J., He, Z. & Sun, M. (2006). Quantum dot-mediated detection of γ-aminobutyric acid binding sites on the surface of living pollen protoplasts in tobacco. *Chemistry and Biology* **13**, 723–731.

Yu, G., Tan, Y., He, X., Qin, Y. & Liang, J. (2014). CLAVATA3 dodecapeptide modified CdTe nanoparticles: a biocompatible quantum dot probe for in vivo labeling of plant stem cells. *PLoS One* **9**, e89241.

Zare-Moghadam, M., Shamsipur, M., Molaabasi, F. & Hajipour-Verdom, B. (2020). Chromium speciation by isophthalic acid-doped polymer dots as sensitive and selective fluorescent probes. *Talanta* **209**, 120521.

Zhang, L., Wang, J., Deng, J. & Wang, S. (2020). A novel fluorescent "turn-on" aptasensor based on nitrogen-doped graphene quantum dots and hexagonal cobalt oxyhydroxide nanoflakes to detect tetracycline. *Analytical and Bioanalytical Chemistry* **412**, 1343–1351.

Zhang, M., Su, R., Zhong, J., Fei, L., Cai, W., Guan, Q., Li, W., Li, N., Chen, Y., Cai, L. & Xu, Q. (2019a). Red/orange dual-emissive carbon dots for pH sensing and cell imaging. *Nano Research* **12**, 815–821.

Zhang, M., Wang, H., Liu, P., Song, Y., Huang, H., Shao, M., Liu, Y., Li, H. & Kang, Z. (2019b). Biotoxicity of degradable carbon dots towards microalgae: *Chlorella vulgaris*. *Environmental Science: Nano* **6**, 3316–3323.

Zhang, M., Wang, H., Song, Y., Huang, H., Shao, M., Liu, Y., Li, H. & Kang, Z. (2018). Pristine carbon dots boost the growth of *Chlorella vulgaris* by enhancing photosynthesis. *ACS Applied Bio Materials* **1**, 894–902.

Zhang, M., Wang, H., Wang, B., Ma, Y., Huang, H., Liu, Y., Shao, M., Yao, B. & Kang, Z. (2019c). Maltase decorated by chiral carbon dots with inhibited enzyme activity for glucose level control. *Small* **15**, 1901512.

Zhang, N., Zhang, L., Ruan, Y. F., Zhao, W. W., Xu, J. J. & Chen, H. Y. (2017). Quantum-dots-based photoelectrochemical bioanalysis highlighted with recent examples. *Biosensors and Bioelectronics* **94**, 207–218.

Zhang, S., Zhang, D., Ding, Y., Hua, J., Tang, B., Ji, X., Zhang, Q., Wei, Y., Qin, K. & Li, B. (2019). Bacteria-derived fluorescent carbon dots for highly selective detection of P -nitrophenol and bioimaging. *Analyst* **144**, 5497–5503.

Zhang, X., Jiang, M., Niu, N., Chen, Z., Li, S., Liu, S. & Li, J. (2018a). Natural-product-derived carbon dots: from natural products to functional materials. *ChemSusChem* **11**, 11–24.

Zhang, X., Yin, J., Kang, C., Li, J., Zhu, Y., Li, W., Huang, Q. & Zhu, Z. (2010). Biodistribution and toxicity of nanodiamonds in mice after intratracheal instillation. *Toxicology Letters* **198**, 237–243.

Zhang, X., Yu, X., Wang, J., Wang, Q., Meng, H. & Wang, Z. (2018b). One-step core/multishell quantum dots-based fluoroimmunoassay for screening of deoxynivalenol in maize. *Food Analytical Methods* **11**, 2569–2578.

Zhao, J., Deng, J., Yi, Y., Li, H., Zhang, Y. & Yao, S. (2014). Label-free silicon quantum dots as fluorescent probe for selective and sensitive detection of copper ions. *Talanta* **125**, 372–377.

Zhao, W., Xiang, Y., Xu, J., He, X. & Zhao, P. (2020). The reversible surface redox of polymer dots for the assay of total antioxidant capacity in food samples. *Microchemical Journal* **156**, 104805.

Zheng, M., Ruan, S., Liu, S., Sun, T., Qu, D., Zhao, H., Xie, Z., Gao, H., Jing, X. & Sun, Z. (2015a). Self-targeting fluorescent carbon dots for diagnosis of brain cancer cells. *ACS Nano* **9**, 11455–11461.

Zheng, M., Wang, Y., Wang, C., Wei, W., Ma, S., Sun, X. & He, J. (2018). Green synthesis of carbon dots functionalized silver nanoparticles for the colorimetric detection of phoxim. *Talanta* **185**, 309–315.

Zheng, X. T., Ananthanarayanan, A., Luo, K. Q. & Chen, P. (2015b). Glowing graphene quantum dots and carbon dots: properties, syntheses, and biological applications. *Small* **11**, 1620–1636.

Zheng, Y., Zhang, H., Li, W., Liu, Y., Zhang, X., Liu, H. & Lei, B. (2017). Pollen derived blue fluorescent carbon dots for bioimaging and monitoring of nitrogen, phosphorus and potassium uptake in *Brassica parachinensis* L. *RSC Advances* **7**, 33459–33465.

Zheng, Z., Zhou, Y., Li, X., Liu, S. & Tang, Z. (2011). Highly-sensitive organophosphorous pesticide biosensors based on nanostructured films of acetylcholinesterase and CdTe quantum dots. *Biosensors and Bioelectronics* **26**, 3081–3085.

Zhou, R., Li, M., Wang, S., Wu, P., Wu, L. & Hou, X. (2014). Low-toxic Mn-doped ZnSe@ZnS quantum dots conjugated with nano-hydroxyapatite for cell imaging. *Nanoscale* **6**, 14319–14325.

Zhu, S., Song, Y., Zhao, X., Shao, J., Zhang, J. & Yang, B. (2015). The photoluminescence mechanism in carbon dots (graphene quantum dots, carbon nanodots, and polymer dots): current state and future perspective. *Nano Research* **8**, 355–381.

Zou, Z., Du, D., Wang, J., Smith, J. N., Timchalk, C., Li, Y. & Lin, Y. (2010). Quantum dot-based immunochromatographic fluorescent biosensor for biomonitoring trichloropyridinol, a biomarker of exposure to chlorpyrifos. *Analytical Chemistry* **82**, 5125–5133.

Zuo, P., Lu, X., Sun, Z., Guo, Y. & He, H. (2016). A review on syntheses, properties, characterization and bioanalytical applications of fluorescent carbon dots. *Microchimica Acta* **183**, 519–542.

(*Received 1 February 2021; revised 26 May 2021; accepted 27 May 2021*)